INFORMATION TO USERS

This manuscript has been reproduced from the microfilm master. UMI films the text directly from the original or copy submitted. Thus, some thesis and dissertation copies are in typewriter face, while others may be from any type of computer printer.

The quality of this reproduction is dependent upon the quality of the copy submitted. Broken or indistinct print, colored or poor quality illustrations and photographs, print bleedthrough, substandard margins, and improper alignment can adversely affect reproduction.

In the unlikely event that the author did not send UMI a complete manuscript and there are missing pages, these will be noted. Also, if unauthorized copyright material had to be removed, a note will indicate the deletion.

Oversize materials (e.g., maps, drawings, charts) are reproduced by sectioning the original, beginning at the upper left-hand corner and continuing from left to right in equal sections with small overlaps.

Photographs included in the original manuscript have been reproduced xerographically in this copy. Higher quality 6" x 9" black and white photographic prints are available for any photographs or illustrations appearing in this copy for an additional charge. Contact UMI directly to order.

Bell & Howell Information and Learning
300 North Zeeb Road, Ann Arbor, MI 48106-1346 USA
800-521-0600

Université d'Ottawa · University of Ottawa

The Molecular Cloning, Cellular Expression, and Functional Study of Human Caveolin-1

Philip Harold Links

B.Sc. University of Alberta, 1996.

A THESIS SUBMITTED IN PARTIAL FULFILLMENT OF THE REQUIREMENT OF THE DEGREE OF MASTERS OF SCIENCE
in

THE FACULTY OF GRADUATE STUDIES

Department of Biochemistry
Ottawa Heart Institute
University of Ottawa

Abstract

This thesis will discuss the molecular cloning, cellular expression, and functional study of human caveolin–1. This 21 kDa inter-membrane protein is found in cell surface invaginations termed caveolae (Gk: *little caves*). The expression of caveolin-1 has been shown to be sufficient to form caveolae in cell culture. Caveolin-1 was cloned from human adipose tissue by RT-PCR, sequenced and subcloned into vectors for its eukaryotic over-expression. The eukaryotic expression vectors contained either myc or myc and poly-histidine epitopes to assist in purification. Vectors containing antisense caveolin-1 and a ribozyme targeting caveolin-1 were also created for the targeted disruption of caveolin-1. Caveolin-1 cDNA was transfected into McA-RH7777 rat hepatoma cells, human fibroblasts, human umbilical vein endothelial cells (HUVEC), and Cos-7 cells to evaluate candidate cell lines for stable expression models. Stable cell lines over expressing caveolin-1 were generated in McA-RH7777 and HUVEC models.

Confluent HUVEC cells that display cobblestone monolayer morphology were used for the study of transcellular trafficking on Falcon 3-D cell culture inserts. Intact monolayer formation as evaluated by Trans-epithelial electrical resistance (TEER) and was found to be maximal on inserts coated with fibronectin or collagen I, but not collagen IV, laminin or Matrigel. A sensitive horse radish peroxidase assay was established to evaluate monolayer integrity and was found to agree well with TEER measurements in this model. Utilizing radiolabeled inulin and dextran, transcytosis measurements in this model were used to probe the effect of caveolin-1 over-expression on high density lipoprotein (HDL) transcytosis. Caveolin-1 expression was shown to have no effect on HDL transcytosis in this model, and all trafficking could be accounted for by paracellular

trafficking.

We studied the effect of caveolin-1 expression on cellular cholesterol transport and efflux. Caveolin-1 cDNA was cloned from human adipose tissue and subcloned into an expression vector containing a C-terminal myc and a poly-histidine tag. Stable transfectants expressing different levels of human caveolin-1 were generated using rat hepatoma McA-RH7777 cells that do not normally express endogenous caveolin-1. Confocal microscopy showed that caveolin-1 staining was located at the perinuclear region and the plasma membrane. The expressed caveolin-1 was associated with the detergent insoluble membrane fraction. The initial rate of [^{3}H]cholesterol efflux from McA-RH7777 cells to HDL or recombinant discoidal particles (Lp2A-I) was independent of caveolin expression level. Caveolin-1 expression did not alter ^{125}I-HDL binding or association with the cell surface. However, long term (>10 h) cholesterol efflux to HDL or recombinant discoidal particles (Lp2A-I) was positively correlated with caveolin-1 levels (r^2 = 0.94). In addition, incorporation of [^{3}H]acetate and [^{3}H]mevalonate into cholesterol was increased with caveolin-1 expression. Exogenous [^{3}H]cholesterol movement from the plasma membrane to an acyl cholesterol acyl transferase (ACAT) accessible pool was increased in caveolin-1 expressing cells, and this transport was sensitive to progesterone. Thus, through enhanced intracellular cholesterol transport between cellular cholesterol stores and the efflux accessible pool of cholesterol, stable caveolin-1 expression in McA-RH7777 cells increased the rate of equilibration of cholesterol to efflux sites.

Dedications

I dedicate this work to my Grandfather who has been my inspiration throughout.

Acknowledgments

I would like to thank my supervisors Dr. Yves Marcel and Dr. Zemin Yao for their leadership on this new project. I would also like to thank Dr. Roger McLeod for his patient tutelage, without which I would not have had the skills to attack this project. I would like to thank Dr. Xiaohui Zha for her assistance in the microscopy studies to characterize the McA-RH7777 cells, and her help in the assay for cholesterol efflux in these cells. I would like to also thank Dr. Jim Burgess for his constant criticism and advice, which has forced me to be critical of my work. I would like to acknowledge Dr. Khai Tran's assistance in HPTLC, which gave me an invaluable tool to evaluate cholesterol synthesis. I would also like to thank Malcolm Robb, who's invaluable, if somewhat cryptic notes, enabled me to clone caveolin, without which this work would not have been possible. I would also like to thank the members of both Dr. Marcel's and Dr. Yao's labs, for their support during my studies at the Ottawa Heart Institute.

Table of Contents

Table of Figures

Abbreviations

ACAT	**Acyl Cholesterol Acyl Transferase**
CAD	**Coronary Artery Disease**
CE	**Cholesterol Ester**
CETP	**Cholesterol Ester Transfer Protein**
DIM	**Detergent Insoluble Membrane**
GDI	**GDP Dissociation Inhibitor Protein**
GPI	**Glycosylphosphatidylinositol**
HDL	**High Density Lipoprotein**
HRP	**Horseradish Peroxidase**
HUVEC	**Human Umbilical Vein Endothelial Cells**
FC	**Free Cholesterol**
LCAT	**Lecithin:Cholesterol Acyltransferase**
LDL	**Low Density Lipoprotein**
Lp2A-I	**Reconstituted Discoidal HDL with two ApoA-I proteins**
McA-RH7777	**McArdle Rat Hepatoma 7777 cells**
MMLV RT	**Moloney Mouse Leukemia Virus Reverse Transcriptase**
MTP	**Microsomal Triglyceride Transfer Protein**
NT	**Nucleotide**
PC	**Phosphatidylcholine**
PE	**Phosphatidylethanolamine**
PL	**Phospholipid**
PLTP	**Phospholipid Transfer Protein**
POPC	**1-palmitoyl 2-oleoyl phosphatidylcholine**
SM	**Sphingomyelin**
SR-B1	**Scavenger Receptor B1**
TEER	**Trans Epithelial Electrical Resistance**
TG	**Triglyceride**
VLDL	**Very low density lipoprotein**
Wt	**Wild Type (referring to the parental strain)**

Chapter 1: Introduction and Background

1.1 Historical perspective of atherosclerosis

Atherosclerosis and heart disease will kill more people in North America this year than any other disease. While much progress has been made in understanding the mechanisms of this disease, many questions and paradoxes remain. In the early 1970's the Framingham Heart Study was convened to determine risk factors that correlate with death as a result of coronary artery disease (1). This study made two major observations, first low density lipoprotein (LDL) cholesterol levels correlate with risk of death as a result of coronary artery disease (CAD). Secondly high density lipoprotein (HDL) levels are inversely correlated with the risk of death as a result of CAD. While considerable progress has been made in understanding the implications of the first finding of this study, a comprehensive explanation for the negative correlation between HDL and death remains to be elucidated.

An understanding of the apparent protective role of HDL has been complicated by the poorly defined metabolism of HDL (2). Reverse cholesterol transport is currently accepted as the means of protection mediated by HDL (3). This concept hinges on HDL's ability to scavenge cholesterol from the peripheral tissues (4). Once HDL absorbs cholesterol in the periphery, it transfers cholesterol to apoB-containing lipoproteins (5), that return cholesterol to the liver for elimination in the bile. This process is termed *reverse cholesterol transport* (Fig. 1B) (6). HDL is thought to scavenge cholesterol from engorged foam cells that accumulate below the endothelium of the artery (7). This work will attempt to address how lipoproteins traverse the endothelium to gain access to the foam cells below, and to define the mechanism by which HDL removes cellular

cholesterol.

1.2 Lipoproteins

Lipoproteins (Lp's) are a broad family of macromolecules, which serve to solubilize lipid for transport in the aqueous environment of the circulation. This mechanism of transport is conserved throughout animals and insects (8). These macromolecules are made of protein (apolipoprotein) and lipid components. Lipoproteins are classified by their buoyant density upon ultra-centrifugation.

Lp Class	**Buoyant density**	**Apolipoproteins**
Chylomicron	d < .098 g/ml	ApoB-48, ApoA-I, II & IV, ApoC-I, II & III, ApoE
VLDL	.098 < d < 1.006 g/ml	ApoB-100 ApoC-I, II & III, ApoE
IDL	1.006 < d < 1.019 g/ml	ApoB-100 ApoC-I, II & III, ApoE
LDL	1.019 < d < 1.063 g/ml	ApoB-100
HDL	1.063 < d < 1.21 g/ml	ApoA-I, II & IV, ApoC-I, II & III, ApoE

Apolipoproteins belong to two major classes, exchangeable and integral non-exchangeable lipoproteins. The first class is characterized by repeated amphipathic α-helices which mediate the reversible interaction between the protein and phospholipids. Apolipoprotein A-I is a prototypical exchangeable protein of 28 kDa, composed of 11 amphipathic alpha helices (3). In the case of non-exchangeable apolipoproteins, the interaction with lipid is irreversible. The mechanism by which apolipoprotein B is thought to associate irreversibly with lipid, is through extended regions of β–sheet structure found within this mammoth 550 kDa protein (9).

Figure 1: Models of cholesterol efflux and reverse cholesterol transport

A, Illustration of the two models for HDL mediated cholesterol efflux. At left, specific efflux where SR-BI is diagrammed as the specific intercessor allowing cholesterol to be transferred to nascent HDL. At right, non-specific or diffusional efflux where nacent HDL interacts with the plasma membrane and is able to remove cholesterol without an accessory protein factor. B, A schematic diagram of reverse cholesterol transport. Discoidal preβ HDL is shown forming spherical HDL_3 through the action of lecithin:cholesterol acyltransferase (LCAT). HDL and apoB containing lipoproteins undergo reciprocal exchange of triglyceride and cholesteryl ester, which loads apoB-containing lipoproteins that are cleared by the liver. C, A model of HDL maturation. HDL proceeds from preβ HDL to HDL_3 (7.2-8.8 nm) then HDL_2 (8.8-12 nm) through HDL_1. This is achieved through the action of LCAT and the sequestration of peripheral free cholesterol in the core of the lipoprotein as cholesteryl ester.

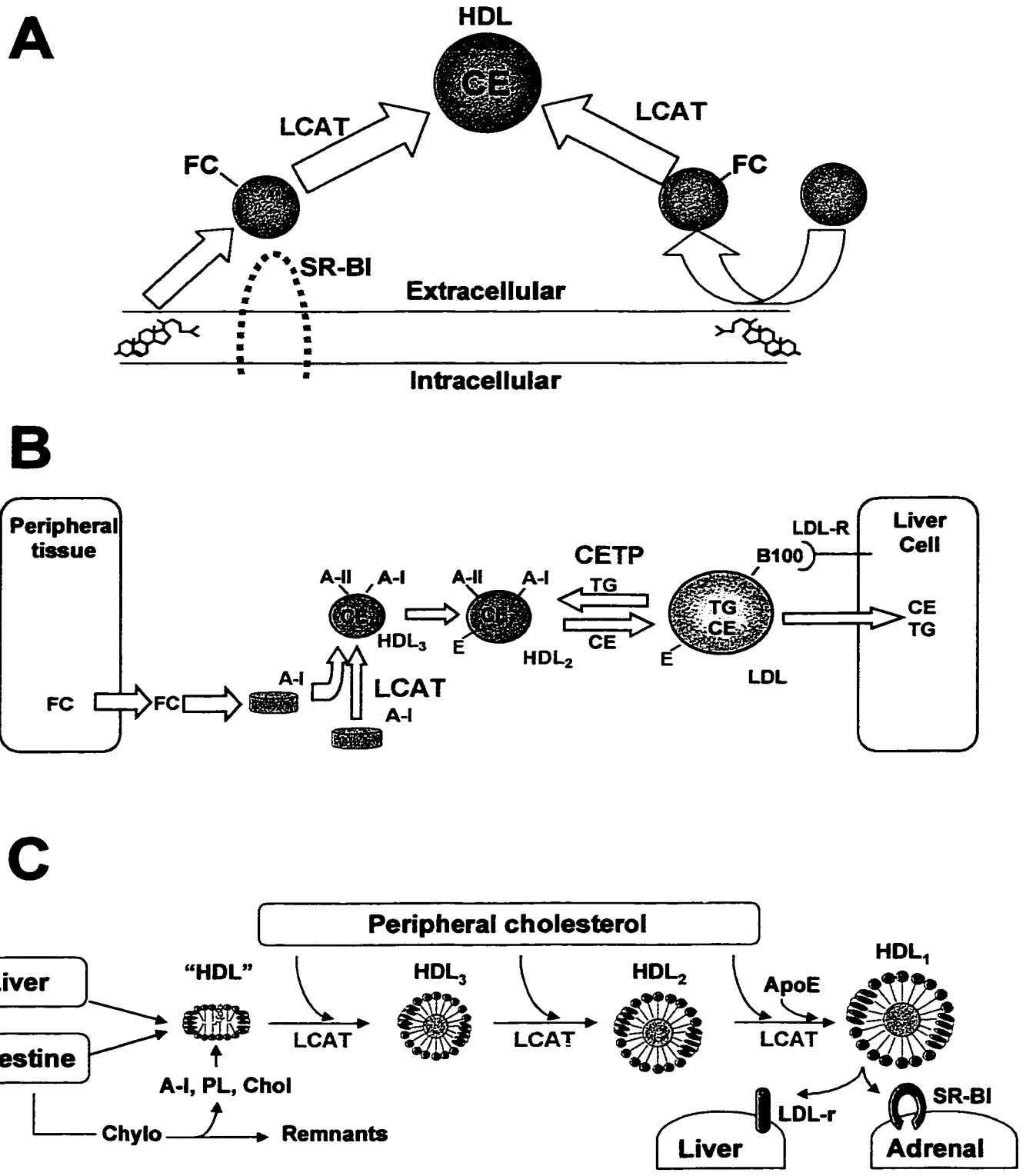
A
HDL
CE
LCAT
LCAT
FC
FC
SR-BI
Extracellular
Intracellular
B
Peripheral tissue
FC
FC
A-I
LCAT
A-I
A-II
A-I
CE
HDL3
A-II
A-I
CE
E
HDL2
CETP
TG
CE
TG
CE
E
LDL
B100
LDL-R
Liver Cell
CE
TG
C
Peripheral cholesterol
Liver
Intestine
"HDL"
A-I, PL, Chol
Chylo
Remnants
LCAT
HDL3
LCAT
HDL2
ApoE
LCAT
HDL1
LDL-r
SR-BI
Liver
Adrenal

1.21 ApoB-containing lipoproteins

ApoB-containing lipoproteins are composed of a non-exchangeable apoB and a phospholipid monolayer, which envelops the core of the lipoprotein and is composed of non-polar lipids including triglycerides (TG) and cholesteryl esters (CE) (10). ApoB-containing lipoproteins have two major sites of synthesis in humans, the liver and the intestine (11). The intestinal production of apoB-containing lipoproteins serves to transport exogenous (dietary) lipids while the hepatic production serves to transport endogenously synthesized lipids (12). In intestine only 48 % of the entire apoB gene product is translated, leading to the production of apoB 48. This is achieved through deaminination of the apoB RNA at NT 6666 leading to a stop codon (11). This apoB 48 stabilizes the large intestinal class of lipoprotein termed chylomicrons (12). These lipoproteins range in size up to 1200 nm engorged with dietary TG and CE. These lipoproteins also carry a complement of exchangeable lipoproteins including apoA-I apoA-II and apoC's.

The hepatic secretion of endogenously synthesized lipids is facilitated by the integral full-length apoB 100. These lipoproteins are predominantly secreted as very low density lipoproteins (VLDL), with one apoB per particle (13). These lipoproteins, in addition to a core enriched with TG, carry on their surface a complement of exchangeable apolipoproteins (14). These exchangeable proteins can govern functions such as receptor binding (apoE) or cofactors for lipolysis (apoC-II) of the lipoprotein (15, 16). Through catabolism in the circulation, VLDL are converted into IDL and finally LDL. Through this conversion the density of these particles shifts from $d < 1.006$ g/ml to $1.019 < d < 1.063$ g/ml as the TG core is hydrolyzed by lipoprotein lipase and hepatic lipase (17, 18).

Also as these particles circulate they are acted upon by CETP which enriches them in CE (19). This process of cholesterol transfer from HDL to apoB-containing lipoproteins will be expanded further as *reverse cholesterol transport* in section 1.3

The removal of cholesterol from the plasma is largely mediated through the interaction of LDL and IDL with the LDL receptor (LDL-R) (20). The LDL-R is capable of recognizing either apoB 100 or apoE for successful Ca^{2+}-dependent ligand binding. Once bound, the receptors cluster into clathrin coated pits, and are internalized by endocytosis (21). Through a process of vesicular trafficking the receptor-ligand complexes are transported to the late endosome where acidic conditions allow the separation and recycling of the LDL-R to the plasma membrane.

1.22 High density lipoproteins

High density lipoproteins compose a broad distribution of particles which have a heterogeneous lipid and protein composition (22). Unlike apoB 100 found on LDL, the apolipoproteins, which maintain the structure of HDL, are exchangeable. Typically apoA-I is found on all HDL particles however the numbers of protein molecules per lipoprotein can vary from two to five or more. Other exchangeable apolipoproteins found on HDL include apoC's, apoD and apoE. Large domains of these proteins are composed of amphipathic α-helical regions, which confers their exchangeable property. These regions are multiples of 22 to 33 amino acids, which on one face of the long axis of the helix contain hydrophobic residues and on the other face contain hydrophilic residues (3). The mechanism of interaction of these proteins with the lipoprotein surface is a hydrophobic interaction where the helix dips into the phospholipid heads of the monolayer (9).

This family of apolipoproteins evolved from a common ancestral gene some 500 million years ago (23). From predictions based on nucleotide homology, the amphipathic helices, which comprise these proteins, arose through a series of gene duplication events. With the exception of apoA-IV all maintain a three intron, four-exon gene structure (Fig. 2B). By comparing the rate of synonymous substitution within domains one can infer functional significance of a particular domain. For example, helix 8 within apoE, which encompasses the LDL-R binding region, reveals the most highly conserved region within apoE (24) and by contrast the non-synonymous substitution rate for apoA-II is one of the highest rates observed for a mammalian gene (24).

HDL exists as three density subclasses, with HDL_2 being both the most buoyant and the largest, HDL_3 being intermediate and preβ HDL being the least buoyant and the smallest. HDL_2 particles are further divided by size into subclasses (from largest to smallest) HDL_{2b}, HDL_{2a}. The HDL_3 sub-fraction contains the subclasses HDL_{3a}, HDL_{3b}, and HDL_{3c} (25). These classifications group peaks of HDL by density which overlap and represent a continuum of variable size and lipid composition. By dry mass HDL tends to be 50% apolipoprotein 3-5% TG, 25% PL and ~15% CE.

ApoA-I is synthesized and secreted by both intestinal and hepatic cells in approximately equal amounts (26). In the case of intestinal secretion, apoA-I is secreted on chylomicrons. During the catabolism of the core triglycerides of this particle, extraneous surface phospholipids may be shed as discs stabilized with apoA-I (27).

Figure 2: Exchangeable apolipoprotein evolution and gene structure

A. Schematic representation of apolipoprotein gene evolution. The progenitor probably most closely resembled apoC-I. The original divergence is predicted to have occurred 570 x 10^6 years ago, this is roughly coincident with the divergence between vertebrates and invertebrates. The square boxes indicate gene duplication events. The divergence between apoA-II and apoC-III is predicted to have occurred 285 x 10^6 years ago. B. Gene structure representation of the exchangeable lipoproteins. the wide bars represent the exons while the thin lines represent the intronic sequences and 5' and 3' flanking sequence. Shading indicates regions of homology between different genes. Notice that all genes except apoA-IV share a common four-exon three-intron gene structure (23).

A

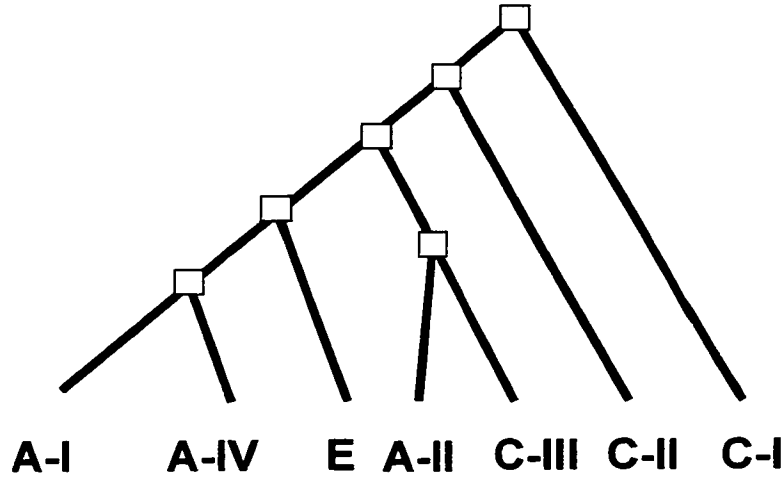

B

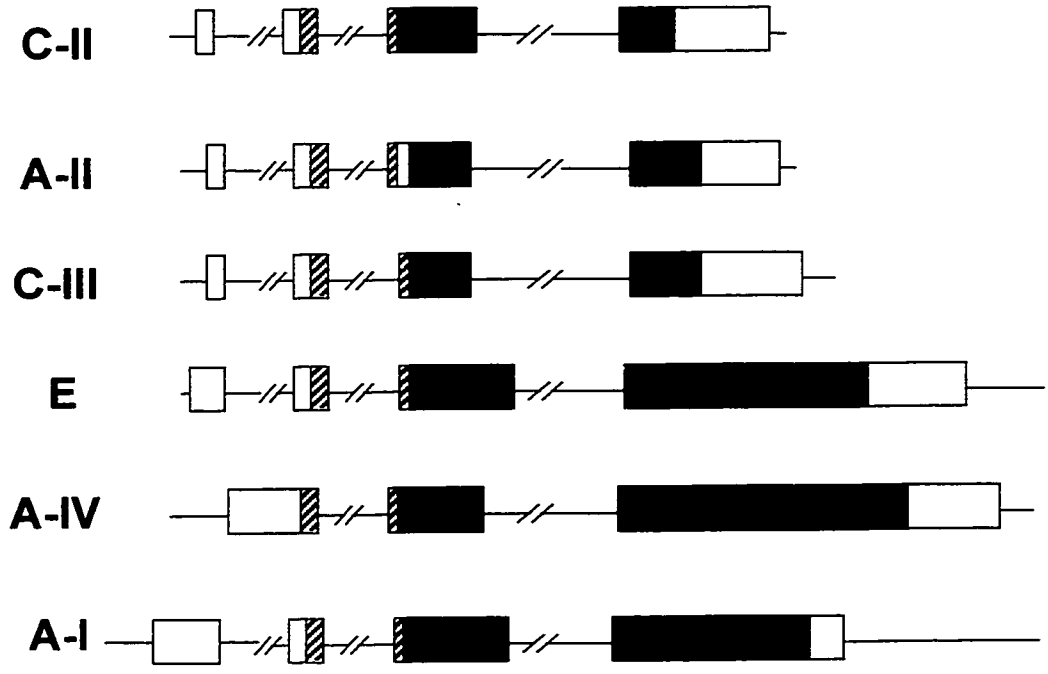

Lipid free apoA-I has also been shown to be capable of recruiting phospholipid from the cell surface for disc formation (28). Under normal conditions discs are not seen in human plasma, but they are seen in patients with defects in lecithin:cholesterol acyl transferase (LCAT) activity (29).

The use of HDL derived cholesterol for steroidogenesis in the adrenal gland appears to require a specific HDL receptor, SR-BI (30). This receptor is capable of binding HDL and mediating the selective uptake of lipids from these particles (31). This receptor does not appear to be an endocytic receptor and its function is under active investigation. Interestingly this receptor has been reported within cell surface invaganations that are termed caveolae (32). While the SR-BI mediated cholesterol delivery may serve as an important mode in adrenal function, knock out animals do not reveal any change in CAD (30).

1.3 Reverse cholesterol transport

Reverse cholesterol transport was a hypothesis, presented in 1968 by Dr. John Glomset at the University of Washington. He had discovered a plasma cholesterol acyltransferase (LCAT) activity and proposed the need for an enzyme that converted free cholesterol (FC) to CE on HDL particles (33). He postulated that free cholesterol might be transferred from a cellular membrane to a HDL particle by physical equilibration and the CE that was generated would be subsequently cleared by the liver. At the time of this postulate there was no known interaction of HDL with apoB- containing lipoproteins. It was only with the discovery of CETP that a transfer of cholesterol from HDL to apoB-containing lipoprotein particles was suggested (34). It is now known that there are also

transfer proteins that are capable of transferring PL such as phospholipid transfer protein (PLTP) between different lipoprotein classes (35).

It is currently believed that the protective function of HDL in CAD, may be through its role in reverse cholesterol transport (Fig. 1B) (36). HDL is thought to mediate the efflux of cholesterol from the plasma membrane of cells to its lipid monolayer (Fig. 1A) (37). Through the action of LCAT the free cholesterol found in the lipid monolayer which encapsulates HDL is esterified to cholesteryl ester (38). ApoA-I is a sufficient co-factor for LCAT in this reaction (39). Cholesterol ester is then sequestered into the core of the HDL particle. As the HDL particle forms a hydrophobic core of cholesteryl esters, it shifts from a preβ electrophoretic mobility to a α-migrating mobility and to a HDL_3 density (Fig. 1.C). Cholesterol ester-enriched HDL particles are acted upon by CETP, transferring CE to apoB-containing lipoprotein particles in exchange for TG (5). This exchange swells the HDL particles further into the HDL_2 density range (Fig. 1C). The reciprocal transfer of TG for CE is responsible for the loading of apoB-containing particles with CE for elimination by the liver (40). The rationale for the disposal of cholesterol in the liver is that few peripheral cells contain the enzymes necessary for cholesterol degradation (41). Partial degradation can be achieved through conversion by sterol 27-hydroxylase as seen in macrophage (41). However, complete elimination of sterols through bile acid production creates the need for transport to the liver (36). In this process HDL could serve as a first step in the removal of cholesterol from peripheral cells. In this initial step LCAT could serve to load HDL with cholesterol esters. However if reverse cholesterol transport protects against CAD, LCAT deficiency should be atherogenic.

LCAT deficient patients do not exhibit a high incidence of CAD (42). Despite the reduction of HDL in their plasma, there does not seem to be wide spread deposition of cholesterol in the peripheral tissues (29). Some tissues in these patients are severely affected, namely the cornea, kidneys and erythrocytes. This would suggest that these tissues are dependent on a LCAT mediated elimination of cholesterol (38). This is currently one of the major paradoxes within the HDL field, and raises serious questions about the validity of the Glomset hypothesis.

There are currently two models for HDL mediated efflux from the cell surface (Fig. 1A) (43). Diffusional efflux describes the desorption of cholesterol from the cellular membrane and its movement down a physicochemical gradient onto a HDL particle (44). This mechanism is contrasted by evidence for a specific efflux mechanism (45). The proof of a specific binding site for HDL or apoA-I has been confounded by the fact that no membrane protein has been identified as a mediator of cholesterol efflux (3). Recent reports have implicated SR-BI as a mediator of cholesterol efflux (46, 47). However others have reported that SR-BI is able to bind many other lipoproteins suggesting that its role as a specific intercessor of HDL mediated cholesterol efflux may be questionable (48). Interestingly SR-BI seems to be located in specialized membrane invaginations termed caveolae (49). While other proteins such as HDL binding protein (HBP) have been proposed as receptors of HDL, studies of SR-BI remain the most germane (50). The role of a specific binding site of HDL with the plasma membrane remains an important area of investigation, both for elucidation of reverse cholesterol transport and for the metabolism of HDL at the cell surface. This domain may be plasma membrane caveolae.

During the writing of this thesis the causative defect in Tangiers disease was identified as mutations in the ABC-1 gene (ATP binding cassette). Tangiers patients are characterized by an absence of plasma HDL. With the elucidation of the causative defect by positional cloning, the mechanism of ABC-1 function in reverse cholesterol transport is actively under investigation. While ABC-1 is beyond the scope of this thesis, a recent publication has proposed that it acts as a phosphatidyl serine (PS) flippase.

1.4 Caveolae

Caveolae are 50 to 100 nm cell surface invaginations, which have been characterized by electron microscopy as being un-coated. This is in contrast to the clathrin coated pits in which the LDL receptor and other endocytic receptors have been found (51). These caveolae are specialized regions of the plasma membrane which contain free cholesterol and sphingomyelin. The association of ras, src and small G-proteins implicate caveolae as a likely locale for cell signaling (52). A 21-24 kDa protein named caveolin is sufficient to drive the formation of caveolae. This protein serves to maintain the structure of these plasma membrane domains and anchors signaling molecules through a unique scaffolding domain (53). In this way it sequesters both protein signaling factors through protein-protein interaction as well as maintaining a local environment that is favorable to lipid signaling substrates.

Caveolin proteins belong to a gene family that includes three members (in humans). These three genes are caveolin-1, caveolin-2 and caveolin-3. Caveolin-1 and 2 are both found in *C. elegans*, suggesting an important evolutionary function. Interestingly, a yeast homologue has not yet been found. Caveolin-1, 2 and 3 have similar intron-exon structure, and are found on the same chromosome (54). In mice they

are found on chromosome 6, and in humans chromosome 7q31. The close similarity in intron-exon structure suggests that they may have arisen through gene duplication events. Also conservation of key amino acids in functional domains suggests domains which may be important to caveolin function. In fact in two Italian kindreds have been identified which have mutations in one of these key domains and show disrupted caveolin-3 oligomerization, which leads to an autosomal dominant form of limb girdle muscular dystrophy (55).

1.41 Caveolin isoforms and tissue distribution

The genes for caveolin-1, 2 and 3 encode four different proteins. Caveolin-1 encodes two gene products, which arise as a result of an alternative initiation site, which occurs at amino acid 32. This gives rise to two caveolin-1 isoforms α and β (56) (Fig. 3A). Caveolin-2 and 3 share other functional domains with caveolin-1 including a stretch of 33 hydrophobic amino acids, which are thought to mediate its interaction with the plasma membrane (57). The final topology of all caveolin isoforms result in both the N and C termini facing the cytosol. The tissues in which the isoforms of caveolin are found seem to intimate distinct isoform functions. Caveolin-1 is enriched in the epithelia, and adipose tissue. Caveolin-2 has a similar distribution, but is also found highly expressed in the lung (58). Caveolin-3 is found predominantly in the muscle and heart (59). In the tissues where caveolin-1 and 2 are expressed they may function in concert as well as independently.

Figure 3: Caveolin isoforms and topology

A. Schematic representation of caveolin isoforms 1, 2 and 3. α and β isoforms ofcaveolin-1 are generated by an alternative initiation site at AA 35. The putative intermembrane hydrophobic region of caveolin-1 is indicated from A.A. 100 to 141. B, Proposed topology of caveolin is diagramed as the intermembrane regions inserts into but not through the membrane bilayer, exposing both the C and N termini to the cytosolic side of the membrane.

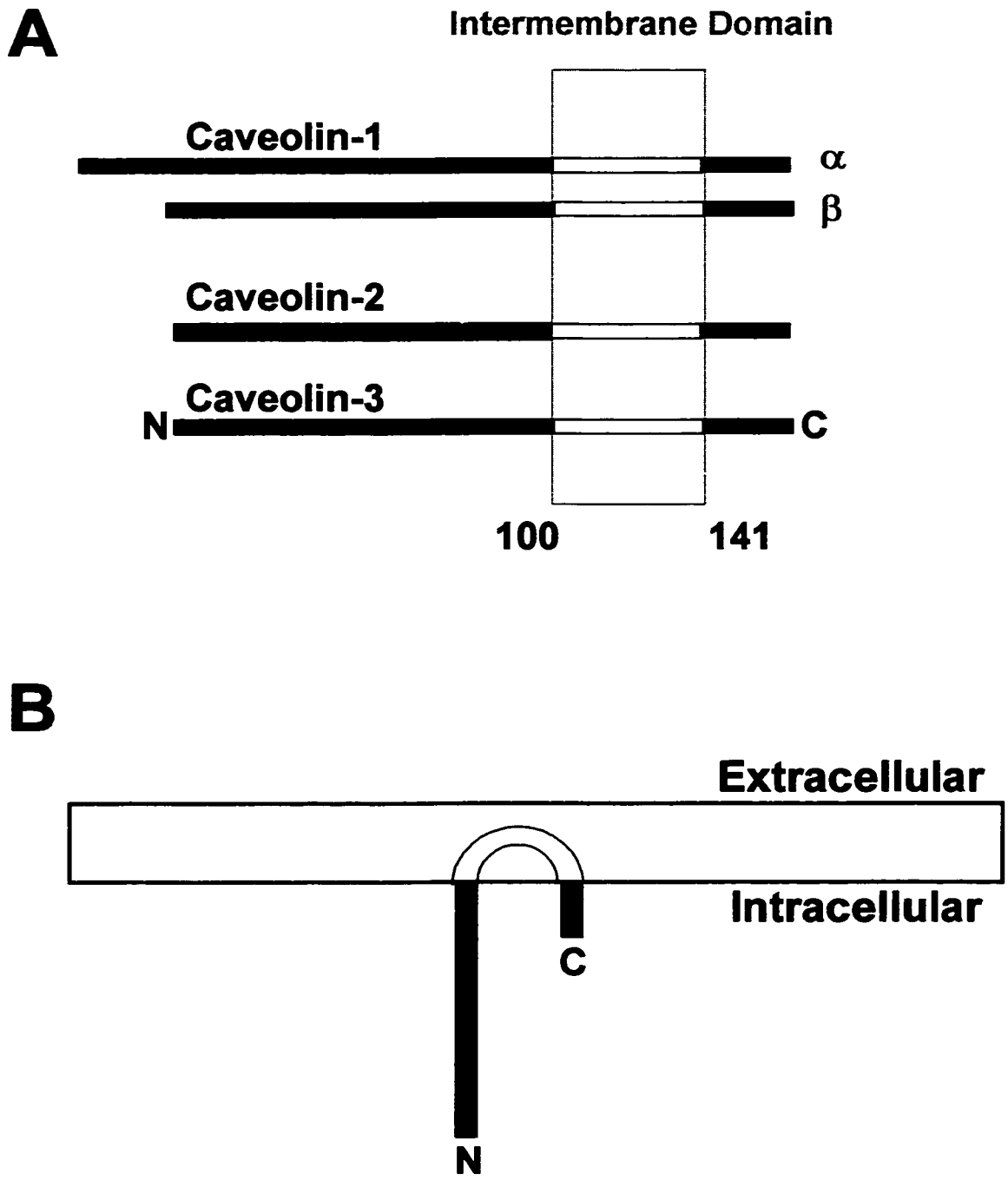
A
Intermembrane Domain
Caveolin-1
α
β
Caveolin-2
Caveolin-3
N
C
100
141
B
Extracellular
Intracellular
C
N

Caveolin forms caveolae through ordered aggregation, which can be homo or hetero-oligomeric (60). In-vitro experiments showed that three cholesterol molecules bind two molecules of caveolin-1. This probably represents the basic unit of packaging. These subunits then aggregate into higher order structures with 16-18 molecules of caveolin (61), which probably represent subunits of intact caveolae. On the cell surface caveolae can often cluster together, and EM has revealed that caveolae superstructures may exist on the surface of cells as striations (62). Much of the experimental work in defining caveolae has relied on its insolubility in Triton X-100. When cell membranes are solubilized with Triton X-100, caveolin enriched membranes will float upon sucrose density ultra-centrifugation (63). This has been adopted as one of the functional assays within the field to assess caveolae formation. The difficulty that has arisen is that many researchers feel that co-fractionation of other proteins within this caveolar fraction, constitutes functional localization to the caveolae. While this is provocative it does not serve as a proof of caveolar localization, merely enrichment within this fraction under specific experimental conditions. Some proteins such as eNOS and $G_{\alpha}i$ have been further shown to interact with caveolin directly; strengthening the argument for their caveolar localization (64).

The association of caveolin-1 with lipid occurs co-translationally (65). This raises the question of whether caveolae are assembled in the ER or later in the Golgi apparatus or plasma membrane. Parton and colleagues (65) have shown that caveolin-1 oligomerization and detergent insolubility can be divorced. Their data suggest oligomerization occurring first in the ER and detergent insolubility occurring later in the Golgi apparatus. The detergent resistant characteristic of caveolae represents oligomeric

caveolin-1 in association with its lipid complement. The synthesis of glycosphingolipids in the early Golgi would argue that the detergent resistant characteristic should be acquired after ER exit of caveolin-1. There is precedence for assembly to occur within the Golgi complex, as hemagglutinin oligomers are formed in the ER but do not adopt detergent insolubility until the Golgi apparatus (66). Likewise, vonWillebrand factor forms inter-chain disulfide bonds (as dimers) in the ER before oligomerization occurs in the Golgi apparatus (67).

Caveolae can form through homo-oligomerization of caveolin-1 or hetero oligomerization between caveolin-1 and 2 (68). This has been shown by co-immunoprecipitation studies of caveolin-1 and 2. Interestingly, only caveolin-1 but not 2 levels are altered in transformed cells (abl and ras) (69). In these cells caveolae disappear from the cell surface, but detergent insoluble caveolin-2 complexes remain. The detergent resistant property of caveolin is thought to result from its association with sphingolipids. Also in an insect cell expression model (Sf-21 cells) caveolin-1 expression but not caveolin-2 is sufficient to drive caveolae formation (70). This has led to caveolin-2 being labeled as an "*accessory protein*".

Figure 4: Caveolin domain structure

A. Schematic diagram of functional domains within caveolin. Palmitoylation sites at A.A. 133, 143 and 156 are indicated. B. Distance legend for diagrams A and C, numbers represent amino acid boundaries of structural domains in caveolin-1. C. Proposed pentapartite structural domain model based on computer algorithm maps (Appendix D). α denotes proposed α–helices, β represents regions of β-sheet and η represents hydrophobic inter-membrane domain.

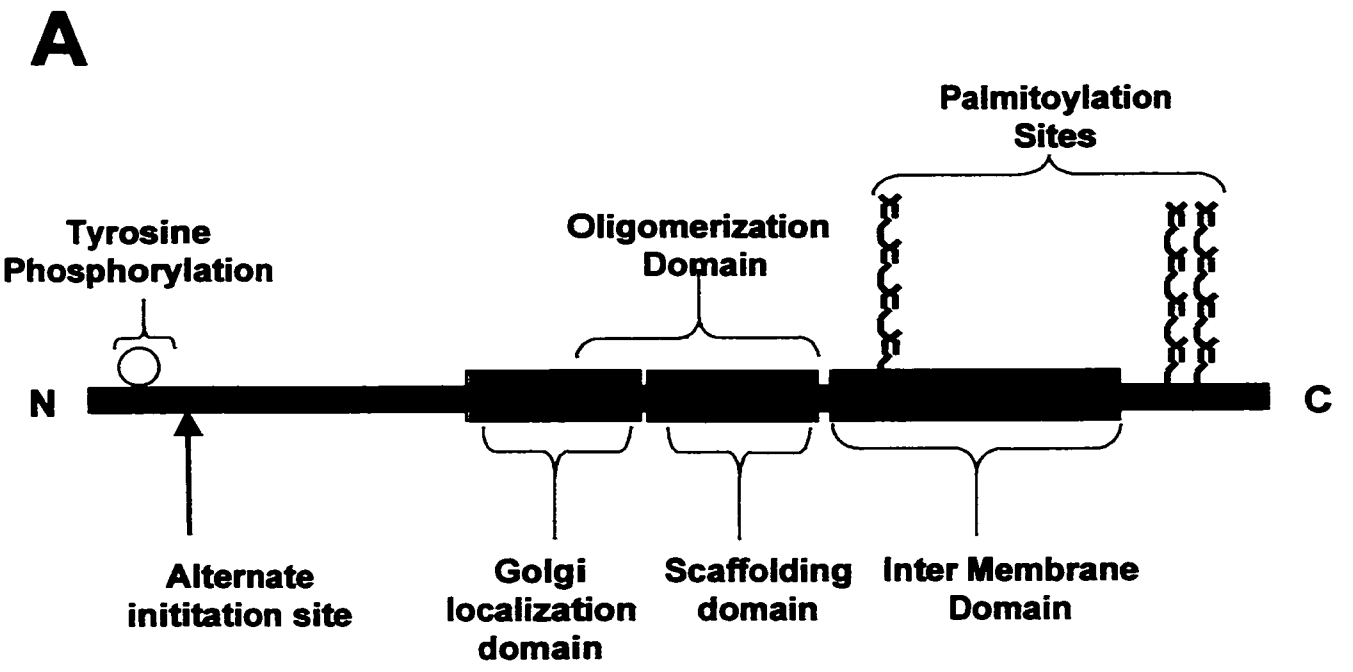
A
Palmitoylation Sites
Tyrosine Phosphorylation
Oligomerization Domain
N
C
Alternate inititation site
Golgi localization domain
Scaffolding domain
Inter Membrane Domain

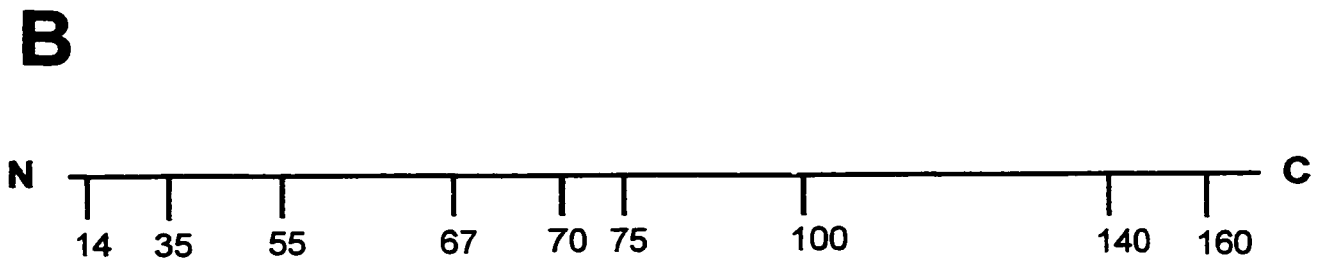
B
N
C
14
35
55
67
70
75
100
140
160

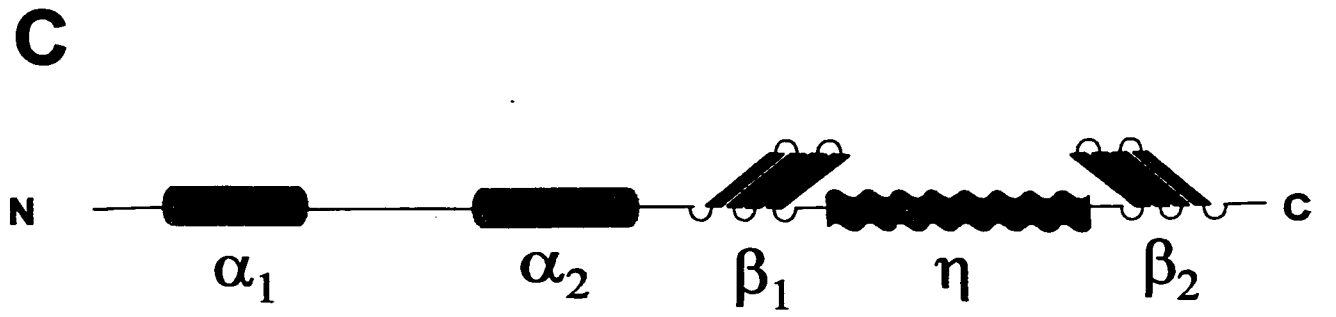
C
N
C
α1
α2
β1
η
β2

1.42 Caveolin structure

Caveolin adopts a hairpin structure as it inserts into the membrane, with both the N and C termini facing the cytosol (Fig. 3B). Mutagenesis of caveolin-1 has implicated a portion of caveolin that is involved in homo-oligomerization (Fig. 4)(71). This was observed using short expression constructs of caveolin-1 expressed in *E. coli*. These expressed proteins were assayed for the ability to float within a sucrose gradient. One construct expressing amino acids 61 to 101 was found to float at the same density as full-length caveolin-1. This region is termed the oligomerization domain (72). A second domain exists, termed the scaffolding domain, that functions to support or bind signaling molecules (53). The proof for this interaction has also come from in-vitro binding studies of a GST caveolin construct 61 to 101. The scaffolding domain extends from 81 to 101, despite the fact that the binding studies involved the 61 to 101 GST fusion construct. This delineation is made through sequence comparison of caveolin-1 with Rab GDI proteins (73). As shown in figure 5A, caveolin-2 and 3 also have regions, which are similar to these Rab GDI's. A schematic diagram of GDI function in cell signaling is included in appendix A.

Caveolin was originally characterized as one of the major phosphoproteins found in cells transformed with vSrc. At this point the 21 kDa phosphoprotein was termed virally induced phosphoprotein-21 (VIP-21) (61). It was later shown that VIP-21 shared complete sequence homology with a protein purified in a vesicular compartment of MDCK cells. At this point the name was changed to caveolin. Later the precise site of phosphorylation of caveolin was shown to be tyrosine 14 (74). It seems that the constitutive phosphorylation, which is seen in the vSrc-transformed state, is dissimilar

from native caveolin where it is typically unphosphorylated. In 3T3-L1 cells, caveolin-1 undergoes a rapid phosphorylation in a time-dependant fashion when stimulated by insulin (75). It seems that the insulin-dependent phosphorylation of caveolin-1 is not mediated by a kinase activity of the insulin receptor but rather by c-Src that is found to co-purify with caveolin-1 (76). C-Src has been shown to phosphorylate GST-caveolin-1 in vitro, and further in vitro peptide phosphorylation assays have indicated that tyrosine 14 is phosphorylatable by Src kinases. This phosphorylation of caveolin-1 on residue 14 means that only the α isoform of caveolin-1 could be phosphorylated (Fig. 4A) as the β isoform lacks the N terminal 35 A.A. (Fig. 3A).

Src interacts directly with the oligomerization domain (61 to 101) as shown by in-vitro binding studies using GST caveolin-1. The region of interaction is believed to be between A.A. 81 to since a GST protein stretching from 1 to 81 was incapable of binding to Src (77). This delineation was corroborated by inactivation of Src auto-phosphorylation by a peptide from the region 81 to 101. It is noteworthy, however, that the authors have at their disposal a GST caveolin construct from 81 to 101 but the binding of Src to this peptide was not shown (77). Peptides from caveolin-3 but not 2 have also been shown to inhibit auto-phosphorylation of Src in vitro (77). Using phage display techniques a degenerate peptide library was used to determine what patterns were found within proteins that recognized the scaffolding domain. Two patterns were elucidated ϕXϕXXXXϕ and ϕXXXXϕXXϕ where ϕ is an aromatic residue usually phenylalanine. These motifs are found in Gα proteins Src as well as eNOS (78).

Figure 5: The GDI homology and phosphorylation sites within caveolin

A. Comparison of caveolin-1 domain 91–101 with known GDI's. Red letters indicate homology between this domain and other known GDI proteins. Similar domains are also indicated for human caveolin-2 and mouse caveolin-3. B. Comparison of Caveolin-1 domain 9-14 to other known substrates of src. Homologous amino acids are indicated in red and * indicates conservation of amino acids between all caveolin-1 species cloned to date.

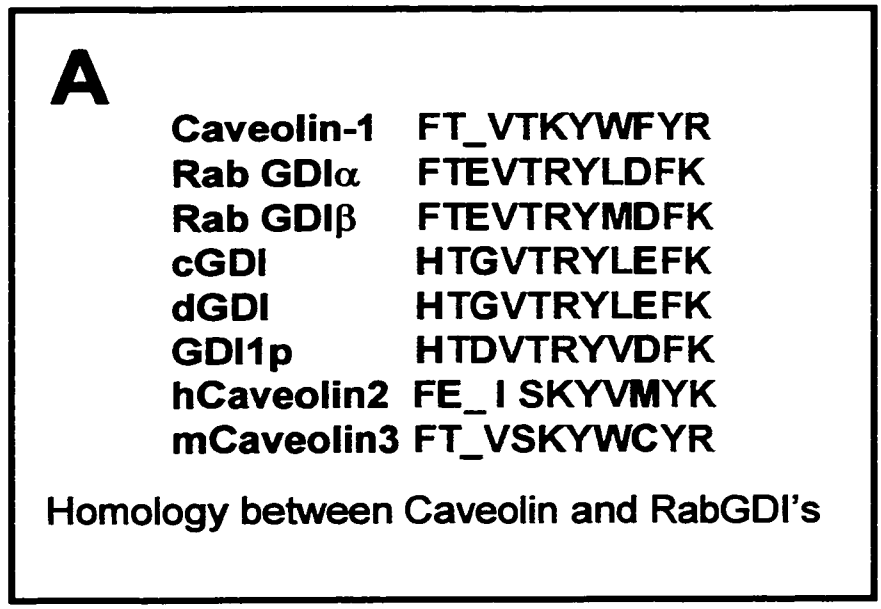
A
Caveolin-1 FT_VTKYWFYR
Rab GDIα FTEVTRYLDFK
Rab GDIβ FTEVTRYMDFK
cGDI HTGVTRYLEFK
dGDI HTGVTRYLEFK
GDI1p HTDVTRYVDFK
hCaveolin2 FE_I SKYVMYK
mCaveolin3 FT_VSKYWCYR
Homology between Caveolin and RabGDI's

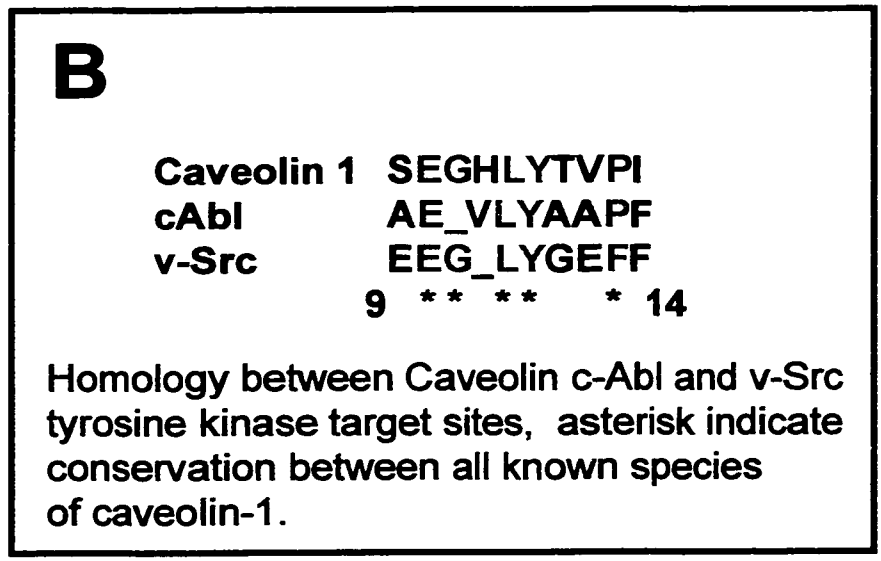
B
Caveolin 1 SEGHLYTVPI
cAbl AE_VLYAAPF
v-Src EEG_LYGEFF
9 ** ** * 14
Homology between Caveolin c-Abl and v-Src tyrosine kinase target sites, asterisk indicate conservation between all known species of caveolin-1.

1.43 Caveolar constituents

Caveolae are a specialized type of lipid raft (79). The term raft was introduced to describe a lateral organization of lipids within the plane of the membrane (80). This is in contrast to the *fluid mosaic model*, which predicts that lipids move freely throughout the plane of the membrane (81, 82). These rafts of glycosphingolipids and cholesterol seem to function as domains, which serve to order lipids and proteins for processes such as signaling or membrane transport (82). These domains have been defined by their insolubility to detergent and their floatation characteristics upon gradient ultracentrifugation. Lipid rafts are capable of sequestering specific classes of proteins, particularly glycosylphosphatidylinositol (GPI) linked proteins (83).

There is an ever-growing list of molecules which are classified as localizing within caveolae. This definition has led to a divide in the field, as some researchers feel that co-localization of proteins within the same fraction of a caveolae preparation constitutes co-localization. Other researchers believe that only direct interaction between caveolin and the protein of interest shows that they may co-localize in vivo. Coincident staining by imuno-fluorescence has been difficult, as methods to stain caveolin require cell permeabilization. With the advent of green fluorescence protein (GFP) and construction of GFP-caveolin this problem may rapidly disappear. Of many molecules which have been ascribed a caveolar distribution, eNOS remains one of the most relavant (84).

This enzyme is responsible for the conversion of L-arginine to nitric oxide (NO), which is a potent mediator of vascular tone. This enzyme has been intensely studied in both its physiological role and its intracellular function. ENOS expression has been

shown to correlate with cellular cholesterol levels, as HMG Co-A reductase inhibitors are known to increase its expression. Its role in caveolae has only recently been identified (85). Many of the modifications, namely acylation and phosphorylation which modulate caveolin, are also found in eNOS. It is now known that co-translational myristoylation of eNOS is required for its targeting to the plasma membrane. While eNOS is known to cycle on and off the plasma membrane, it is unlikely that myristoylation will regulate this trafficking, since myristoylation of proteins is typically irreversible (86).

ENOS localization on the plasma membrane is dynamically regulated by bradykinin. Bradykinin is a potent vasodilatory peptide that is degraded by angiotensin converting enzymes (ACE). If bradykinin is able to reach the cell surface, it may act through an increase in intracellular calcium, promoting the binding of calcium to calmodulin (87). Caveolin and calmodulin are thought to regulate the activation of eNOS through opposite effects, caveolin inhibiting and calmodulin stimulating its activity (88).

ENOS is one of the few proteins for which there is compelling evidence of caveolar localization. This protein differs in that there is co-immunoprecipitation data, which suggests caveolin-1 binds directly to eNOS. This interaction has been studied using antibodies against both caveolin-1 and eNOS (85). Further, caveolin-1 has been shown to have a functional role with eNOS in that the interaction with caveolin-1 inhibits eNOS activity (64). The localization of proteins to caveolae domains may require other criteria to define proteins as localized to caveolae. One potential approach may be the collection of ligand protected within caveolae (89). However the mechanical production of caveolae will continue to be criticized as homogenization may lead to the artifactual enrichment of a candidate ligand.

1.44 Caveolin function

Assigning a function to this cell surface microdomain has been one of the central difficulties since its discovery. There has been no shortage of postulates as to a potential function for this microdomain even the invention of a new term, *potocytosis* to describe a postulated endocytotic function (90). The reason for this has been difficulty in assigning molecules that interact specifically with this microdomain. Molecules such as transferrin were once thought to localize to the caveolae through receptor mediated interaction, but none of these has stood the test of time. Many researchers have resorted to intracellular ligands to probe the function of caveolae by attacking the intracellular tails of caveolin. In this way one of the most promising potential functions for caveolae is as a locale to concentrate and transduce cellular signals. If the protein eNOS is also considered, these locales can be thought of as a site not just to manage in-coming signals but as a way for the cell to communicate with the extracellular milieu.

One of the other functions now being actively investigated is the role for caveolae in the intracellular transport of cholesterol (81). As this site serves as an area where cellular cholesterol can be concentrated within easy reach of extracellular removal mechanisms, it may be a site where cholesterol may be removed from the cell through efflux. This role for caveolin in cholesterol efflux is strengthened by the fact that cholesterol sequesterants or caveolin disrupting agents such as progesterone or NEM disrupt not only caveolae but also cholesterol efflux (91). Some researchers have also shown a correlation between caveolin expression levels in various cell types, and efflux potential (92).

1.5 Rationale and Aims

The aim of this work is to probe the potential interaction between HDL and caveolae. Two primary questions will be addressed with two different model systems. The first aim is to elucidate the mechanism of HDL's movement from the lumen of the artery through the endothelium. There is some evidence that lipoproteins may traffic through endothelial cells via non-coated vesicles of a size that is consistent with caveolae (93). Further studies with other ligands such as albumin suggest that they may also traffic via a similar mechanism (94). It seems that this mechanism may require caveolin-1. This will be determined experimentally by first generating a cell culture model of the endothelium, then recombinant DNA techniques will be employed to disrupt caveolin levels in these cells. This model will then be used to ask whether HDL traffics through the endothelium via caveolin-1 mediated transport. The second aim is to understand how HDL removes cholesterol from cells. To probe the role of caveolin in cholesterol efflux stable cell lines expressing caveolin-1 will be generated. The first issue that will be addressed is whether there is a relationship between caveolin and HDL mediated efflux. Then the model will be used to explore and elucidate the mechanism whereby caveolin is involved in cholesterol efflux. This work will show for the first time that caveolin expression alters cholesterol cycling. This novel observation stems from an increase in cholesterol synthesis and cholesterol esterification in McA- RH7777 cells.

Chapter 2: Experimental Procedures

Materials

DNA restriction and modification enzymes were purchased from New England Biolabs. Oligonucleotides, primers and ultra pure agarose were obtained from Gibco BRL. All reagents for cell culture were purchased from Life Technologies Inc. The pCDNA3.1 mychisB- plasmid was obtained from Invitrogen, T7 sequencing kit was obtained from Pharmacia. Anti-caveolin polyclonal antibody was obtained from Transduction labs (cat #C13630). Monoclonal anti-myc was produced from hybridomas obtained from the ATCC (1-9E10.2). ^{125}I was obtained from NEN, ^{35}S dATP was obtained from NEN, [^{3}H]cholesterol and [^{3}H]acetate were obtained from ICN. Primers were purchased from Gibco BRL, Acrylamide was of analytical grade from BioRad. All other reagents were of analytical grade and obtained from standard commercial sources.

Methods

Preparation of Caveolin-1 Expression Plasmid – RNA was obtained from human adipose tissue (obtained by approval of the human ethics committee) and purified by the GTC-D purification method (95). RNA was reverse transcribed using an oligo dT primer and MMLV-RT, and the caveolin-1 cDNA was amplified by PCR using primers, 5' cggaattccatccagccacgg 3' and 5' cggggtaccaggtatacttctatcc 3' that contained EcoRI and XhoI restriction sites respectively (underlined). PCR was performed using preamplification (10 cycles at an annealing temperature of 45° C) and amplification periods (20 cycles at an annealing temperature of 60° C). The product was subcloned into pCMV5. The construct was sequenced and subcloned into pCDNA3.1 myc his –B. This

construct incorporates a c-terminal myc and a histidine tag adding only two amino acids (Ala and Leu) between the c-terminal Ile of caveolin-1 and the myc epitope.

Cell culture and Transfection – McA-RH7777 cells were grown to 60% confluency in DMEM containing 10% FBS and 10% Horse Serum. Stable transfection was performed as described perviously by the Ca^{2+} dispersion method (96). Stable transformants were selected in 500μM G418, clonaly expanded and screened for expression by western blot (97). HUVEC cells were cultured in 199 medium supplemented with 10% FBS. For experiments where HRP activity assays were performed, phenol free media was used. HUVEC cells were transfected using lipofectamine and were selected in 500μM G418, clonaly expanded and screened for expression by western blotting.

Immunofluorescence - Cells were cultured on poly-lysine coated cover-slip plastic dishes (MatTek Ashland, MA) for two days. After fixation with 4 % paraformaldehyde, cells were permeabilized with 0.1 mg/ml saponin in PBS for 10 min. A polyclonal anti-caveolin antibody was added for 30 min, then cells were washed with M1 media (150 mM NaCl, 5 mM KCl, 1 mM $CaCl_2$, 1 mM $MgCl_2$, 20 mM HEPES pH 7.4; supplemented with 2 mg/ml glucose) containing 2 mg/ml BSA (98). A rhodamine conjugated anti rabbit antibody was added for 30 min, and laser scanning confocal immunomicroscopy was performed using a BioRad MRC 1024 on an Olympus IX70 with a 60x NA 1.4 objective.

Cellular cholesterol efflux to HDL and Lp2A-I– Cells were maintained at 37 °C at 7 % CO_2 on 12-well Falcon dishes. HDL and Lp2A-I were prepared as described previously (99). Cells were incubated with 15 μCi of [^{3}H]cholesterol for 12 h in the presence of 2.5 μg/ml Sandoz 58-035 ACAT inhibitor. Cells were rinsed with PBS containing 2 mg/ml

fatty acid free BSA (PBS-BSA) and placed in serum free DMEM with 2 mg/ml BSA (DMEM-BSA), HDL or Lp2A-I was added at a concentration of 50 μg/ml. Efflux determinations were made as described previously (100).

HDL Binding and Association- Cells were plated onto 6-well Primaria culture dishes. HDL was iodinated by the MacFarlane method (101). Cells were rinsed with PBS-BSA, then incubated with radiolabeled HDL for 1 h in the presence or absence of 40-fold excess unlabelled HDL. Experiments were performed on ice for binding assays and at 37 °C for cell association assays. Cells were rinsed three times with PBS-BSA, and collected in 0.5 N NaOH for counting and protein determination (102).

Cell surface cholesterol influx and efflux - [^{3}H]cholesterol was dissolved in ethanol and dispersed in DMEM-BSA (< 0.1 % final ethanol concentration) and 5 μg/ml HDL. Labeling medium was incubated for 30 min at 37 °C as described previously (103). Cells were then incubated in the labeling medium for the indicated times, washed twice with PBS-BSA, and collected in 500 μl of 0.5 N NaOH for determination of protein concentration by Lowry or for scintillation counting (102). To verify that the label was associated with the cell surface and had not equilibrated with intracellular pools, cells were treated with 50 nM methyl-β–cyclodextrin after labeling. Cells were sedimented at 2,000 rpm for 5 min, washed twice with PBS-BSA, and lysed in 0.5 N NaOH for protein determination and scintillation counting. To evaluate desorption of cholesterol from the plasma membrane to HDL, cells were labeled with [^{3}H]cholesterol as above, washed, and incubated with 50 μg of HDL for 3 h. Medium was collected for scintillation counting, cells were rinsed twice with 1 ml of PBS-BSA and twice with 1 ml of PBS, and collected in 500 μl of 0.5 N NaOH for scintillation counting and protein determination.

[^{3}H]Acetate and [^{3}H]Mevalonate incorporation - Cells were seeded at $1.2x10^5$ cells/well onto 6-well Primaria dishes. Serum-free medium was added 2 h prior to the addition of 100 μCi/ml [^{3}H]acetate. Cells were then labeled for up to 2 h, rinsed with 1 ml of PBS-BSA, rinsed twice with 1 ml of PBS, and collected into 2 ml of 1:1 (v/v) methanol and H_2O. In some experiments, cells were labeled with 100 μCi/ml [^{3}H]acetate or 10 μCi/ml [^{3}H]mevalonate in DMEM-BSA for 90 min at 37 °C or 15 °C. Cells were then rinsed twice with 1 ml of PBS, and collected into 2 ml of 1:1 (v/v) methanol and H_2O. Lipids were extracted and resolved by TLC using a diethylether : hexane : acetic acid (105:40:1.5; v/v/v) solvent system. Radioactivity associated with triglyceride, free cholesterol, cholesteryl ester and phospholipid was quantified by scintillation counting.

Plasma membrane cholesterol conversion to Cholesterol Esters. – [^{3}H]cholesterol was dissolved in ethanol and dispersed in DMEM-BSA (< 0.1 % final ethanol concentration) containing 5 μg/ml HDL. Labeling media was incubated for 30 min at 37 °C as described previously (103). Cells were then incubated in the labeling medium for the indicated times, washed twice with PBS-BSA, and collected in 500 μl of 0.5 N NaOH for determination of protein concentration (102) or for scintillation counting. Cells were either continuously labeled or subjected to a 1 h pulse and 2 h chase (in the case of rate determination). Lipids were then extracted and analyzed by TLC as described above.

Chapter 3: Caveolin-1 Cloning and Transient Expression

3.1 Rationale for caveolin expression system

The goal of this project was to establish stable cell models to investigate the function of caveolin-1 on cholesterol efflux and to evaluate the possibility that caveolin-1 expression was capable of increasing transcytosis. In order to do this the cDNA of caveolin was required; therefore a cloning strategy was adopted. In addition, cell models had to be evaluated for the generation of stably expressing caveolin cell lines. Criteria for cell line selection included transfection efficiency, physiological relevance, endogenous caveolin levels, and potential for transcytosis study.

3.2 Caveolin-1 cloning

In order to begin the molecular assembly of cellular expression vectors for caveolin-1, a RT-PCR strategy was devised. The strategy involved first the isolation of RNA from a tissue in which caveolin-1 is highly expressed. Human adipose tissue was chosen as it contains high levels of human caveolin-1 and tissue was available from reduction mammoplasty procedures (obtained according to standards set by the human ethics research committee at the OCH). The RNA was isolated and purified as outlined in material and methods. This RNA was then used as a template for a reverse transcription reaction in which an oligo dT primer was used to exclusively amplify the mRNA in the preparation. The RNA dependent DNA polymerase reverse transcriptase used was MMLV. This reverse transcription yielded DNA-RNA hybrid strands, which were then used as a template for the final PCR.

The PCR reaction that was designed utilized the incorporation of unique restriction sites into the primers. This strategy conveyed two major advantages. First the

homology to the caveolin-1 template strand served to amplify only the target gene of interest from the mixed population of DNA/RNA duplex. Secondly with the incorporation of these unique restriction sites, the PCR product could be easily cloned into the expression vector pCMV5. The restriction sites chosen were EcoRI and KpnI for their ability to cleave near to the ends of a PCR fragment. The PCR reaction was performed in a two-part reaction designated the *Preamplification* and *Amplification* reactions. The preamplification cycles were intended to allow the PCR reaction to proceed with an optimal reaction temperature for the regions of the primers, which were homologous to the target gene. This preamplification was allowed to cycle ten times before the annealing temperature was increased to the optimal melting temperature of the entire primer. During the amplification cycle there should be templates, which have incorporated the unique restriction sites of the primers. The PCR product was then analyzed by agarose gel electrophoresis and a 600 N.T. product was produced as expected. This PCR product was then generated on a larger scale, using the original RNA/DNA hybrid as a template in 20 x 25 µl reaction tubes. The product of these reactions was then pooled and an aliquot was again used for verification of size on agarose gel.

The PCR product was then digested with EcoRI and KpnI to create 4 base pair overhangs, which allowed forced insertion into the pCMV5 vector. After the digestion of PCR product and vector with EcoRI and KpnI the DNA fragments were PAGE purified. These fragments were then used for ligation reactions and transformation into DH5α *E.coli*. Clones were then assayed by restriction digest for the presence of the caveolin-1 fragment. Further restriction digests were then performed to ensure that the

fragment was correct. This construct was termed pCAV1 for pCMV5 containing full-length caveolin-1. This construct was amplified using the CsCl centrifugation method (104), and sequenced using a T7 DNA polymerase kit with both sense and anti-sense primers. Sequencing revealed two single nucleotide differences between pCAV1 and the sequence for human caveolin-1 in Genbank (Z18951) (105). The first difference was that at NT 100 where a cytosine is substituted for a thymidine, this substitution changes amino acid 33 from alanine to valine. The second difference occurs at NT 433 where again a cytosine is substituted for a thymidine. In this case amino acid 144 changes from a threonine to an isoleucine. It is not possible to assign these differences solely to PCR error, as both of these differences are conservative substitutions and in fact the amino acid encoded at 144 in pCAV1 is found to be isoleucine in all other species of caveolin-1 cloned. Thus these differences are more likely to represent allelic variation due to different tissue sources than PCR error.

Figure 6: Sequencing of human caveolin-1

Caveolin-1 was sequenced with a T7 polymerase kit from Pharmacia with primers in both sense and antisense orientations. Two differences from the human caveolin-1 sequence in genebank were noted (Z18951). The first difference is a T-to-C substitution, which leads to an alanine to valine substitution at amino acid 33. The second difference is again a T-to-C substitution changing a threonine to isoleucine at amino acid 144. Both substitutions are conservative and probably represent allelic polymorphisms, the alteration at amino acid 144 encoding isolucine has been reported in all other caveolin-1 species cloned, except human.

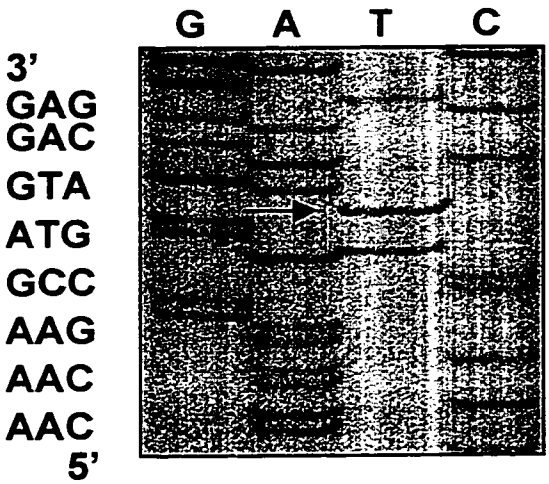
G A T C
3'
GAG
GAC
GTA
ATG
GCC
AAG
AAC
AAC
5'

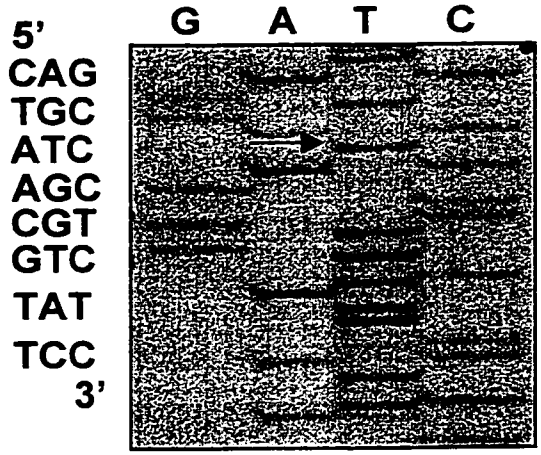
5'
G A T C
CAG
TGC
ATC
AGC
CGT
GTC
TAT
TCC
3'

3.3 Transient expression of pCav1

The pCMV5 based expression systems have been used for both stable and transient expression in cell culture model systems (106). Using this vector system various cell types were evaluated for their utility as a cell culture model for caveolin-1 expression. Cell types, which were evaluated, included Cos-7 cells, human foreskin fibroblasts, HUVEC cells, and McA-RH7777 rat hepatoma cells. Cells were transfected using lipofectamine, then collected 48 h post transfection into SDS-PAGE loading buffer. Samples were then resolved by 10% SDS-PAGE, transferred to nitrocellulose, and Western blotted using a polyclonal antibody against caveolin-1. In fibroblasts, transfection of pCAV1 did not lead to elevations in caveolin-1 expression (data not shown). These cells expressed endogenous caveolin-1, which reacted with the polyclonal anti caveolin-1 antibody. Also these cells exhibit characteristic 200 and 400 kDa homo-oligomers of caveolin-1 (107). The Cos-7 and McA-RH7777 cells proved to be more amenable to transfection. Cos–7 cells had only a very small amount of cross reacting endogenous caveolin-1 which was also seen as high molecular weight oligomers (Fig. 7). McA-RH7777 cells had no endogenous caveolin-1 and expressed recombinant caveolin-1 at high levels. In these cells homo-oligomers were also formed after transfection, which suggests that the caveolin-1 gene product may be functional (data not shown). Also in these cells there appears to be a doublet at 21kDa which supports correct α and β processing of caveolin-1 (data not shown). Transfection into the HUVEC cells proved very difficult as had been reported previously (108). However at high concentrations of pCav-1 DNA, expression levels were raised above background. These cells showed characteristic α and β bands as well as two larger molecular species which probably

represent acylation or phosphorylation states of caveolin-1. In addition to the transfection difficulties with these cells, there was difficulty in identifying the transfected gene product from the endogenous caveolin. In order to resolve this, an epitope tagging strategy was adopted.

3.4 Epitope tagging of caveolin-1

A myc epitope was selected for epitope tagging at the c-terminus of caveolin-1. Others had adopted a similar strategy for probing the interactions of ras with caveolin-1 (109). A di-glycine was also added as a swivel to allow the epitope more accessibility and to reduce interference of the epitope tag with protein folding and secondary structure. This tag was added to the caveolin-1 protein immediately proximal to the stop codon. This was done again using PCR cloning where the myc epitope was encoded by the 100 NT 3' primer. The PCR procedure included a pre-amplification phase, which was intended to overcome the low melting temperature of the annealing region of the myc primer. The fragment was confirmed by restriction digest and prepared on a large scale for sub cloning into pCMV5. The strategy also incorporated a BglII site 3' of the myc epitope and a KpnI site at the very 5' terminus of the PCR fragment (Fig. 10). The fragment was subcloned into pCMV5, EcoRI to KpnI. The addition of a BglII site allows removal of the caveolin-1 fragment from pCMV5 and leaves the myc tail in the vector. This created a myc-tailed vector for the expression of other proteins, if the insertion is EcoRI to BglII and in frame with the myc tail. The sequence encoding the myc epitope was also altered to introduce a BclI site within the myc tail to aid in rapid diagnostics of the myc tail. This alteration of the nucleotide sequence was done so as not to alter the primary amino acid sequence of the myc epitope. The construct was confirmed by

restriction diagnostics and sequencing, creating a C terminal myc tailed caveolin-1 in pCMV5. This construct was termed pCAV1myc (Fig. 10).

Transient transfection with this construct in Cos-7 cells led to a puzzling observation, while expression of a 21 kDa protein which cross-reacted with polyclonal anti-caveolin was achieved (Fig. 7B), it was not detectable with an anti myc antibody (Fig. 7A). This was puzzling as the 9E10 anti-myc antibody clearly reacted with positive controls (Fig. 7A), indicating it was able to recognize myc epitopes by western blot. Since pCAV1myc had been sequenced and was found to be correct, a defect in cloning was ruled out. Also the expression of a 24 kDa protein which was cross reactive with anti-caveolin antibodies suggested that the transgene was translated as caveolin-1 (Fig. 7B). Thus it was assumed that there must be a post-translational disruption of the myc epitope which was preventing its detection. The junction point of the pCAV1myc construct was reviewed and evidence was found for cleavage at a di-glycine motif by enzymes, such as the protease elastase or V-8 (110). With this consideration in mind a new strategy was adopted for the generation of a myc tagged caveolin-1.

A strategy was devised which would allow the insertion of caveolin–1 into a commercially available vector which incorporates a myc and his epitope into the protein of interest. The vector chosen was pCDNA3.1 myc his B-, from Invitrogen. The insert for this construct was again generated by PCR using EcoRI and XhoI primers. The PCR product was digested and inserted into the Invitrogen vector. Restriction digests showed that insertion was successful and the new caveolin construct was termed pCAV1mychis for human caveolin-1 in pCDNA3.1 myc his B- (Fig. 10). This construct was amplified by the CsCl method (104), and transfected into Cos-7 cells using the Ca^{2+} PO_4 method of

transfection. In this experiment pCAV1myc was also transfected. Detection by western blot yielded proteins of the expected size, which were reactive with anti-caveolin antibody but not with the anti-myc antibody (Fig. 7).

In an attempt to corroborate this finding, HepG2 cells were transfected with the pCAV1 myc his construct. In this experiment the protein expressed was cross reactive with the 9E10 anti myc antibody by western blot. With this apparent discrepancy in the detection of myc tailed caveolin by western blot, HUVEC cells were transfected with pCAV1 myc his to determine whether the myc epitope was detectable in these cells. HUVEC cells were transfected using the Ca^{2+} method and caveolin-1 was found to be expressed and also formed high molecular weight oligomers and a doublet at 28kDa (Fig 8). Taken together these results suggest that the sensitivity of the myc epitope to proteoylysis may vary between cell lines. In the HepG-2 and HUVEC cell lines the myc tailed proteins are expressed and detectable with 9E10 anti myc antibody by western blot.

Figure 7: Western blot of caveolin-1 transient expression in Cos-7 cells

Cells were transiently tranfected with caveolin-1 DNA by the Ca^{2+} method as described in materials and methods. Cell lysates were subjected to SDS PAGE and transferred to nitrocellulose. The membrane was probed with A. mono clonal anti-myc antibody or B. poly clonal anti-caveolin antibody and visualized by chemiluminescence.

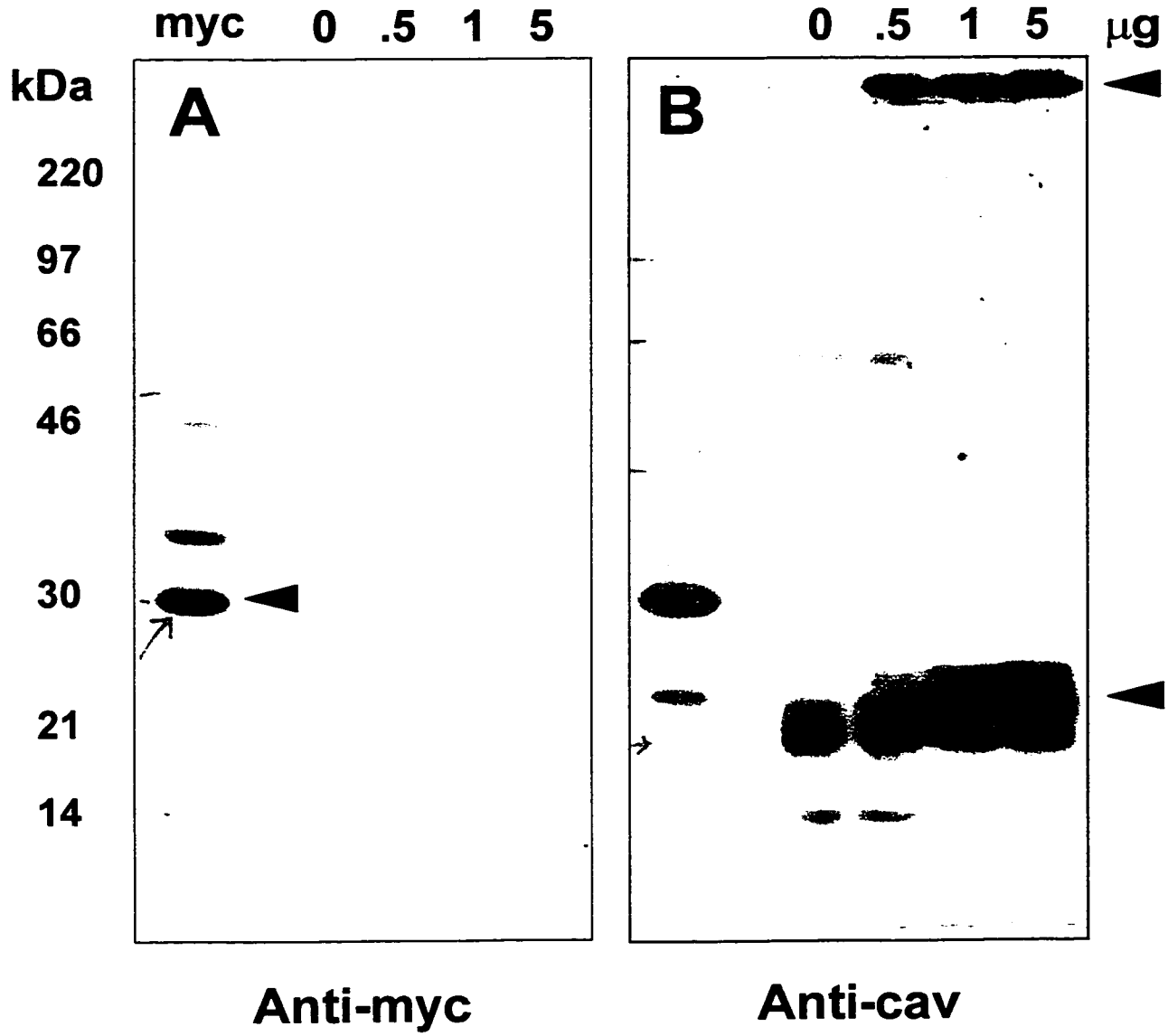
myc 0 .5 1 5
0 .5 1 5 µg
kDa
A
B
220
97
66
46
30
21
14
Anti-myc
Anti-cav

Figure 8: Transient expression of caveolin-1 in HUVEC cells

Western Blot of transient transfection of HUVEC cells, with pCav1 myc his. Cells were transfected with pCav1 myc his using the Ca^{2+} method described in Materials and Methods. Panel A shows western blot with 9E10 monoclonal anti myc antibody. Caveolin-1is shifted slightly higher as a result of the epitope tag. Panel B shows western blot with anti caveolin polyclonal antibody. Note large molecular mass bands which represent caveolin oligomers at MW > 200 kDa

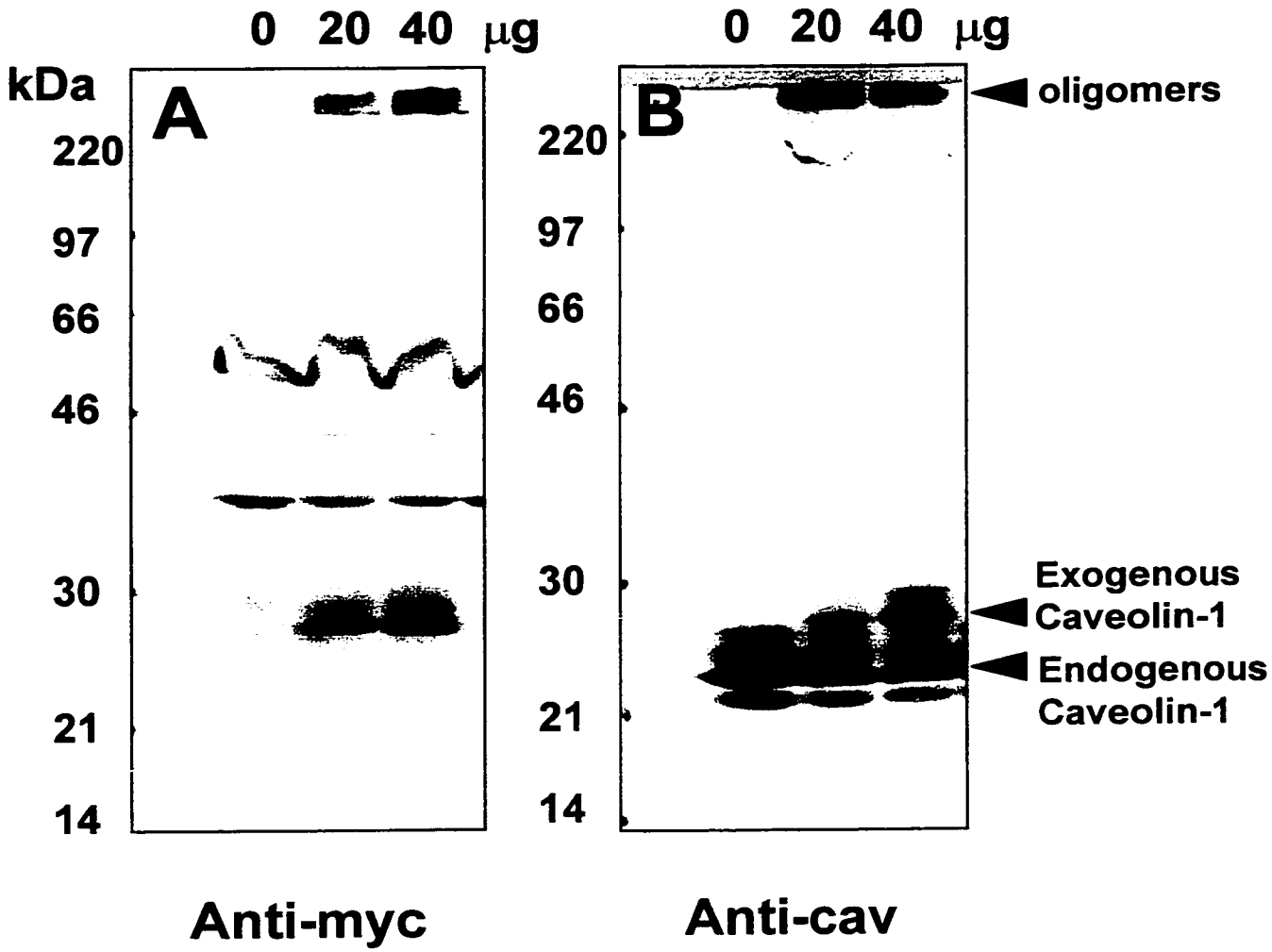
0 20 40 μg
kDa
A
220
97
66
46
30
21
14
Anti-myc
0 20 40 μg
B
220
97
66
46
30
21
14
oligomers
Exogenous Caveolin-1
Endogenous Caveolin-1
Anti-cav

3.5 Antisense Caveolin

In addition to caveolin-1 over-expression, an effective tool to probe caveolin-1's role in HUVEC membrane function would be the ability to decrease caveolin-1 protein levels. In order to do this a construct was designed that encode antisense caveolin-1. In this way the antisense mRNA would be transcribed and hybridize with endogenous sense transcripts of caveolin-1. These duplex strands of RNA are unstable and are degraded by RNAseH. This construct was designed by inverting the sense cDNA of caveolin-1 backwards and upside-down. Reversing the restriction sites with which the caveolin-1 fragment was inserted into pCMV5 did this. Engineering primers, which encoded KpnI at the 5' end and EcoRI at the 3' end, reversed the fragment's orientation and reading strand. This PCR product was generated and cloned into pCMV5, generating the construct pαCAV1, for antisense caveolin-1 in pCMV5 (Fig. 10). This construct was then used for transient transfection of HUVEC cells. With increasing concentration of pαCAV1 the endogenous caveolin-1 was reduced in HUVEC cells as detected by Western blot (Fig. 9A). This confirms that this antisense strategy can lead to a decrease in the endogenous protein of interest. The pαCAV1 construct can also be used for the generation of stable cell lines, making the generation of HUVEC cells with reduced caveolin-1 levels possible. This antisense construct was also used to generate an inducible antisense construct utilizing Invitrogen's pIND system (Fig. 10). This construct was generated by removal of antisense caveolin-1 from pαCAV1 and insertion into pIND KpnI to EcoRI. This inducible antisence construct in addition to an inducible sense caveolin-1 construct (Obtained from Charles Baum, University of Chicago) will be powerful new tools to investigate the function of caveolin-1 (Fig. 10).

Figure 9: Antisense caveolin-1 strategies

A. HUVEC cells were transiently transfected with antisense caveolin-1 using the lipofectamine. Cell lysates were normalized to cell protein and subjected to SDS-PAGE. The samples were western blotted with polyclonal anti caveolin antibody and subjected to chemilumenescence. B. Illustration of plasmid utilized for the construction of a ribozyme against caveolin-1. The ribozyme is driven by a U1 snRNA promoter and resistance is conferred by a Zeocin selection marker. C. Schematic diagram of caveolin-1 ribozyme RNA encoding 5' nuclear localization sequence and 3' stabilization element.

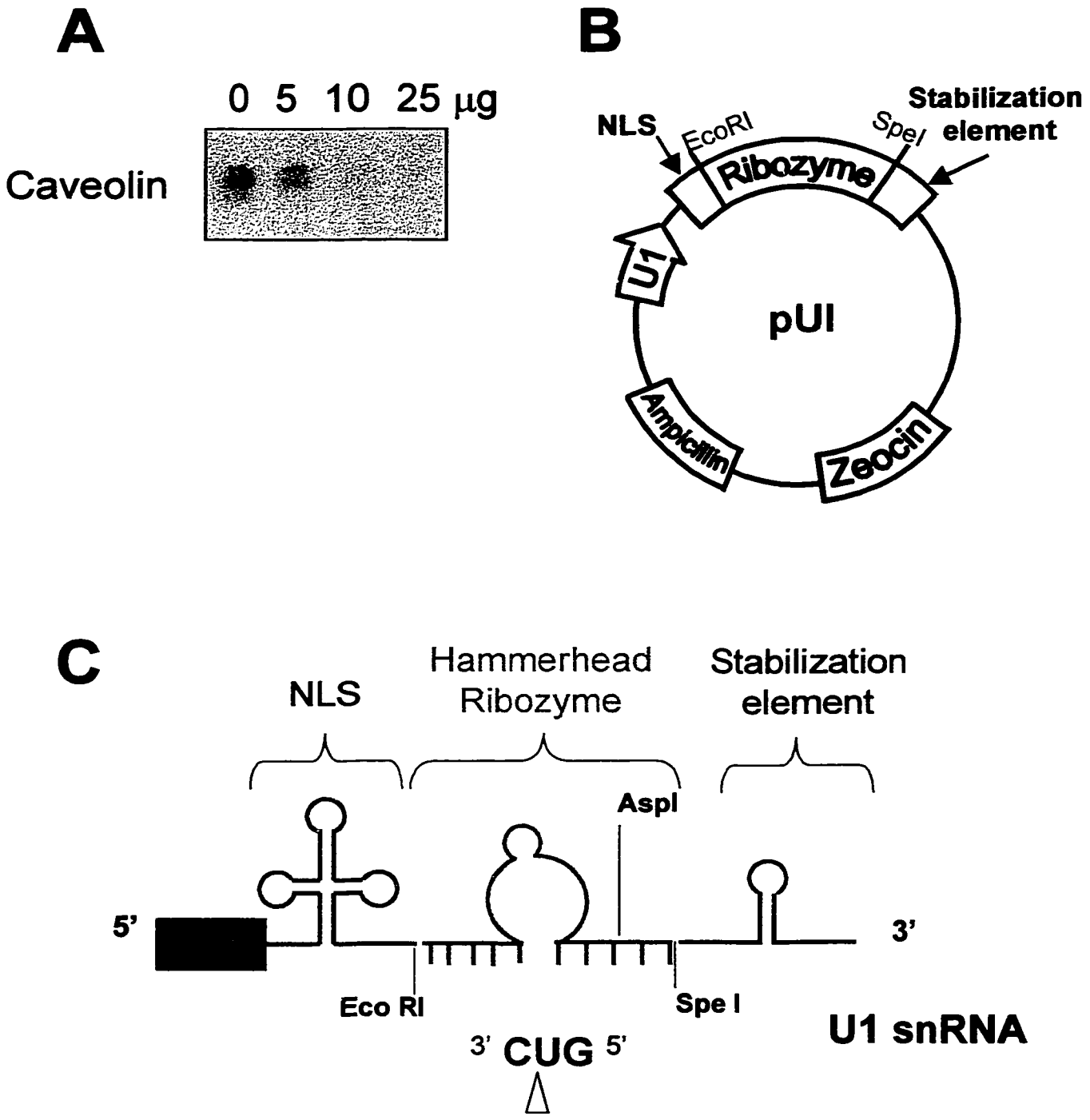
A
0 5 10 25 µg
Caveolin
B
NLS
EcoRI
SpeI
Stabilization element
Ribozyme
U1
pUI
Ampicillin
Zeocin
C
NLS
Hammerhead Ribozyme
Stabilization element
AspI
5'
3'
Eco RI
Spe I
3' CUG 5'
U1 snRNA

A second antisense construct was built using hammerhead ribozyme technology. Simply put, catalytic RNA can be generated such that it targets a particular region of mRNA with a target sequence that includes a $^{3'}GUC^{5'}$ sequence (Fig. 9C). After successful binding, cleavage of the target strand is made by the catalytic ribozyme, leading to degradation of the target RNA. To design a caveolin-1 ribozyme, caveolin-1 mRNA was modeled using RNAfold software (111) in an attempt to identify GUC sequences that were not contained in regions of secondary structure. As a result of the heavy computing power required to model the entire sequence, truncated sequences were modeled and secondary sequence that was conserved across overlapping constructs was assumed to be formed. Using this method a target site was identified outside regions of predicted secondary structure, and a hammerhead ribozyme was built with arms flanking the sequence at A.A. 53. This construct is diagrammed in figure 9C and at the time of writing this construct appears to be functional in cell culture.

All of the human caveolin-1 constructs that I have generated are shown below (Fig. 10). The first two constructs make use of the pCMV5 vector, which contains a powerful CMV promoter, which drives high levels of protein expression in eukaryotic systems. For the generation of stable cell lines these constructs require the co-transfection of a second plasmid encoding a neomycin selection marker. The third construct uses a pCDNA3.1-based vector, which also exploits the CMV promoter for eukaryotic expression. This plasmid also encodes a neomycin selection marker so that co-transfection for stable eukaryotic expression is not required. The inducible constructs employ a concatamer of E/GRE sites to promote the binding of an RXR heterodimeric nuclear receptor to the promoter region of these plasmids (appendix C).

Figure 10: Caveolin-1 expression vectors

Expression constructs for human caveolin-1 are diagrammed in blue. Antisense constructs for human caveolin-1 are diagrammed in red. Myc epitope tags are represented in red and his epitope tags in green. All plasmids utilize ampicillin resistance for prokariotic selection. Neomycin markers for eukariotic selection are denoted Neo. E/GRE concatamers are indicated by nested arrows.

pCav1

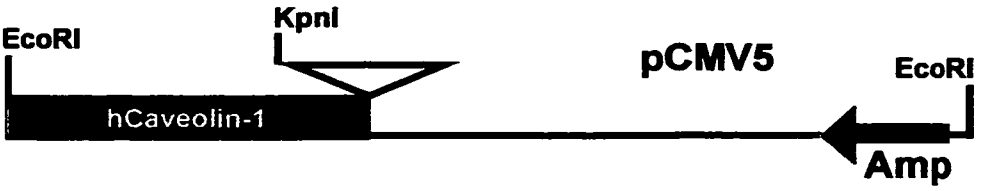

pCav1myc

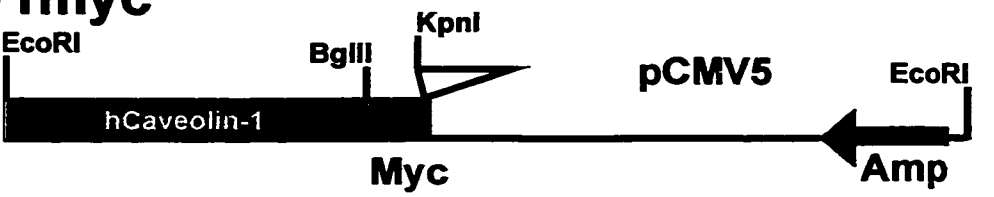

pCav1mychis

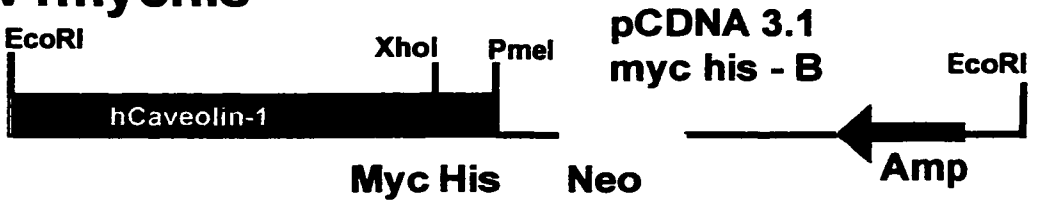

pαCav1

pαCav1 IND

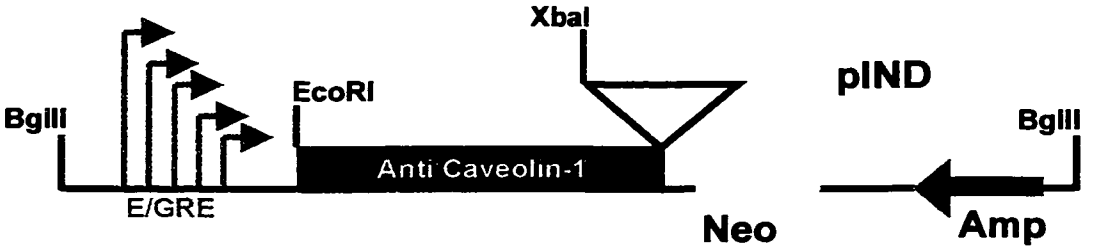

pCav1 IND

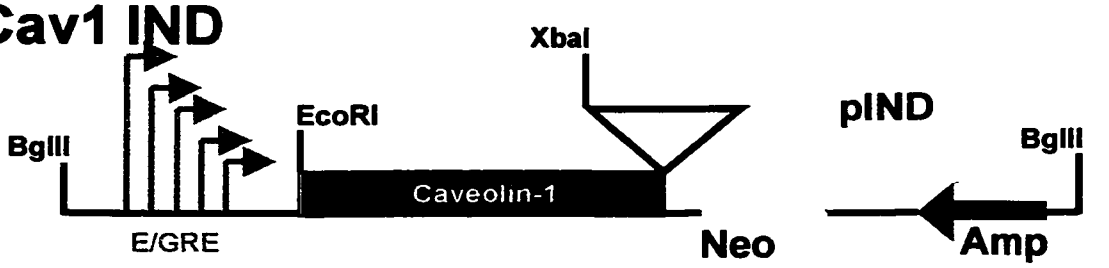

Chapter 4: Expression of Caveolin-1 in HUVEC Cells and the Development of a Transcytosis Model System

4.1 Rationale

Epithelial cells serve as a barrier to regulate the passage of macromolecules and ions between separated compartments (112). Epithelial cells achieve this by establishing tight junctions and zones of adherence (zonula adherens) which seal monolayers preventing the nonspecific paracellular transport of molecules. This allows regulated endocytosis and trans-cellular trafficking to control the movement of molecules from one side of an epithelial barrier to the other. Very little work has been preformed to explain how lipoproteins traverse the endothelium of the artery. There have been some provocative electron microscopy studies which have implicated caveolae in transcytosis of lipoproteins (113). Since the original electron microscopy data was presented there have been several attempts to evaluate transcytosis of lipoproteins in cell culture systems (114, 115). This work had been focused on transcytosis of LDL but had not established the role of caveolin-1 in the process.

In order to explore the potential transcytotic function of caveolin-1, an endothelial cell model was selected. The cell line that was chosen was the HUVEC ECV 304 immortal cell line (116). This cell line was a spontaneous transformant, which led to the production of this immortal clone. By exploiting the cobblestone morphology of the HUVEC cells, we sought to perform direct experiments to explore the movements of macromolecules across intact cell monolayers. With the exception of trancytotic studies of the IgA receptor trafficking, most other models rely on microscopic evidence for transcytosis (117). There are very few biochemical models of trancytosis in cell culture

(118, 119). Other approaches to investigate transcytosis include separation of binding, endocytosis and trafficking through different biochemical approaches (118). Utilizing the transwell system we sought to perturb transcytosis in the HUVEC cell system by over-expressing caveolin-1.

The Falcon transwell 3D cell culture system was chosen in this study for its utility as a biochemical method of exploring the transcytosis of macromolecules. 12 well Falcon dishes with transwell inserts were chosen, largely due to the prohibitive cost of each disposable insert. Each well was assembled under sterile conditions where transwell chambers had to be removed from packaging and properly seated in the well to prevent leakage. These inner chambers had a filter diameter of .8 cm and a pore size of 3 μm. Cells were cultured on the inner chamber of this transwell chamber as diagramed in figure 11. The filter can be coated with various matrix coatings to encourage improved cell growth and monolayer formation.

Figure 11: Transwell 3-D cell culture system

Schematic diagram of the Falcon 3D-cell culture system. Cells were cultured on the filter insert on the inner transwell chamber. Hydrostatic pressure was minimized by adding 1.5 ml of media to the apical chamber and 2.5 ml of media was placed in the outer chamber. TEER measurements were made with a Millicell-ERS cell culture Voltmeter. Platinum electrodes were placed as illustrated for TEER measurements without contacting the plastic with the probes.

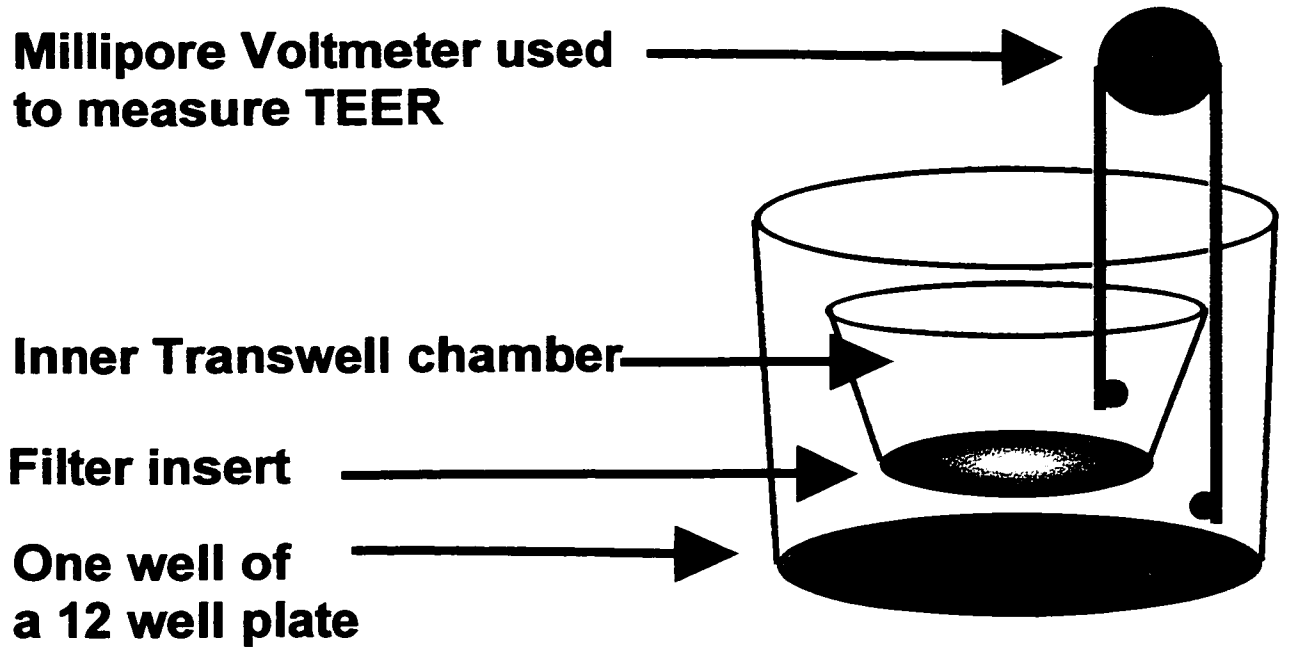
Millipore Voltmeter used
to measure TEER
Inner Transwell chamber
Filter insert
One well of
a 12 well plate

The formation of intact monolayers in this system can be evaluated by inserting probes into the upper and lower chamber of the well, and measuring the resistance across the monolayer. This measurement of TEER is used as a measure of monolayer integrity. The level of media in the upper and lower chamber was maintained at equal levels to minimize the potential effects of hydrostatic pressure. Once an intact monolayer has been established target ligands can be introduced into either the apical or basal compartment and their appearance in the opposite chamber can be monitored.

4.2 Generation of stable cell lines

In order to generate stable cell lines over-expressing human caveolin-1, the myc tailed vectors described in chapter two were employed. These two vectors employed either a single myc tail or a myc and poly histidine tail (Fig. 10). The first vector used was the myc and his tailed vector in pCDNA3.1. This vector employs a neomycin selection marker on the plasmid. This plasmid was transfected into HUVEC cells using the lipofectamine procedure outlined in Materials and Methods. After twenty-four hours cells were transferred to media that contained 500 μM G418 (a neomycin analogue). After 14 days the transfected cells displayed significant cell death and colonies developed from individual progenitors. These colonies were removed to 24-well dishes and expanded as individual clones. These clones were then screened by Western blot for their expression of myc tagged caveolin-1. Figure 12 shows some of the clones derived from the pCDNA based caveolin construct.

It was noticed that after ten passages some of these clones showed decreased expression of caveolin-1. In order to ensure long term stable expression of caveolin-1 cell lines were also generated using the pCMV5 based myc tagged caveolin. To generate

cell lines using this vector a co-transfection strategy was employed where the selection marker is introduced on a second vector, in this case pSV2neo. The cell line generated with this vector is shown in figure 12A (Clone C2) in comparison to the cell lines generated with the pCDNA3.1 construct (Clone 5-2 and 2-8). We speculate that the cell lines built with the pCDNA construct may exist as episomal plasmids in some of the cell colonies. The stable expression levels of the pCMV5 based construct may be explained by more efficient integration into the host genome. This speculation can be formally tested to establish whether these plasmids have different efficiencies of integration into the host genome.

Noteably in all clones overexpressing caveolin-1 there was no change in the expression level of eNOS (Fig. 12B). Caveolin-1 has been proposed to be a negative regulator of eNOS function through direct inhibitory binding. The inhibition of eNOS activity appears to correspond to an altered intracellular distribution when bound to caveolin-1. Utilizing these cell lines the effect on eNOS function and distribution could be easily addressed.

Figure 12: HUVEC stable cell lines

A. Western blot of stable HUVEC cell lines over expressing caveolin-1. Note endogenous α and β forms of caveolin. The pCavMyc vector was used to generate C-2 while the pCav1 myc his construct was used to generate clones 5-2 and 2-8. Note that the clones expressing myc and his tags are shifted slightly higher. Panel B shows expression levels of eNOS by western blot.

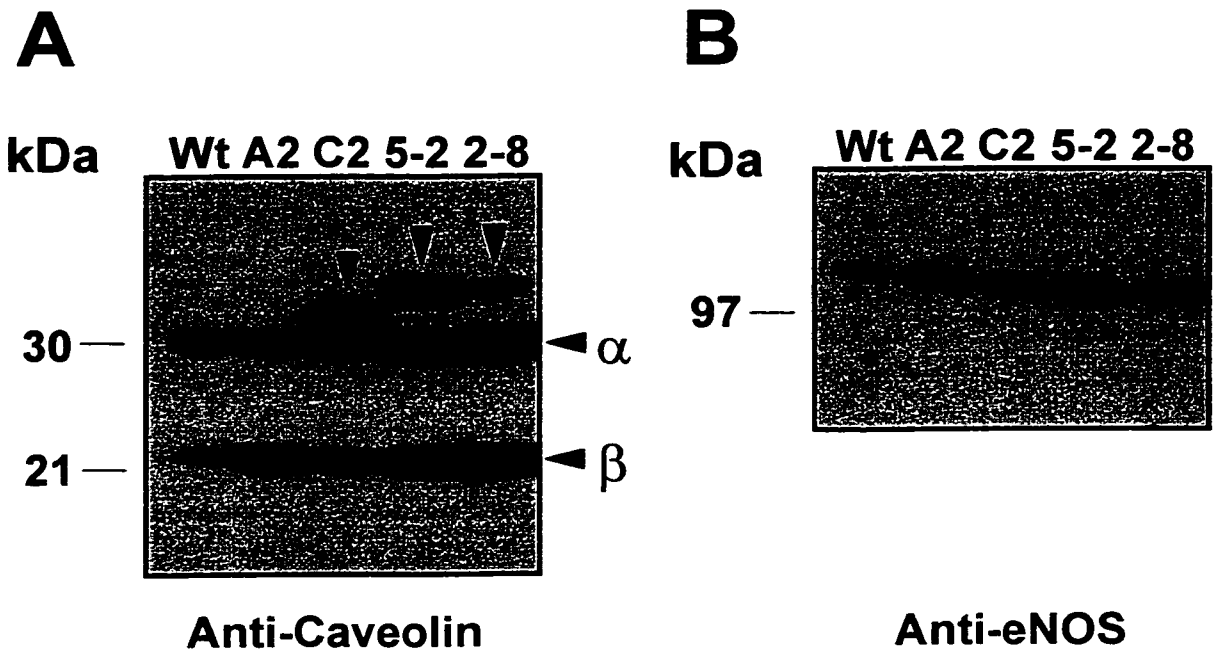
A
kDa
Wt A2 C2 5-2 2-8
30
21
α
β
Anti-Caveolin
B
kDa
Wt A2 C2 5-2 2-8
97
Anti-eNOS

4.3 Evaluation of growth matrices and membrane inserts

Using the Falcon 3D-cell culture system we determined optimal growth conditions for these endothelial cells. The importance of optimal growth conditions is underscored by the central weakness of this Transwell approach, which is the incomplete formation of an intact monolayer. Without the complete formation of an intact monolayer trafficking events can be attributed to paracellular trafficking, or leakage. In order to minimize the contribution of paracellular trafficking, the trans-epithelial resistance of the monolayers was measured. The trans-epithelial electrical resistance (TEER) is the resistance, which is established as the monolayer reaches confluence, through the formation of tight junctions. As intact monolayers form, the resistance measured across the insert increases. This measure of confluency and tight junction formation helps to ensure that the paracellular trafficking component is minimized.

Trans-epithelial measurements of resistance can reflect differences in confluency as the time required to establish TEER varies depending on the number of cells plated. HUVEC cells were plated at three different cell densities and their transepithelial resistance was measured over ten days. Cells plated at the lowest cell density (1×10^5 cells/ml) took the longest period of time to establish high TEER values. Higher cell densities of 1×10^7 cells/ml in a .8 cm diameter dish seemed to achieve high TEER values most rapidly. Using this cell density for further experiments, various matrix coatings were explored for their utility in improving monolayer integrity as evaluated by TEER.

Figure 13: HUVEC growth on coated inserts

Cells were maintained at 37 °C at 7 % CO_2 in M199 media containing 10 % FBS. Twelve well Falcon plates were used to suspend inserts with a pore size of 3 μM. A. Growth of wild type (wt) HUVEC cells and caveolin-1 expressing clone 3-8 on transwell inserts coated with collagen I. Cells were plated at 1 x 10^{-7} cells per well, TEER measurements were made using a Millicell ERS voltmeter. B. Establishment of TEER values on Matrigel (proprietary matrix by Becton Dikenson for endothelial cells)

A

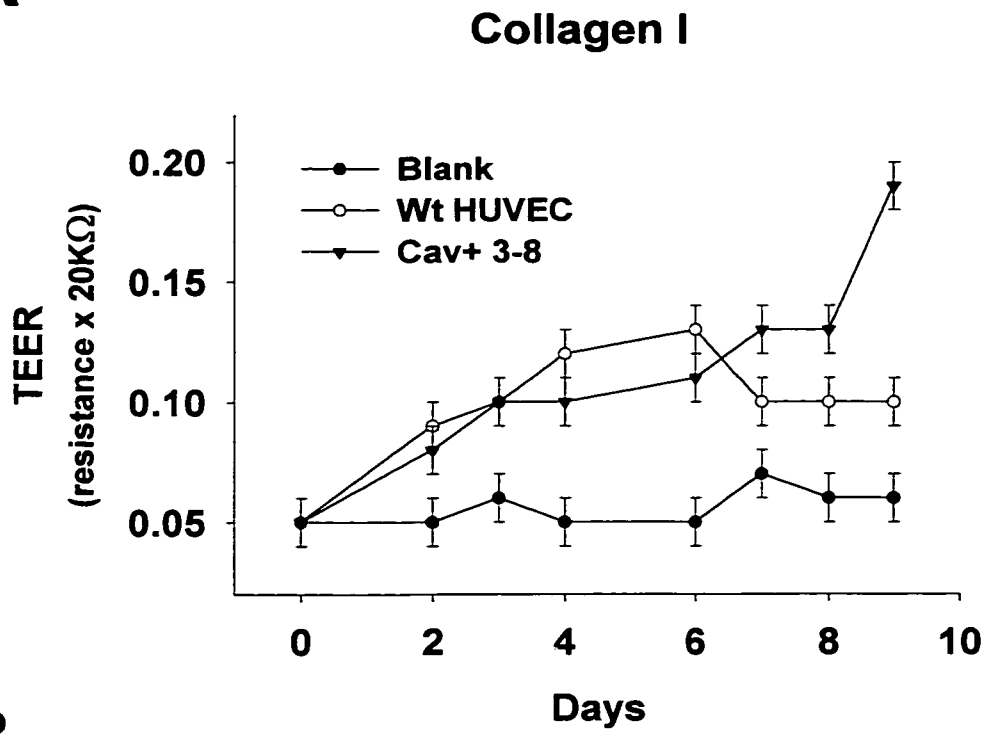
Collagen I
Blank
Wt HUVEC
Cav+ 3-8
TEER
(resistance x 20KΩ)
0.20
0.15
0.10
0.05
0
2
4
6
8
10
Days

B

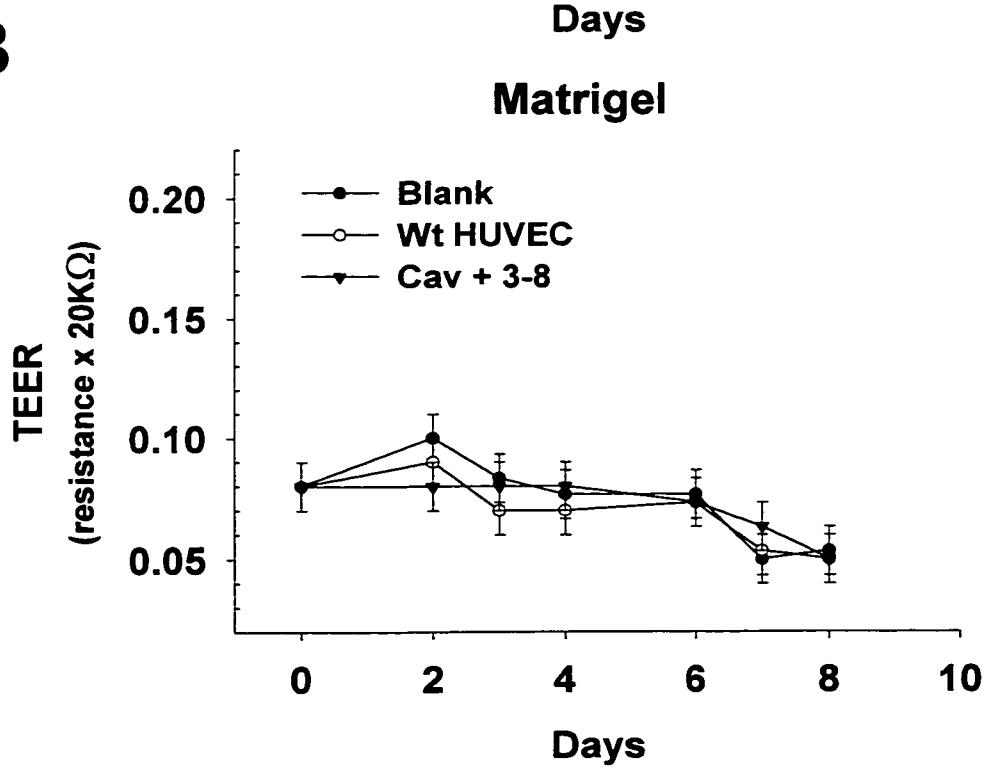
Matrigel
Blank
Wt HUVEC
Cav + 3-8
TEER
(resistance x 20KΩ)
0.20
0.15
0.10
0.05
0
2
4
6
8
10
Days

Cells were cultured on .8 cm, twelve well inserts, which were coated with various matrix coatings. The types of matrix that were investigated, included collagen I, collagen IV, fibronectin, laminin, and Matrigel (a proprietary preparation produced by Becton Dickinson). Experiments showed that not only matrix coating and cell confluency can effect TEER values but also individual clones seem to have different abilities for achieving high TEER values (Fig. 13). For example clone 5-2 which showed lower TEER values in cell density experiments still showed TEER values which were 30×10^{-4} Ohms lower than parental or caveolin-1 expressing clone 2-8. This impaired ability to maintain high TEER was also seen on all matrices tested for this clone (2-8). Clone 3-8 and parental HUVEC cells showed increased TEER values when cultured on plates coated with fibronectin and collagen I (Fig. 13). This data suggests that utilization of filters which have matrix proteins coated on them encourage cell growth, which leads to higher TEER. The largest increase in TEER was seen utilizing inserts coated with collagen I and fibronectin. The ability of a given clone to establish high TEER seems to vary, and the inability to establish high TEER values can be improved by coating the filter inserts with matrix proteins.

4.4 Development of non isotopic assay for transcytosis

In order to evaluate the integrity of the cell monolayers a biochemical evaluation of membrane integrity was developed. Horse Radish Peroxidase (HRP) was chosen as a non radioactive marker, which is not actively transported across HUVEC monolayers. This marker conveys a number of advantages, first its small size should allow the detection of paracellular trafficking in the monolayer of cells. Secondly it is amenable to the development of very sensitive colorometric assays, but can also be tracked by

radioisotopic methods such as ^{125}I labeling. Most significantly this assay can be used as an internal control in radio-isotopic assays of other ligands.

For this work HRP was added to the upper or lower chamber of a transwell dish. After the course of the experiment the media from the opposite chamber was collected and assayed for the presence of HRP. The HRP was detected by a colorometric reaction in which HRP acts on the substrate o-Dianasiadine to cause a pink color change which is detectable at 450 nm. To assay the appearance of HRP in the opposite chamber of a transwell dish a micro assay was developed where a 50 µl sample of media could be evaluated for the presence of HRP through this colorometric detection method. This system which was developed was very robust and sensitive; samples as small as 5 µl of media could be assayed. Concentrations of HRP as low as .015 µg/ml could be detected, and the reaction was linear over two orders of magnitude (maximum of 5 µg/ml). Quantities of HRP lying outside this range could be determined using serial dilutions. This methodology allowed evaluation of HRP trafficking at the same time that a second radiolabelled protein was assayed.

4.5 Comparison of HRP and albumin transcytosis

Albumin is a protein that is thought to traffic across endothelial cells via caveolae mediated vesicular transcytosis (120). This protein was selected as a convenient marker to evaluate trafficking across HUVEC monolayers. Cells were seeded onto transwell filters and allowed to reach confluency as evaluated by a TEER greater than 0.1 x 20kΩ. ^{125}I-albumin and HRP (1 mg/ml) were added to the upper chamber of the transwell compartment and their appearance in the lower chamber was tracked with respect to time. The trafficking of HRP and albumin were evaluated in wild type and caveolin-1

over-expressing HUVEC cells. The transport of albumin, which has been shown in microscopy studies to traffic in caveolae, was not increased in this model where caveolin-1 was over-expressed. The appearance of HRP in the opposite chamber was not different between caveolin-1 expressing and parental cells. Further experiments suggested that caveolin over-expression was not sufficient to increase trafficking of albumin in this model. To better compare the trafficking of albumin and HRP in this model equimolar concentrations of the two ligands were added to either the top or bottom of the transwell chamber and their appearance in the opposite chamber was monitored. Both of these ligands were labeled with ^{125}I to improve inter-comparability. This experiment showed that trafficking of these ligands in three hours was less than 3 % of the initial 20 μg/ml that was introduced. Also the transport of albumin was actually less than that of HRP when the samples were added at equal concentrations.

	Top to Bottom	*Bottom to Top*
HRP	2.7 +/- 0.1%	1.6 +/- 0.6%
Albumin	0.8 +/- 0.2%	0.4 +/- 0.01%

Table 1
The appearance of ligands in opposite chambers of a wild type culture of HUVEC cells. Values are expressed as a molar percentage of ligand appearing in the opposite well after a 3 h incubation.

The previous work on transport of albumin, used lung epithelium by microscopic methodologies (121). This model employs a different cell type, which may not interact with albumin in the same manner. It is also difficult to say whether the appearance in the opposite chamber is a result of trafficking or leakage. Methods to evaluate intra-cellular trafficking usually involve the use of energy poisons or reduced temperature both of which cause loss of TEER in other endothelial model systems.

Further investigation of this system was continued with cell line C2, which showed higher caveolin-1 expression than 2-8 or 5-2, which were used, in the previous experiments (Fig. 12). This cell line also was able to maintain high TEER values under the experimental conditions used. Additional ligands, which were used to probe this model included, HDL, inulin and dextran. Inulin and dextran were used to try to dissect intracellular movement from paracellular movement. Dextran is a very large branched polysaccharide (> 500 kDa) while inulin is a smaller polysaccharide purified from dahlia tubers (~5 kDa). These two markers served as markers of paracellular and transcellular transport respectively. In all of the experiments performed the transport of specific ligand was equivalent to the transport of these two markers. This suggests that studies utilizing this HUVEC cell model in this culture system display biochemical characteristics of leakiness. Any difference in transcytosis imparted by the over expression of caveolin-1 cannot be detected, as the background contribution of apparent paracellular trafficking is too great. Caveolin-1 knockout constructs are diagramed in figure 10, which will address whether caveolin-1 is involved in transcytosis.

Figure 14: Transcytosis of HDL is independent of cav-1 over-expression

Cells were plated at $1x10^{-7}$ cell per well onto 12 well falcon transwell inserts. Cells were cultured to confluence as determined by TEER >.1 kΩ. Equimolar ^{125}I-HDL concentrations were added to the apical and basal Transwell cambers. HUVEC cells denoted A-2 are mock transfected and C-2 are caveolin-1 over-expressing cells. A. ^{125}I-HDL which has moved from the upper chamber into the lower chamber in 1hr. B. ^{125}I-HDL which has moved from the lower chamber into the upper chamber in 1hr. C. [^{3}H]Dextran transported from the basal chamber appearing in the apical chamber after 1h D. [^{3}H]Inulin transported to the apical chamber from the basal chamber after 1 h In all cases the difference in transport rates of each ligand was the same (70 % when A2 and C2 are compared.)

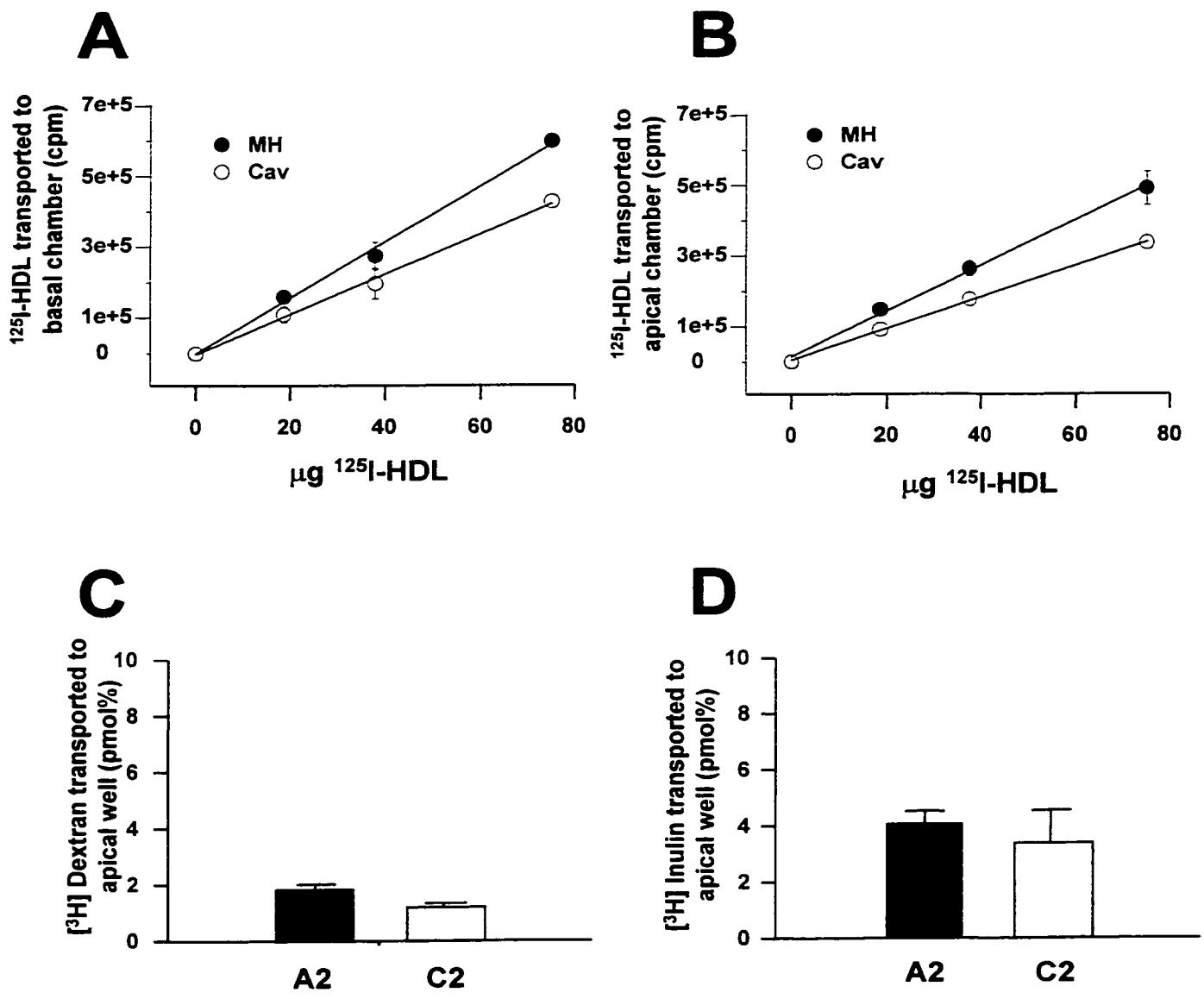
A
B
C
D
MH
Cav
7e+5
5e+5
3e+5
1e+5
0
20
40
60
80
μg 125I-HDL
125I-HDL transported to basal chamber (cpm)
125I-HDL transported to apical chamber (cpm)
[3H] Dextran transported to apical well (pmol%)
[3H] Inulin transported to apical well (pmol%)
10
8
6
4
2
A2
C2

4.6 HDL association with caveolin-1 over-expressing HUVEC cells

If caveolin-1 expression alters the interaction of HDL with cells, this may be detectable at the cell membrane. To investigate the interaction of HDL at the cell surface, binding studies were performed. Experiments were performed in 6-well dishes looking at the properties of HDL interaction with the cell surface. These cells work very well for these types of surface interaction assays as they can withstand rigorous washing that the McA-RH7777 cells can not. These studies revealed that at 0 °C there is no difference in the binding of HDL to the surface of these cells. However it was found that if the experiment was performed at 37 °C there was an increase in the ^{125}I-HDL associated with the caveolin-1 expressing cell line (Fig. 15).

Other researchers have used cell association studies (37 °C) to probe the interaction of HDL with the cell surface (122). It has previously been shown that the cells under these conditions do not degrade HDL. Using this system we also found that this increased association was seen only at high HDL concentrations. This suggests that the alteration in these cells have led to an increase in a low affinity, high capacity site of interaction at the cell surface. We were also able to show that the increase in cell association in the caveolin-1 expressing cells was specific (Fig. 16). Incubating the radiolabelled ligand in the presence of a 40-fold excess of cold ligand competes 50 % of ^{125}I-HDL binding. Under these conditions we see that the non-specific association of HDL to both cell types is equal (Fig. 15). Thus we can conclude that the difference in cell association due to caveolin-1 over expression is specific.

Figure 15: ^{125}I-HDL binding and association in cav-1 expressing HUVEC cells

Cells were grown to confluency in 6-well falcon dishes in M199 media supplemented with 10 % FBS. Cells were rinsed twice with PBS-BSA and ^{125}I-HDL and competitor HDL was added (forty-fold excess). Cells were incubated for 1 h at 4 °C or 37 °C before being rinsed three times with PBS and collected into .5 ml of .5 N NaOH for scintillation counting and protein determination. A. Binding (4 °C) of ^{125}I-HDL to mock transfected HUVEC cells. B. Binding of ^{125}I-HDL to Caveolin-1 transfected HUVEC cell line C-2. C. Association (37 °C) of ^{125}I-HDL to mock transfected HUVEC cells. D. Association of ^{125}I-HDL to Caveolin-1 transfected HUVEC cell line C-2.

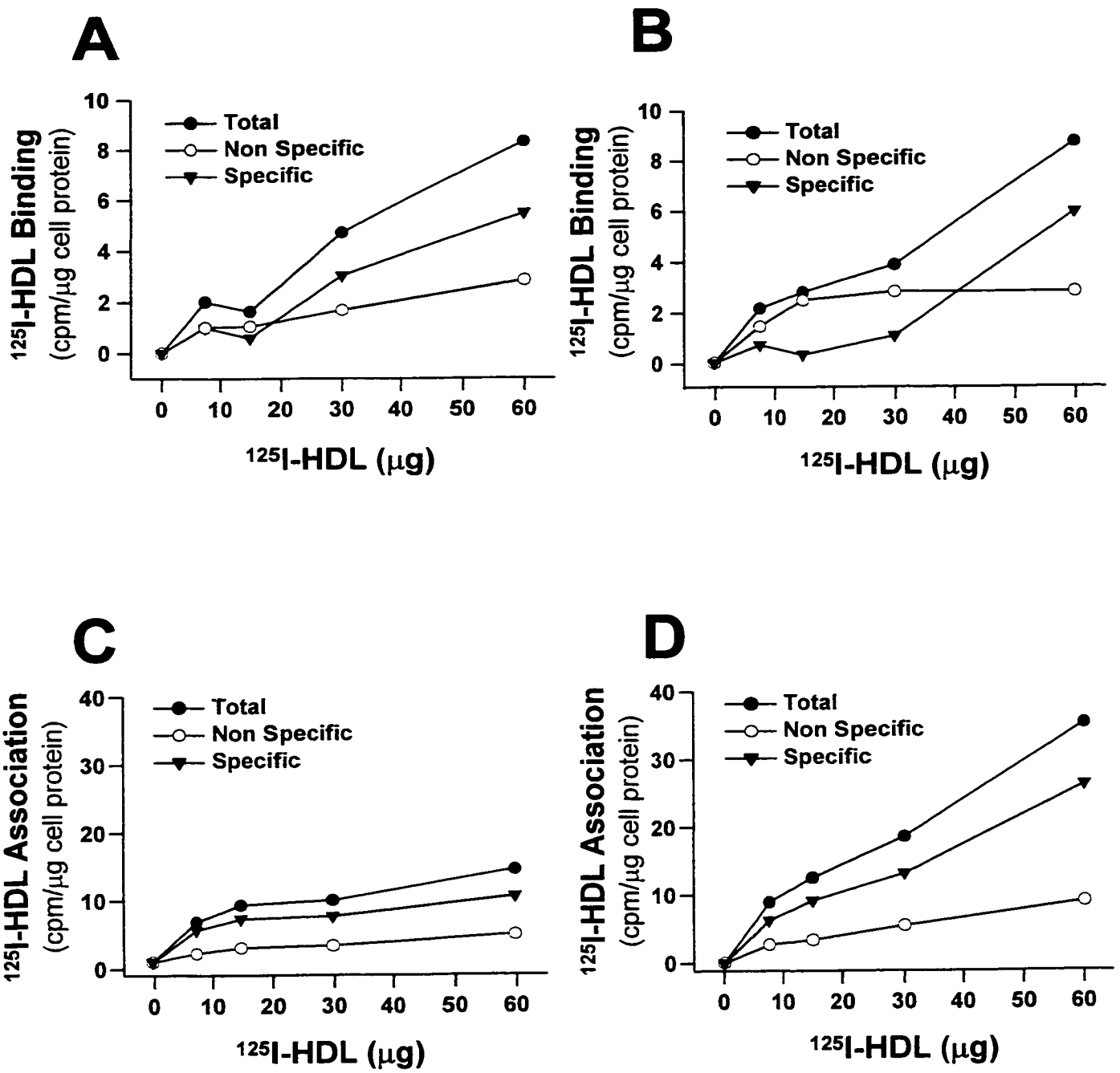
A
B
C
D
Total
Non Specific
Specific
125I-HDL Binding
(cpm/μg cell protein)
125I-HDL Association
(cpm/μg cell protein)
125I-HDL (μg)
0
10
20
30
40
50
60
2
4
6
8

Figure 16: ^{125}I-HDL association is increased with cav-1 expression in HUVEC cells

HUVEC cells were cultured in M199 media supplemented with 10 % FBS to confluency in 6-well Falcon dishes. HUVEC cells denoted A-2 are mock transfected and C-2 are caveolin-1 over-expressing cells. A. Cells were rinsed twice with PBS-BSA before 60 μg of ^{125}I-HDL was added to each of the wells. In the case of non-specific association 40-fold excess HDL was added as a competitor. Specific association is determined by subtracting total binding from non-specific binding (n=5). B. Cells were rinsed twice with PBS-BSA before 60 μg of ^{125}I-HDL was added to each of the wells in the presence of increasing concentration of cold HDL competitor. Radioactivity is expressed as a percentage of total association in the absence of cold competitor.

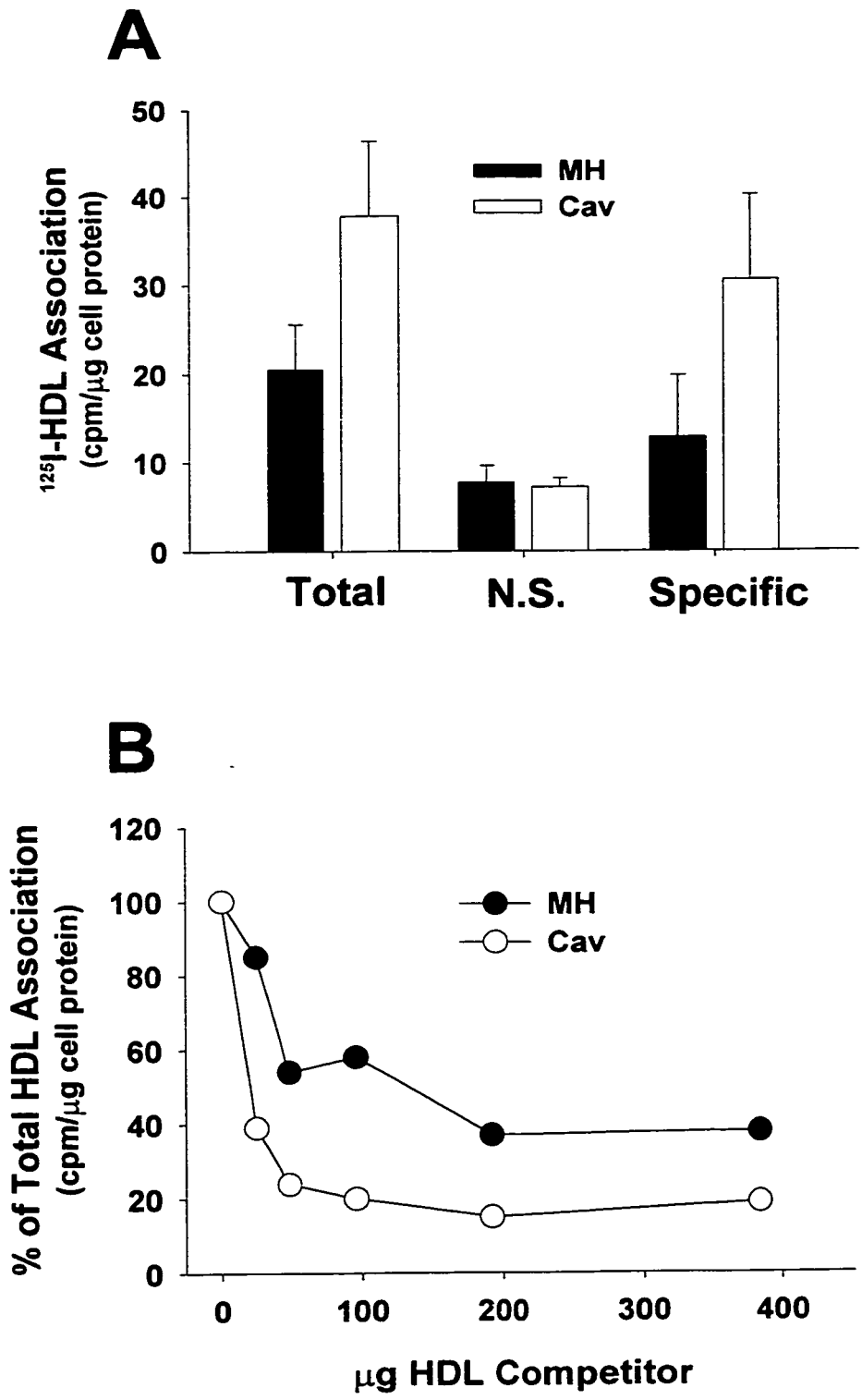
A
^{125}I-HDL Association
(cpm/μg cell protein)
50
40
30
20
10
0
MH
Cav
Total
N.S.
Specific
B
% of Total HDL Association
(cpm/μg cell protein)
120
100
80
60
40
20
0
MH
Cav
0
100
200
300
400
μg HDL Competitor

Chapter 5: Caveolin-1 Expression and Function in McA-RH7777 cells

5.1 Rationale

Caveolae at the cell surface have been implicated as potential sites for the efflux of cellular cholesterol to HDL (43, 49, 123, 124). The co-localization of the HDL binding protein SR-B1 to caveolae has lead to the notion that caveolae may be an active site not only for selective uptake of lipids (49) but also for diffusional cholesterol efflux (46). Caveolae transport has also been recently linked to defects in ABC1, the causative defect in Tangier's disease (125). Transient expression of caveolin-1 in fibroblasts modestly increased cholesterol efflux (126) and antisense methodologies have also implicated caveolin-1 in HDL mediated cholesterol efflux, however the mechanism has not been defined (127). Cholesterol within caveolae is packaged in a highly ordered manner, and efflux may require cholesterol to be localized to more fluid, efflux competent, regions of the plasma membrane (128). While caveolae have been proposed to mediate the efflux of cellular cholesterol (124), a number of cells including hepatoma cells have little or no caveolin-1 (16) but possess high efflux potentials (17). The formal possibility exists that the role of caveolae in cholesterol efflux is not to act as the site for cholesterol efflux, but rather to move cholesterol to the plasma membrane where it may diffuse to efflux competent regions of the plasma membrane.

In this study, we have selected the McA-RH7777 rat hepatoma cell line as a model to study the contribution of caveolin-1 to cholesterol efflux. Hepatoma cells have been reported to produce no caveolin-1 mRNA (129) and have also been shown to demonstrate robust cholesterol efflux properties (37). While there have been reports of

caveolae in primary hepatic tissue (130), caveolin-1 appears to be absent in hepatoma cell lines (92). Thus the McAH7777 cells constituted a good model for the generation of a panel of stably transfected cells expressing a wide range of caveolin-1. We show here that these cells reveal proportionality between caveolin-1 expression level and long term diffusional efflux to HDL and Lp2A-I. This increase in specific efflux is not apparent during initial rates of efflux, but only after extended efflux periods. Using this model, we also analyze the contribution of caveolin-1 to the transport of exogenously introduced cholesterol and the effect of caveolin-1 expression on cholesterol synthesis.

5.2 Generation and Expression of Human Caveolin-1

To ensure that the construct would produce recombinant caveolin-1 we performed transient transfection in HepG2 cells. Immunoblots with a polyclonal anti-caveolin antibody (Transduction labs C136130) revealed no endogenous caveolin in this cell model. The construct produced a recombinant protein of the correct molecular weight which was immunoreactive to both polyclonal anti-caveolin and monoclonal anti-myc antibodies (Fig. 17B). This construct was then used to generate a spectrum of stable caveolin-1 expressing cell lines in the rat hepatoma cell model McA-RH7777 (Fig. 17C).

5.3 Characterization of caveolin-1 localization and function

Stable cell lines were examined by confocal microscopy to determine the intracellular distribution of recombinant caveolin-1. Recent studies have shown that monoclonal antibodies against the N-terminus of caveolin-1 preferentially stain plasma membrane caveolin-1, while C-terminal monoclonal antibodies preferentially stain Golgi caveolin-1 (131). To avoid such preferential staining of PM or Golgi pools of caveolin-1, we utilized a polyclonal anti-caveolin antibody in an attempt to reveal the steady state

distribution of caveolin-1 within these cells. Strong caveolin-1 staining was seen in a peri-nuclear region of the cells, which probably represents the Golgi apparatus. Punctate membrane staining was also seen along the plasma membrane of these cells, and the its intensity correlates with caveolin-1 expression levels (Fig. 18).

One of the prototypical characteristics of caveolin is its insolubility in non-ionic detergents. To ensure that the recombinant caveolin-1 displayed this property in hepatoma cells, detergent insoluble membrane fractions (DIM) were prepared. These membrane preparations were normalized to protein and equivalent protein concentrations were subjected to SDS-PAGE and Western blotting (Fig. 19). These DIM fractions were enriched approximately four fold in caveolin-1 relative to total cell extracts. The caveolin-1 found within these extracts was proportional to the expression level in the different stable clones. By Western blot analysis of whole cell lysates, caveolin-1 expressing cells displayed high molecular mass complexes at 200, 400 and 600 kDa which were disrupted by alkylation and, probably represented homo-oligomers (data not shown).

Figure 17: Cloning of human caveolin-1 and expression in hepatocytes

A, schematic diagram of caveolin-1 expression vector containing C-terminal myc and his epitope tags. CMV, cytomegalovirus promoter, BGH PA, bovine growth hormone poly-adenylation sequence. Insertion of the 3' XhoI site encodes Ala, Leu after the C-terminal Ile of caveolin-1. B, transient expression of caveolin-1 in HepG2 cells that were transfected with increasing concentrations of caveoin-1 cDNA. Cell lysates were collected 48 h post transfection resolved by SDS-PAGE and transferred to nitrocellulose. Caveolin-1 was detected by anti-caveolin (Transduction labs C13630) or anti-myc (9E10) antibody and visualized by chemiluminescence (ECL). C, immunoblot analysis of Caveolin-1 expressed in stably transfected McA-RH7777 cells.

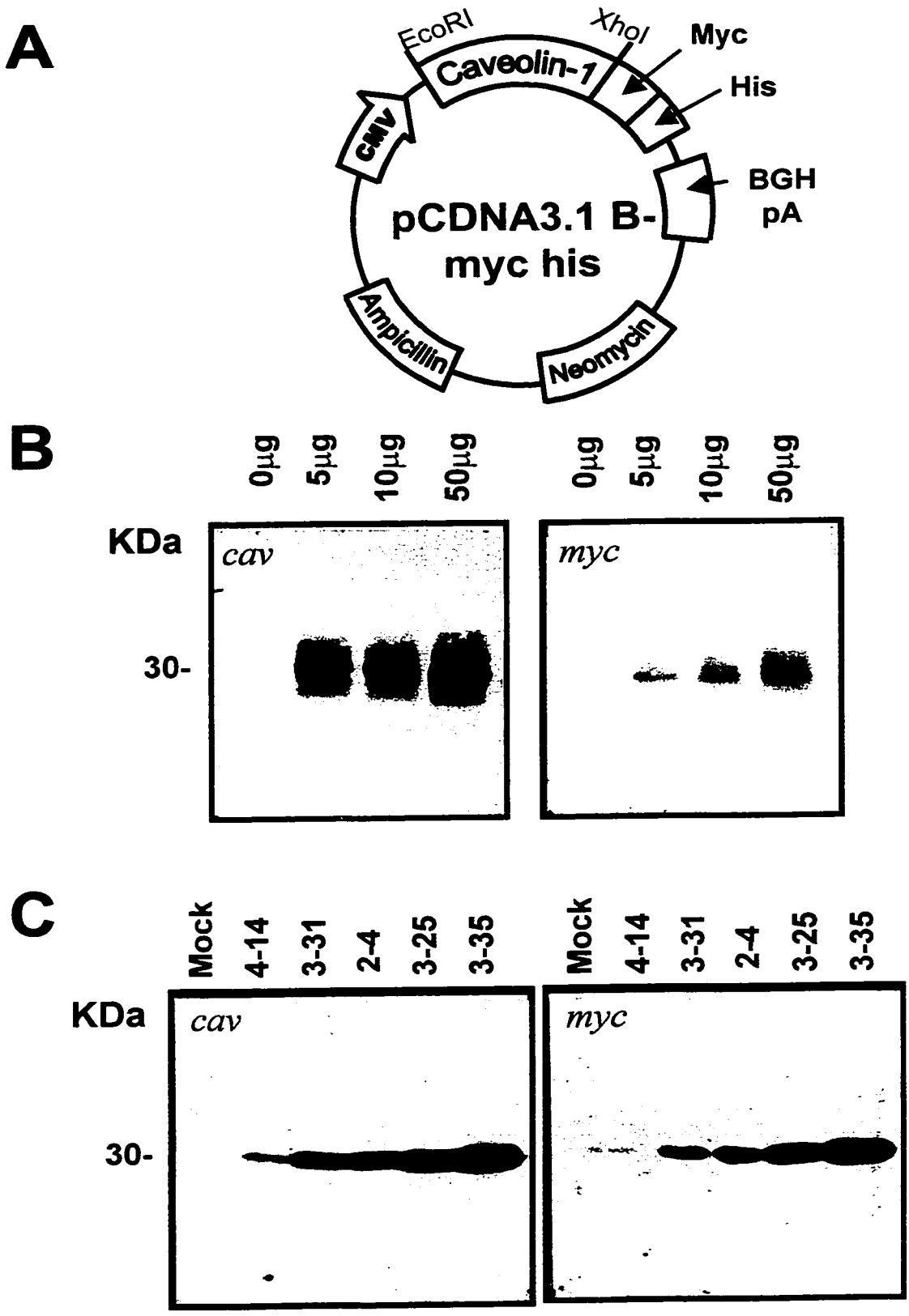
A
EcoRI
XhoI
Myc
His
Caveolin-1
CMV
BGH
pA
pCDNA3.1 B-
myc his
Ampicillin
Neomycin
B
0μg
5μg
10μg
50μg
0μg
5μg
10μg
50μg
KDa
cav
myc
30-
C
Mock
4-14
3-31
2-4
3-25
3-35
Mock
4-14
3-31
2-4
3-25
3-35
KDa
cav
myc
30-

Figure 18: Cellular localization of recombinant caveolin-1 in McA-RH7777 cells

Cells cultured on 35-mm poly-lysine coated, glass bottom dishes were fixed and permeabilized as described in Materials and Methods. Caveolin-1 was detected by an anti-caveolin polyclonal antibody (Transduction labs C13630) followed by Rhodamine conjugated anti-rabbit secondary antibody. Caveolin-1 expression levels are MH < 3-25 < 3-35.

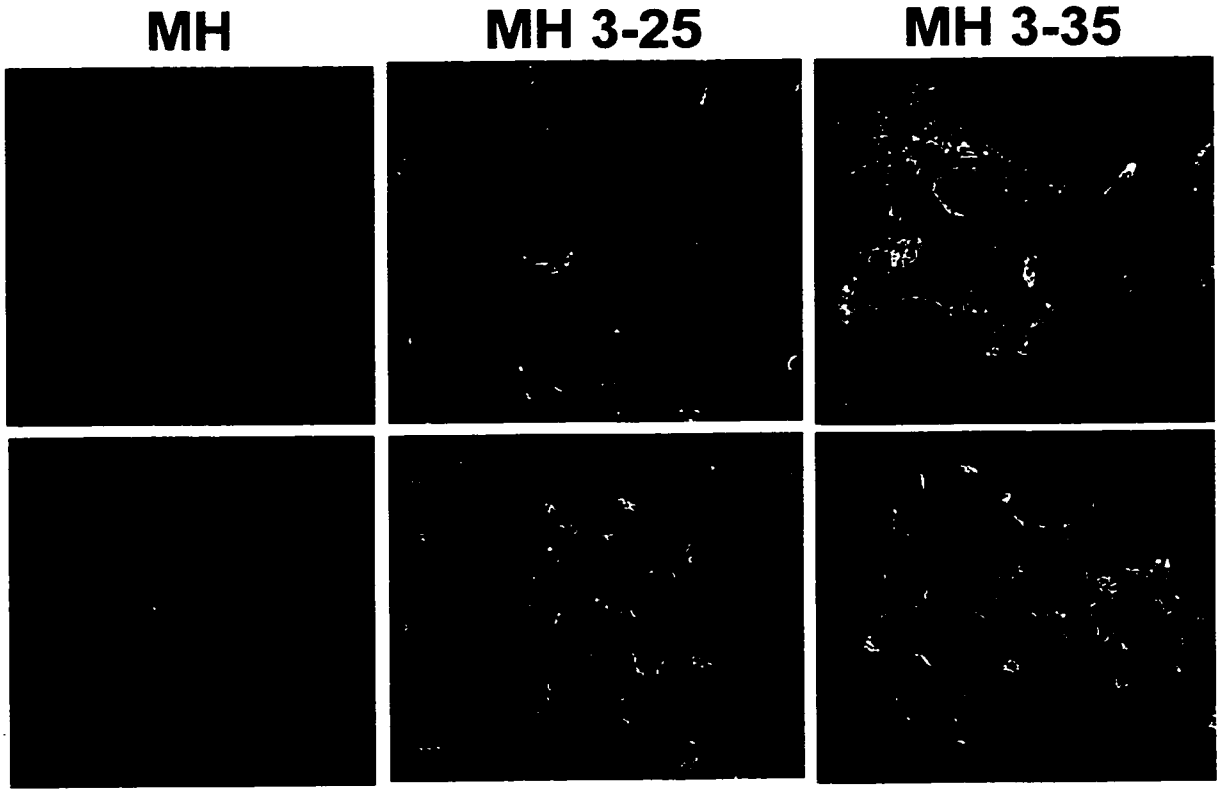
MH
MH 3-25
MH 3-35

5.4 HDL and Lp2A-I mediated efflux

The effect of caveolin-1 expression on cholesterol efflux was determined using cells that were labeled for 12 h with [^{3}H]cholesterol. After this long labeling period, the efflux to HDL was evaluated over a 24 h period. Efflux values are represented after the subtraction of non-specific efflux to a 40-fold excess of fatty acid-free BSA. The efflux to BSA was equivalent between all cell lines (data not shown), indicating that nacent lipoprotein secretion does not account for differences in efflux. During short term (< 6 h) HDL mediated efflux, there was a slight increase in efflux with caveolin-1 expression level (not statistically significant). However efflux to HDL at 10 h and 24 h increased significantly with caveolin-1 expression level (Fig. 20 A and B).

The effect of caveolin-1 expression on cholesterol efflux was also examined using Lp2A-I particles that were prepared with POPC and human apoA-I. Again, the caveolin-1 induced efflux was observed only after prolonged efflux periods (> 6 h) (Fig 20C, D). Furthermore, experiments with lipid free apoA-I also revealed an increase in cholesterol efflux, which required long efflux periods to become apparent (data not shown). These results suggest that increasing caveolin-1 levels increase cholesterol concentration in a compartment that is in slow equilibrium with the efflux accessible pool at the cell surface. Values of specific HDL-mediated efflux after 24 h were compared to the caveolin-1 expression levels, which were semi-quantified by densitometry of Western blots for caveolin-1. A highly significant correlation was seen between caveolin-1 expression level and HDL-mediated cholesterol efflux ($r^2 = 0.94$ data not shown)

Figure 19 Cav-1 is enriched in the detergent insoluble membrane fraction.

Stable McA-RH7777 cells expressing caveolin-1 were solubilized with 1% Triton X-100 for 30 min. Cell membrane fractions were rinsed twice with M1 buffer. The DIM fractions were collected and normalized to protein. Equal amounts of protein per lane were resolved on SDS-PAGE transferred to nitrocellulose and blotted with polyclonal anti-caveolin or anti-myc antibodies as described above.

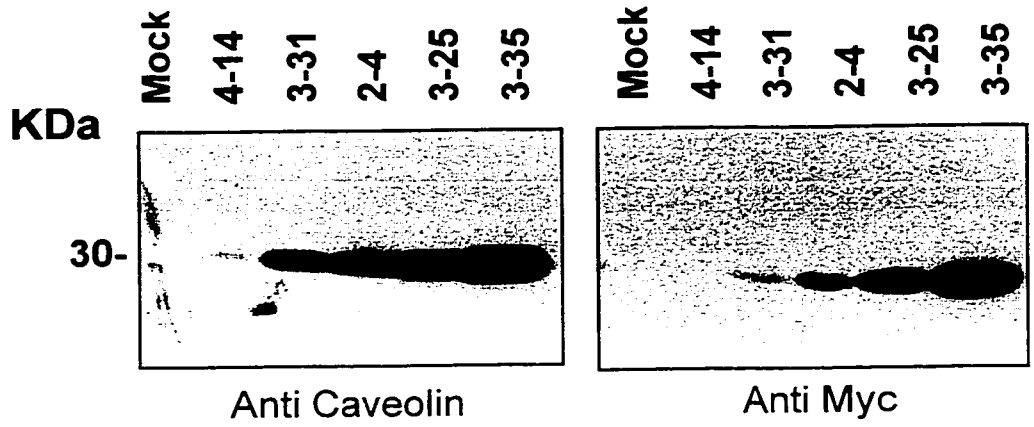
Mock
4-14
3-31
2-4
3-25
3-35
KDa
30-
Anti Caveolin
Mock
4-14
3-31
2-4
3-25
3-35
Anti Myc

Figure 20: HDL and Lp2A-I mediated efflux

A, cells were seeded at 1.5 x 10^4 cells/well on 6-well Primaria plates. After 24 h, complete media was removed, and DMEM-BSA, 15 μCi [^{3}H]cholesterol and 5 μg HDL was added to each well. After a 12 h loading period, cells were rinsed 2 times with DMEM-BSA. Efflux media was then placed on the cells with or without 50 μg of HDL. Each point is the average +/- S.D (n=3). and is representative of three independent experiments. B, HDL mediated efflux was performed as above with an efflux period of 24 h. HDL mediated specific efflux was determined (HDL mediated efflux minus BSA mediated efflux) after a 24 h efflux period. C, Lp2A-I mediated efflux was performed as above with 50 μg of acceptor particle over efflux periods up to 5 h. D, Lp2A-I mediated specific efflux (Lp2A-I mediated efflux minus BSA mediated efflux) represented as % of radiolabel effluxed after 18 h / cell associated counts before efflux. All data are the average +/- S.D. (n=3) and is representative of three independent experiments, * $p < .0005$ ** $p < .0001$.

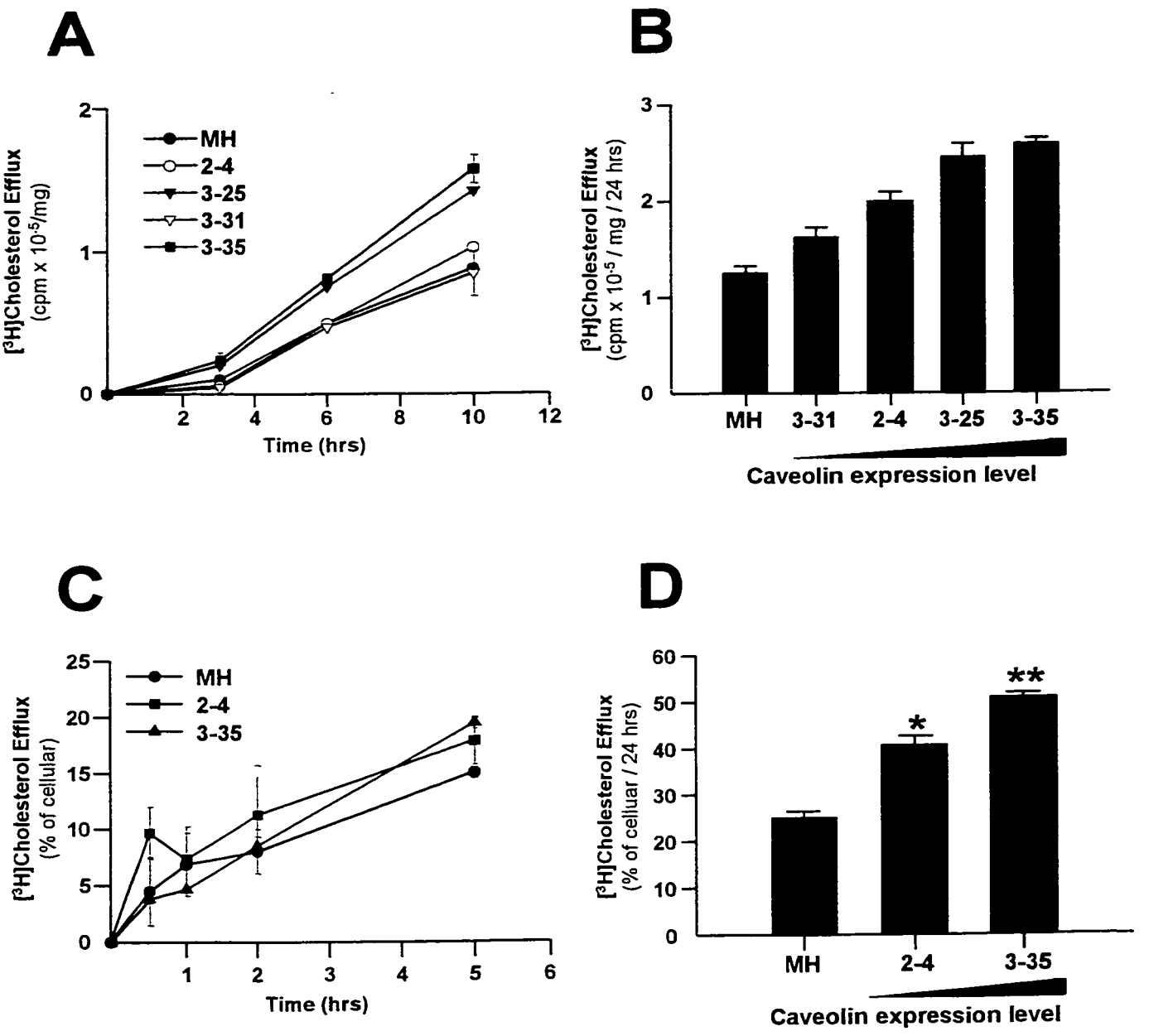
A
[3H]Cholesterol Efflux
(cpm x 10-5/mg)
MH
2-4
3-25
3-31
3-35
Time (hrs)
B
[3H]Cholesterol Efflux
(cpm x 10-5 / mg / 24 hrs)
MH
3-31
2-4
3-25
3-35
Caveolin expression level
C
[3H]Cholesterol Efflux
(% of cellular)
MH
2-4
3-35
Time (hrs)
D
[3H]Cholesterol Efflux
(% of celluar / 24 hrs)
*
**
MH
2-4
3-35
Caveolin expression level

5.5 HDL Binding and Association

The stable cell lines expressing caveolin-1 were then evaluated for HDL interaction at the cell surface. The total binding of ^{125}I-HDL was the same for mock transfected or caveolin-1 expressing cells (Data not shown). Forty-fold excess cold HDL was added to evaluate non-specific binding; specific binding was determined by subtraction of non-specific binding from total binding. Specific binding was not altered by the expression of caveolin-1 in these cells (Data not shown). The cell surface association of ^{125}I HDL was assessed at 37°C. Cell association assays allow the interaction of ^{125}I HDL with the cell surface, which may require lipid domain function. This may be impaired during binding assays performed at 4°C. However total and specific association was unchanged with the over-expression of caveolin-1 in this liver cell line (Data not shown).

5.6 Plasma membrane labeling and efflux

To gain insight into the mechanism by which expression of caveolin–1 would facilitate cholesterol desorption and efflux to HDL, we first examined HDL mediated efflux of cholesterol from the plasma membrane. The enrichment of [^{3}H]cholesterol in the plasma membrane was achieved by incubation of cells with HDL that contained [^{3}H]cholesterol for influx periods up to thirty minutes at 37 °C. The influx of [^{3}H]cholesterol under these conditions was not altered by caveolin-1 expression (Fig. 21A). Methyl-β-cyclodextrin, a potent cholesterol binding but membrane-impermeable agent (132) could remove all the [^{3}H]cholesterol from the cells (Fig. 21B), indicating that [^{3}H]cholesterol from HDL was incorporated into the plasma membrane but not intracellular compartments. We then measured the rate of [^{3}H]cholesterol desorption from the plasma membrane and its transfer to HDL. We found that the short-term desorption and efflux of [^{3}H]cholesterol

from the plasma membrane to HDL was unaffected by caveolin-1 expression (Fig. 21C). Furthermore, expression of caveolin-1 in McA-RH7777 cells did not result in increased HDL interaction at the cell surface. Neither the total binding nor the specific binding of ^{125}I-HDL was increased in cells expressing caveolin-1 (data not shown). Cell surface association of ^{125}I-HDL (37 °C) also revealed no difference in specific or total association with caveolin-1 expression (data not shown).

5.7 [^{3}H]Acetate Incorporation

We next investigated the metabolism of cholesterol within the caveolin-1 expressing cells. Continuous labeling with [^{3}H]acetate showed that the rate of [^{3}H]acetate incorporation into cholesterol was faster in cells expressing caveolin-1 (Fig. 22A), whereas incorporation of the [^{3}H]acetate into CE was unaltered (Fig. 22B). Incorporation of [^{3}H]acetate into triglyceride showed a 50 % increase in caveolin-1 transfected cells (Fig. 22C), while incorporation into phospholipid was decreased (Fig. 22D). Cell lines expressing intermediate levels of caveolin-1 showed rates of [^{3}H]acetate incorporation that were intermediate of MH and 3-35 (data not shown). To determine whether the effect of caveolin-1 on [^{3}H]acetate incorporation into free cholesterol was dependent on vesicular transport, we compared [^{3}H]cholesterol accumulation at 37 °C and 15 °C (data not shown). At 15 °C, transport from the ER and Golgi apparatus to the plasma membrane would be retarded. Under these conditions the incorporation of acetate into cholesterol was reduced, but the caveolin-1 expressing cells still showed a significant increase in [^{3}H]cholesterol ($p < .0005$). To evaluate whether the altered cholesterol metabolism was at the level of HMG-CoA reductase, we evaluated the incorporation of [^{3}H]mevalonate into free cholesterol. At 37 °C, there was a significant increase in

[^{3}H]mevalonate incorporation into free cholesterol in caveolin-1 expressing cells ($p < .0002$) (data not shown). This increase in [^{3}H]mevalonate incorporation into free cholesterol is still significant ($p < .0005$) at 15 °C. The effect of caveolin-1 expression on [^{3}H]acetate and [^{3}H]mevalonate incorporation into cholesterol was insensitive to 15 °C temperature blockage.

Figure 21: McA-RH7777 Cell surface labeling

Cells were seeded at 2 x 10^4 cells per well in 6-well Primaria dishes. One day after plating, cells were rinsed twice with DMEM-BSA. A, HDL mediated cholesterol influx was evaluated by the addition of 50μg of [^{3}H]cholesterol labeled HDL. Cells were incubated for up to 30 min to label cells. Cells were then rinsed twice with DMEM and twice with PBS-BSA. Cells were then collected into 500 μl of 0.5 N NaOH for scintillation counting and determination of cellular protein. B, The [^{3}H]cholesterol labeled cells were then subjected to 50 μM me-β-cyclodextrin mediated efflux for a period of one hour at 37 °C. Media samples were collected and spun at 3000 rpm for 5 min to pellet any cell debris. The supernatant was then removed for scintillation counting. C, Cells were labeled with [^{3}H]cholesterol as in A. HDL mediated efflux of cell surface cholesterol label was then evaluated comparing caveolin expression levels to HDL mediated specific cholesterol efflux. All data are the mean +/- S.D. of three separate determinations.

A

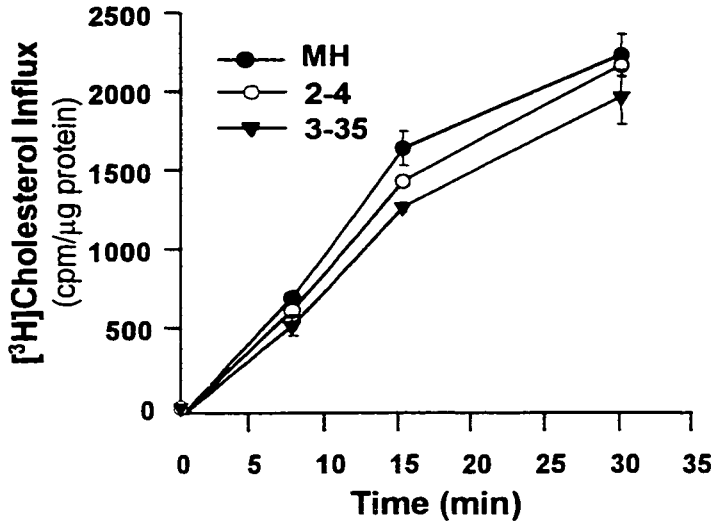
[³H]Cholesterol Influx
(cpm/μg protein)
2500
2000
1500
1000
500
0
MH
2-4
3-35
0
5
10
15
20
25
30
35
Time (min)

B

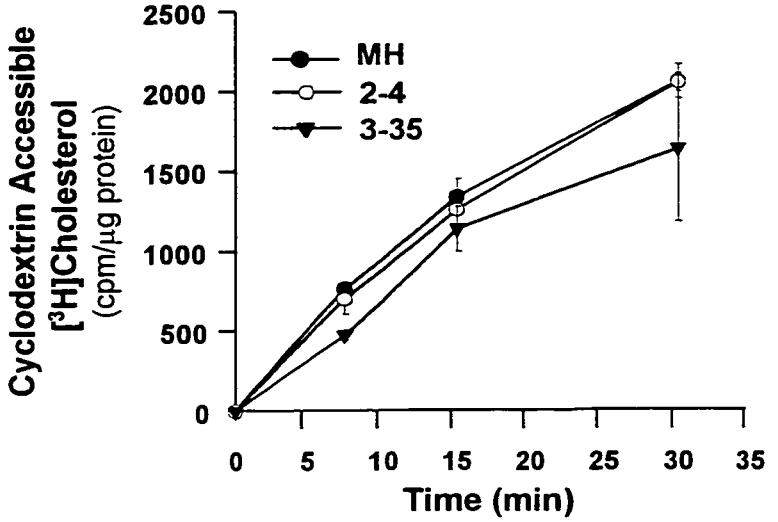
Cyclodextrin Accessible
[³H]Cholesterol
(cpm/μg protein)
2500
2000
1500
1000
500
0
MH
2-4
3-35
0
5
10
15
20
25
30
35
Time (min)

C

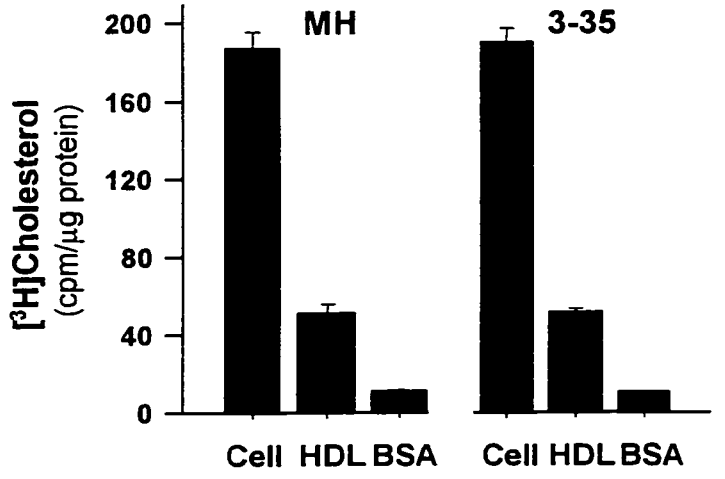
[³H]Cholesterol
(cpm/μg protein)
200
160
120
80
40
0
MH
3-35
Cell
HDL
BSA
Cell
HDL
BSA

5.8 Trafficking of cholesterol from the PM to an ACAT accessible pool

Utilizing the approach used to label the plasma membrane pool of cholesterol, we sought to evaluate the retrograde movement of cholesterol from the plasma membrane to the ER as a function of caveolin-1 levels. The activity of the ER resident protein ACAT, is governed primarily by substrate availability (133). We monitored the conversion of exogenously added [^{3}H]cholesterol to cholesteryl esters. We found that the incorporation of [^{3}H]cholesterol label into cholesterol esters after 2 h increased with caveolin-1 expression (Fig. 23A). When pulse chase experiments were performed, the rate of appearance of labeled cholesterol esters correlated with caveolin-1 expression levels (Fig. 23B). Finally, when the cells were supplemented with serum during the chase, the cells expressing caveolin-1 showed the least sensitivity to decreases in esterification as a result of dilution of the [^{3}H]cholesterol label (Fig. 23C). When cells were incubated with 50 μM progesterone, cholesterol esterification was decreased by > 50 % (data not shown). This effect of progesterone was seen in both caveolin-expressing and mock-transfected cells. The relative decrease in esterification during progesterone treatment was again more pronounced in the mock transfected cells. This increased sensitivity of mock-transfected cells to progesterone treatment mirrors the effect of serum on esterification in figure 23C.

Figure 22: [^{3}H]Acetate incorporation into cellular lipids.

Cells were seeded at 1.2 x 10^5 cells/well onto 6-well Primaria dishes. Serum-free DMEM-BSA was added 2 h prior to the addition of 100 μCi/ml [^{3}H]acetate. Cells were then continuously labeled for up to 2 h, rinsed with PBS-BSA, rinsed two times with PBS, and collected into 2 ml of 1:1 (v/v) methanol and H_2O. A, the synthetic rate of [^{3}H]acetate incorporation into cholesterol was evaluated by continuous labeling. Cells were collected at indicated times and lipids were extracted and separated by TLC. Cholesterol (A), CE (B), TG(C), PL (D), were scraped and radioactivity was quantified by scintillation counting. The values represent the average of two experiments represented as cpm/mg cell protein.

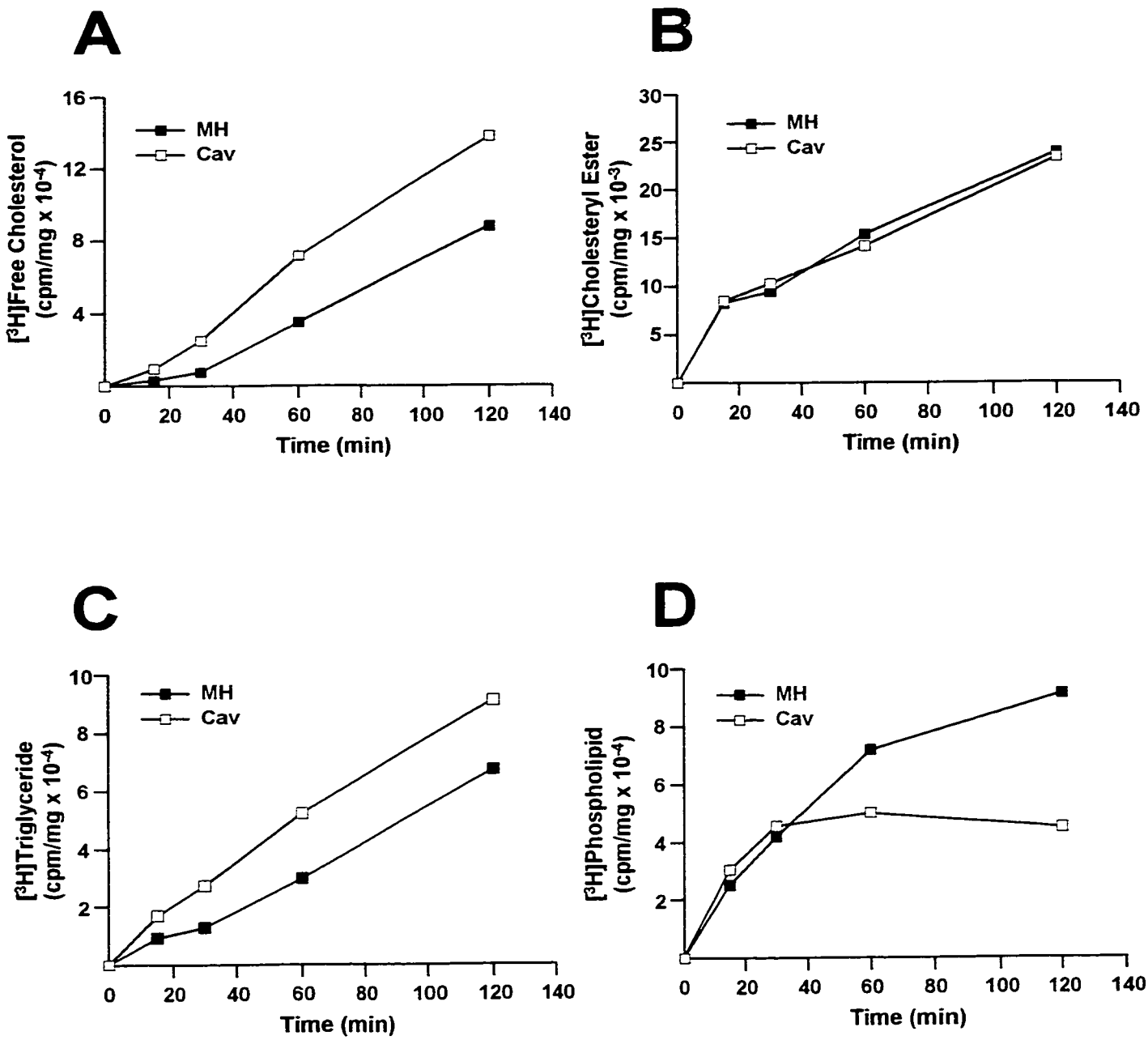
A
[³H]Free Cholesterol (cpm/mg x 10⁻⁴)
16
12
8
4
MH
Cav
0
20
40
60
80
100
120
140
Time (min)
B
[³H]Cholesteryl Ester (cpm/mg x 10⁻³)
30
25
20
15
10
5
MH
Cav
0
20
40
60
80
100
120
140
Time (min)
C
[³H]Triglyceride (cpm/mg x 10⁻⁴)
10
8
6
4
2
MH
Cav
0
20
40
60
80
100
120
140
Time (min)
D
[³H]Phospholipid (cpm/mg x 10⁻⁴)
10
8
6
4
2
MH
Cav
0
20
40
60
80
100
120
140
Time (min)

Figure 23: Incorporation of exogenous [^{3}H]cholesterol into cholesterol esters

A. cells were labeled with [^{3}H]cholesterol for 2 h as described in Materials and Methods. The appearance of this label as cholesterol esters was monitored after 2 h. Cells were washed then lipids were extracted and separated by TLC, cholesteryl esters were then scraped and counted. The levels of [^{3}H]cholesterol esters expressed as cpm/μg cell protein after 2 h. (* $p<.05$ and ** $p<.005$.) B, Cells were pulsed for 1 hr with [^{3}H]cholesterol, cells were rinsed twice with DMEM-BSA andchased for 2 h. Cells were washed then lipids were extracted and separated by TLC, cholesteryl esters were then scraped and counted. Caveolin-1 expressing cells show an increased rate of esterification under these conditions. C, Cells were pulsed for 1 hr with [^{3}H]cholesterol, cells were rinsed twice with DMEM-BSA and chased for 2 h in the presence of 10% FBS. Cells were washed then lipids were extracted and separated by TLC, cholesteryl esters were then scraped and counted. Caveolin-1 expressing cells show smallest decrease in CE formation upon serum treatment.

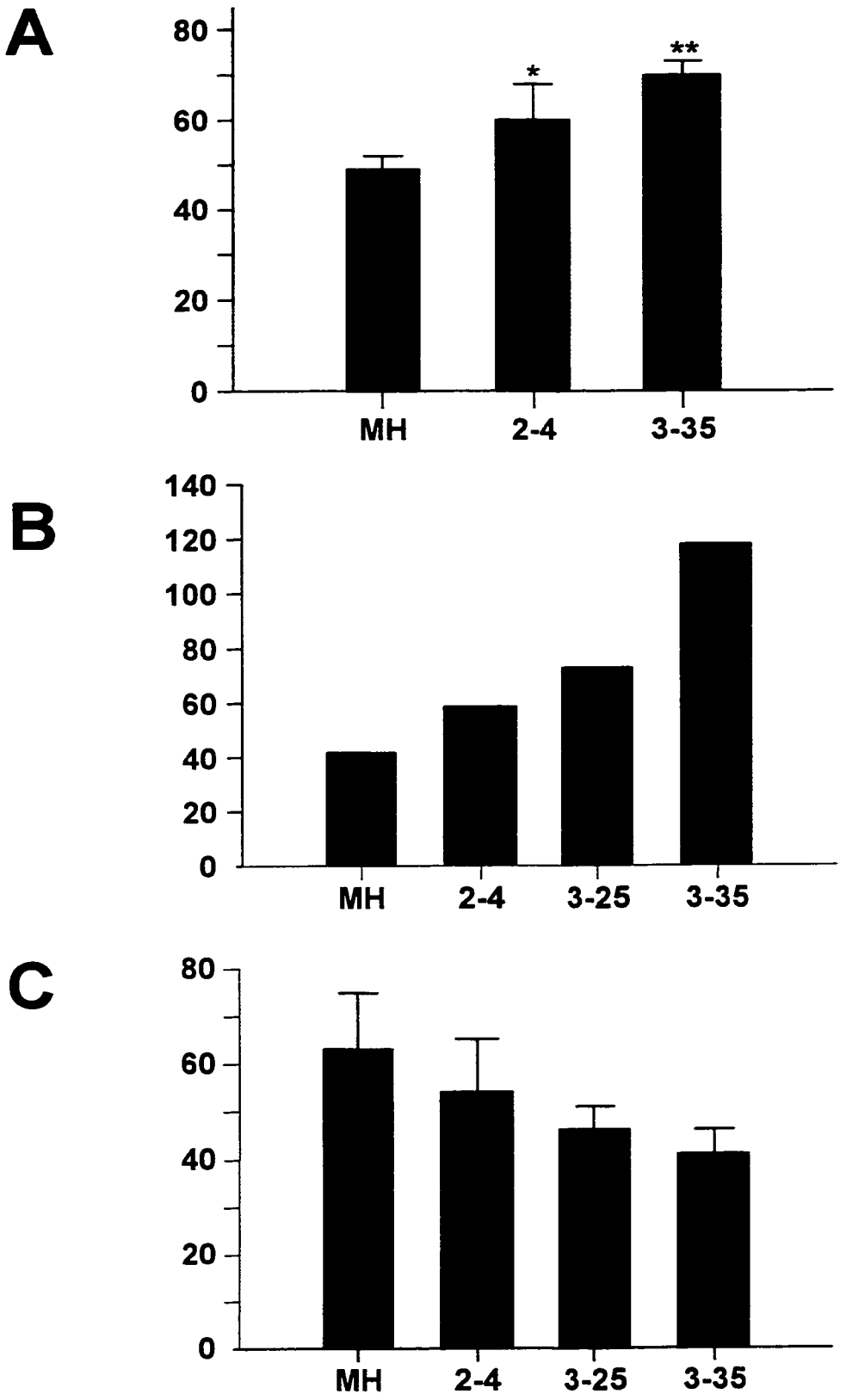
A
80
60
40
20
0
*
**
MH
2-4
3-35
B
140
120
100
80
60
40
20
0
MH
2-4
3-25
3-35
C
80
60
40
20
0
MH
2-4
3-25
3-35

Chapter 6: Discussion

This work sought to create a model to explore the function of caveolin-1 in cell culture. With the successful cloning of caveolin-1 from human adipose tissue, the materials were generated for the creation of cell models. To explore the function of caveolin-1 in cell culture, five novel expression systems and three antisense constructs were built. The expression constructs will allow the manipulation of caveolin-1 through the use of two epitope tags, a myc epitope and a poly-histidine tail. These constructs exploit two different vectors for the generation of stable cell lines, pCMV5 and pCDNA3.1. Finally antisense constructs utilizing inducible antisense RNA and a catalytic ribozyme will allow the study of caveolin-1 function through the generation of knock out cell lines.

A number of cell lines were evaluated for their utility as models for the expression of caveolin-1. The cell lines chosen for stable transfection were the rat hepatoma cell line McA-RH7777 and the human endothelial cell line HUVEC ECV 304. The McA-RH7777 cell line was chosen since no caveolin-1 was detected by western blot so this cell line served as a model to explore the function of caveolin-1 in a cell line that does not normally express caveolin-1. The HUVEC cell line conveyed a number of advantages including its human origin, and its ability to form monolayers. These unique characteristics allow us to test its utility as a transcytosis model. This model is also well suited for microscopy studies due to its flat and extended morphology. Finally the expression of caveolin-1 in these cells makes it a relevant cell model to look at the effects of over expression of caveolin-1.

6.1 Transcytosis

Stable cell lines generated in the HUVEC cell model were evaluated for their utility as a model of transcytosis. To develop this model a cell culture model system was developed using the Falcon transwell 3-D cell culture system. Studies in this system required the generation of a number of novel assays to evaluate the formation of an intact monolayer. In order to evaluate monolayer integrity transepithelial electrical resistance (TEER) measurements were used. This work showed that matrix coatings fibronectin or collagen-I increased the TEER of HUVEC monolayers to the greatest extent. In order to evaluate the monolayer integrity by biochemical methods a colorometric assay using HRP was developed. Also ^{125}I-HRP and ^{125}I-albumin were used to probe the monolayer integrity. The polysaccharides [^{3}H]dextran and [^{3}H]inulin were used in an attempt to evaluate specificity of trafficking of ^{125}I-HDL in this system. The work to date suggests that caveolin-1 expression in this system does not increase the transcytosis of any of the ligands studied. Any trafficking observed in this system can be explained through the sensitive biochemical assays developed, as paracellular transport.

Other critical issues found with this model include the high cost of the Falcon transwell system and the maintenance of sterility during the manipulations required to assay membrane integrity. Also the culture time required and the preparation of cell monolayers and reagents suggests that extensive studies with this model will be prohibitively expensive and time consuming. However, this work has made significant progress in the development of this model system. Namely the improvement of TEER values using matrix coatings, the optimization of cell culture conditions for rapid formation of monolayers and the development and evaluation of six biochemical

measures of monolayer integrity.

Finally the role of caveolin-1 in transcytosis remains largely unresolved. This model suggests that the over-expression of caveolin-1 in HUVEC cells does not cause perturbations in transcytosis as evaluated in the transwell culture system. This does not however rule out caveolin-1 playing a role in transcytosis. To address whether caveolin-1 plays a role in transcytosis an antisense strategy will need to be employed. Transcytosis studies have been performed using EM techniques to track the movement of immunogold labeled particles through the endothelium (121). Simonescu showed that both albumin and lipoproteins traffic through uncoated vesicles whose size is consistent with caveolae. Other biochemical methods to evaluate transcytosis require the independent biochemical analysis of binding uptake and appearance on the opposite side of the cell (118). Attempts are on going to establish direct cell culture assays of transcytosis but as yet these models are in their infancy (119).

6.2 Caveolin-1 over-expression in HUVEC stable cell lines

The HUVEC stable cell lines were explored for their cell surface interaction with HDL particles. At high HDL concentrations cells over expressing caveolin-1 were found to have increased HDL association. This may indicate a change in a low affinity high capacity binding site on the surface of these cells. This interaction was explored since a putative HDL receptor SR-B1 has been reported to be localized in the caveolae (49). This model of caveolin-1 over expression may serve as a meaningful model to probe the relationship between caveolin expression and Cla-1 (the human homologue of SR-B1). At the time of this work we do not have Cla-1 antibodies available, so further exploration of the potential interaction of caveolin-1 with SR-B1 and HDL association will require

more molecular tools.

It is also noteworthy that in these endothelial models of caveolin over expression the expression level of eNOS is not perturbed. Caveolin-1 expression does not seem to affect the expression of eNOS, however it may alter the intracellular distribution of eNOS. Caveolin-1 has been shown by immunoprecipitation to co-precipitate with eNOS suggesting a direct interaction (64). Also caveolin has been shown to repress the function of eNOS working in opposition to the stimulatory effects of calmodulin (88). It would be interesting to use these endothelial cells over expressing caveolin-1 as models to explore the interaction of eNOS with caveolin-1. If caveolin-1 acts as an inhibitor of eNOS activity then these cell lines may produce less NO.

6.3 Caveolin-1 Over expression in McA RH7777 cells

The potential role of caveolin-1 in HDL-mediated cholesterol transport was first presented by Fielding et. al. (124). Since this seminal observation, the mechanism whereby caveolin may affect cholesterol efflux has not been defined. We have generated a panel of stable cell lines that express human caveolin-1, which are used here to study the role that caveolin-1 plays in cholesterol trafficking and efflux. The selection of a hepatoma cell line, which does not express endogenous caveolin-1, also provides a model to study the effects of caveolin-1 on cholesterol synthesis, transport and storage. Our independent cloning of caveolin-1 reveals two sequence differences from the current sequence listed in Genebank acc #Z18951. Considering the conservative nature of these substitutions and the fact that the codon for amino acid 144 encodes a residue that is found in caveolin-1 of all other non human species cloned to date, we propose that these

differences represent allelic variations in human caveolin-1 and that isoleucine 144 is the wild type form.

Utilizing these stable cell lines, we observe an intracellular distribution of caveolin-1, which mirrors the distribution in cell types that normally express caveolin-1 (131). Expression of autologous caveolin-1 in other cell types has been shown to be sufficient to drive the formation of cell surface caveolae (134). The strong Golgi staining and increased punctate plasma membrane staining correlate with increased expression levels of caveolin-1. The functionality of caveolin-1 was confirmed by its enrichment in the DIM fraction (Fig. 19), which suggests that the recombinant caveolin-1 retains detergent insolubility in this cell type, and therefore associates with lipid domains that confer such insolubility. Also the presence of high molecular weight oligomers, which are disrupted upon extensive boiling and NaOH treatment suggests that the recombinant caveolin is capable of forming homo-oligomers.

With this model we sought to determine whether stable caveolin-1 expression affects cholesterol efflux and the underlying mechanisms. Using long-term cholesterol labeling method, which labels all internal as well as plasma membrane cholesterol, no difference was noted in initial rates of efflux to HDL (Fig. 20A) or the well-defined efflux acceptor Lp2A-I (Fig. 20C) as a function of caveolin-1 expression. However, long-term incubations (between 10h and 24 h) revealed an increase in HDL-mediated specific cholesterol efflux, which was proportional to caveolin-1 expression level reaching two fold greater levels in the highest expressing cell line (Fig. 20B). The efflux observed in the presence of 40-fold excess fatty acid free BSA (non specific efflux) was significantly less than that mediated by HDL and equivalent between cell lines, demonstrating that the

difference in [^{3}H]cholesterol detected in the efflux media at 10 h or 24 h cannot be attributed to nascent lipoprotein secretion. The effect of caveolin-1 expression levels on cholesterol efflux requires prolonged efflux periods to become apparent. Under the same conditions efflux experiments using Lp2A-I (Fig. 20D), or lipid-free apoA-I (data not shown) revealed an increase in [^{3}H]cholesterol efflux as a function of caveolin-1 expression after long efflux periods. Therefore, the effect of caveolin-1 expression in the McA-RH7777 cell model appears restricted to long-term diffusional cholesterol efflux. This suggests that caveolin-1 levels may correlate with an increase of cholesterol in a cellular compartment that is in slow equilibrium with the membrane pool accessible to HDL-mediated diffusional efflux.

Fielding et al. (127) showed that transfer of fibroblasts that had been conditioned in medium containing 7 % plasma into a medium containing 80 % plasma lead to an acute increase in caveolin-1 expression after 90 min. This increase coincided with a 2-fold increase in cholesterol efflux to 80 % plasma measured within a 3 min efflux period. These data and that derived from other experiments (16), in which the cells respond to an acute increase in the concentration of medium cholesterol, present an interesting and informative contrast to the experiments presented here, where the cells stably express caveolin-1 and are cultured in constant serum concentration. In our experiments, stable expression of different levels of caveolin-1 does not induce increased initial rates of cholesterol efflux, but augments a cellular pool of cholesterol that is in slow equilibrium with the efflux-accessible pool of caveolae at the plasma membrane. This suggests that in the steady state, caveolin-1-associated cholesterol represents a buffer or recycling pool, that is not rapidly efflux accessible. In contrast an acute cellular cholesterol loading

causes the cells to present cholesterol that is rapidly efflux accessible (18).

In an attempt to explain the mechanism whereby caveolin-1 expression affects only long-term HDL mediated cholesterol efflux, we investigated the interaction of HDL with the cell surface. We found no difference in HDL binding or association between caveolin-1 expressing and mock transfected cells. This was also seen at 37 °C during cell association assays, which would allow lipid domain interactions or retro-endocytosis. We then characterized cholesterol influx from HDL to the plasma membrane. We found that the influx of free cholesterol was unaltered by the expression of caveolin-1 (Fig. 21A). The radiolabeled cholesterol was confirmed to be at the plasma membrane by methyl-β-cyclodextrin-mediated removal of the entire exogenously added label (Fig. 21B). HDL mediated efflux experiments utilizing this cell surface labeling strategy, showed identical cholesterol desorption properties (Fig. 21C), although clearly caveolin-1 was increased at the plasma membrane (Fig. 18). Thus, binding, association, short-term cholesterol influx and short-term diffusional efflux are all unaltered by the expression of caveolin-1. These experiments suggest that the expression of caveolin-1 by itself does not alter the interaction of HDL with the cell surface. This is noteworthy since of SR-BI and caveolin-1 have been implicated in the selective uptake of cholesterol (32, 49).

The lack of effect of caveolin-1 expression on the initial rates of efflux suggested the possibility of an altered intracellular trafficking mechanism. Incorporation of [^{3}H]acetate into free cholesterol increases with caveolin-1 expression level (Fig. 22A). Since between 64 % (128) and 90 % of the cellular free cholesterol is found at the plasma membrane, as reported by Lange et. al. (135), this increase in cholesterol synthesis may represent an increased rate of delivery to the plasma membrane. Experiments by Smart

et. al. (136) have shown that newly synthesized cholesterol moves first into caveolae and then into the plasma membrane and that this process is accelerated with caveolin-1 expression. Since caveolae have now been implicated in vesicular trafficking and cholesterol transport, we propose that the increased cholesterol synthesis is due to an increase in cholesterol trafficking from the ER to the plasma membrane. We hypothesize that increased caveolin-1 would increase trafficking of cholesterol between the ER and the plasma membrane. This may create the illusion within the cell of a localized deficit in ER cholesterol, which in turn leads to increased cholesterol synthesis. Without a recycling of cholesterol off the plasma membrane, the fluidity of the plasma membrane could be affected by the increased synthesis of cholesterol. To investigate the mobilization of cholesterol off of the plasma membrane we used the short-term exogenous labeling of cholesterol, which we had shown by cyclodextran treatment to be on the plasma membrane. By monitoring the conversion of this cholesterol to cholesteryl ester by ACAT, we can evaluate the movement of cholesterol from the plasma membrane to intracellular stores. We find that caveolin-1 expression correlates with the appearance of cholesterol in this cholesteryl ester pool. By pulse chase experiments this was shown to be reflective of an increase in the rate of cholesteryl ester formation. The movement of caveolin in response to changes in cholesterol content of the plasma membrane has been shown by Anderson and colleagues (137). While cholesterol has been shown to affect caveolin expression (138) and distribution (127), this is the first report that caveolin expression at different steady state levels alters the cycling of cholesterol. Also the appearance of plasma membrane cholesterol as cholesteryl esters could be used as a novel method to evaluate the role of caveolin-1 in vesicular trafficking of cholesterol.

The combined data suggest that the correlation between caveolin-1 expression and long-term diffusional cholesterol efflux to HDL cannot be explained by HDL interactions with the cell surface but rather is due to alterations in cholesterol cycling.

Curriculum Vitae
Philip Harold Links

Address:

Lipoprotein and Atherosclerosis Research Group
University of Ottawa Heart Institute
Room H455, 1053 Carling Ave.
Ottawa, Ontario
K1Y 4E9

Phone: (613) 798-5555 ext. 8713
Fax: (613) 761-5281
Home: (819) 771-1340, (306) 374-8897

Biographical Data:

Place of Birth: Durham, North Carolina
Date of Birth: April 17, 1974.
Citizenship: Canadian and American
Sex: Male
Marital Status: Single

Education:

Secondary (1988-1992)
Walter Murray Collegiate, Saskatoon Saskatchewan. Gifted Program, graduated high honors. Lettered in Atheletics and Academics (in top 10 of graduating class)

(June-Sept. 1991)
University of North Carolina at Chapel Hill summer program, classes in Ecology and American Literature. Invitation and interviewed for Moorehead Scholarship (This is the top entrance award offered by UNC $40,000 for combined leadership academics and athletics).

Undergraduate (1992-1996)
University of Alberta Graduate B.Sc. Chemistry, Minor in Biological Sciences.
Recipient of Top entrance Award (Academic Athletic and Leadership),
Advanced organic chemistry laboratory progam
Varsity Football Running Back.

Graduate (1997-present)
Masters in Science candidate in the Faculty of Medicine, Department of Biochemistry University of Ottawa Heart Institute.

Curriculum Vitae
Philip Harold Links

Distinctions and Awards:

1991 Invitation and interviewed for Moorehead Scholarship (This is the top entrance award offered by UNC $40,000 for combined leadership academics and athletics).
1992 Government of Saskatchewan Scholarship (Academics)
1992 Provincial All Star Football Running Back
1993 Copp Family Scholarship Award University of Alberta ($2,500) This is the top entrance award offered by the University of Alberta for combined Athletics Academics and Community Leadership.
1993 Canada Scholar ($2,000) National Scholarship for Academics
1993 University of Alberta Golden Bear Football Running Back
1994 Summer Studentship, University of Alberta Heritage Medical Research Center
1994 Runner up, University of Alberta Medical Student Research Day, Oral Research Presentation
1995 Summer Studentship, University of Ottawa Heart Institute
1997 Medical Research Council of Canada Studentship
1998 Merk Frostt Award for Best Basic Research Presentation, University of Ottawa Heart Institute Research Day
1999 Best M.Sc Student, University of Ottawa Department of Biochemistry poster presentation
1999 University of Ottawa Teaching award, Teaching Assistant of The Year
2000 Runner up Merk Frostt Award for Best Basic Research Presentation, University of Ottawa Heart Institute Research Day
2000 Runner up University of Ottawa Department of Biochemistry poster presentation
2000 Runner up University of Ottawa Department of Pathology research day

Teaching Positions:

1997 Laboratory Instructor, University of Ottawa Department of Biochemistry
1998 Laboratory Instructor, University of Ottawa Department of Biochemistry
1999 Laboratory Instructor, University of Ottawa Department of Biochemistry
2000 Laboratory Instructor, University of Ottawa Department of Biochemistry

Refereed Papers:

McLeod, R.S., Wang, Y., Rusinol, A., **Links, P.,** Yao, Z.: ApolipoproteinB Sequence Requirements for Hepatic very low density lipoprotein assembly. (1996) *J. Biol. Chem.* **271**, 18445-18455.

Refereed Papers ctd:

Philip H. Links, Xiaohui Zha, Zemin Yao, Michael P. Lisanti and Yves L. Marcel: Stable Expression of Caveolin-1 in McA-RH7777 Hepatoma Cells Does Not Change the Initial Efflux Rate but Increases both Long Term Efflux and Cycling of Cholesterol (2000) *J. Biol. Chem.* **(submitted)**.

Non- Refereed Papers:

Links, P.H., Zha, X., Marcel, Y.:Caveolin-1 Expression and its Role in Cholesterol Efflux in Rat Hepatoma Cells (1998) *Molecular Biology of the Cell* **9,** 97.

Oral Presentations

Links, P.H., Zha, X, Marcel, Y.:Caveolin-1 expression increases HDL mediated cholesterol efflux by increasing cholesterol trafficking (2000) *Heart Institute Research Day*. **Runner up Merk Frosst Award for Best Basic Science presentation**

Links, P.H., Burgess, J., Yao, Z., Marcel, Y.:Caveolin Expression Increases Transcytosis (1998) *Heart Institute Research Day*. **Winner of Merk Frosst Award for Best Basic Science presentation**

Links, P.H., Yao, Z., Marcel, Y.:Caveolin-1 Cloning, Expression and Function (1998) *Department of Biochemistry Seminar Series*.

Links, P., McLeod, R.S., Yao, Z.:Identification of a Degradation Sequence in Human ApoB. (1994) *University of Alberta Faculty of Medicine Research Day*. **Runner Up Best Oral Presentation**

Poster Presentations

Links, P.H., Zha, X., Marcel, Y.:Caveolin-1 Expression and its Role in Cholesterol Efflux in Rat Hepatoma Cells (1999) *Department of Pathology and Laboratory Medicine Research Day*

Appendix A: Rab GDI function and G protein cycling

Schematic diagram of rab GDI function, and small G protein cycling. Small G proteins are loaded with GTP by guanine nucleotide exchange factors, which remove spent GDP for GTP. Small G proteins such as Rab are thought to cycle onto the plasma membrane with the assitance of a guanine nucleotide dissociation inhibitor (GDI). The GDI holds the small G protein (which is armed with GTP) in an inactive conformation. Once the GDI is removed the G protein can fire, hydrolyzing GTP to GDP.

Appendix A

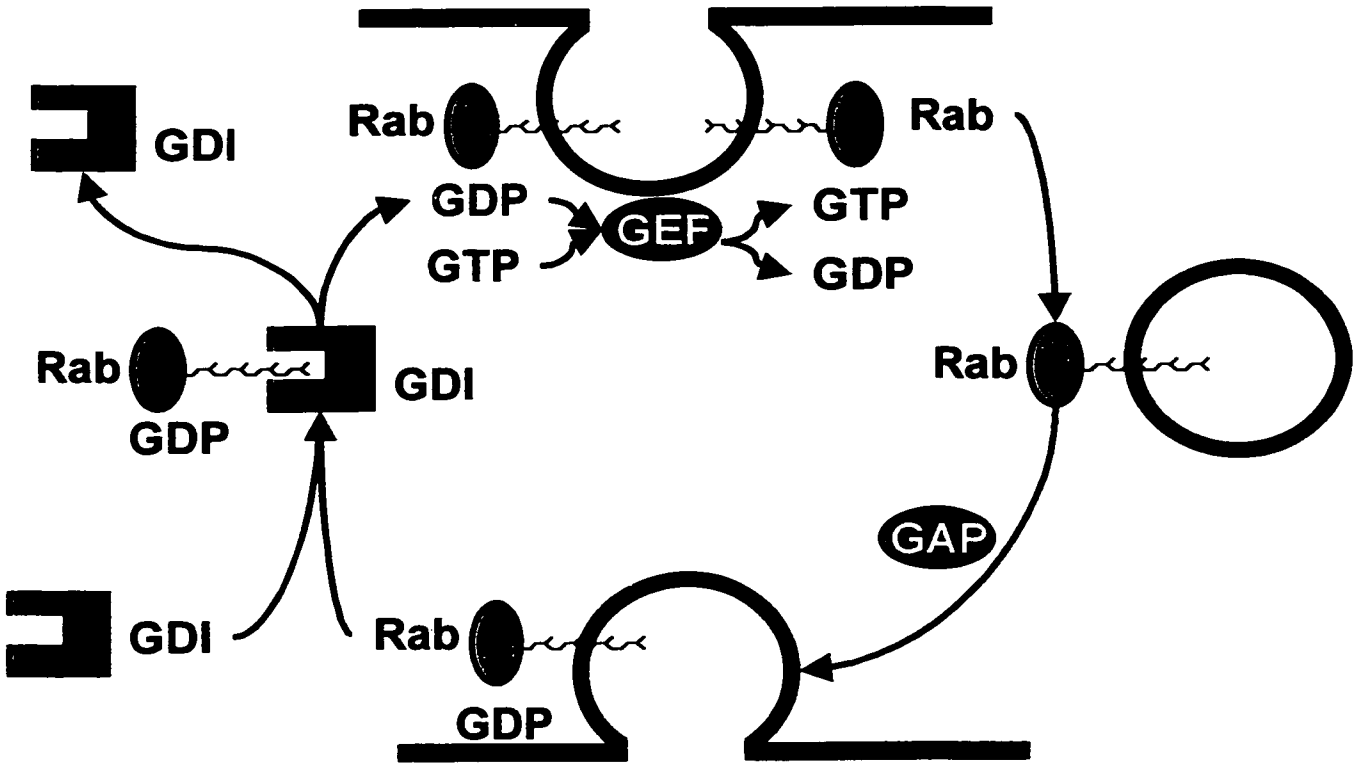

Appendix B: G protein binding to GTP and GDP

Diagram of the cycle of small G proteins between GDP and GTP bound states. The small G protein RAB is illustrated here. The guanine nucleotide exchange factor (GEF) facilitates the removal of spent GDP, while GTPase-activating protein (GAP) loads the small G protein with GTP.

Appendix B

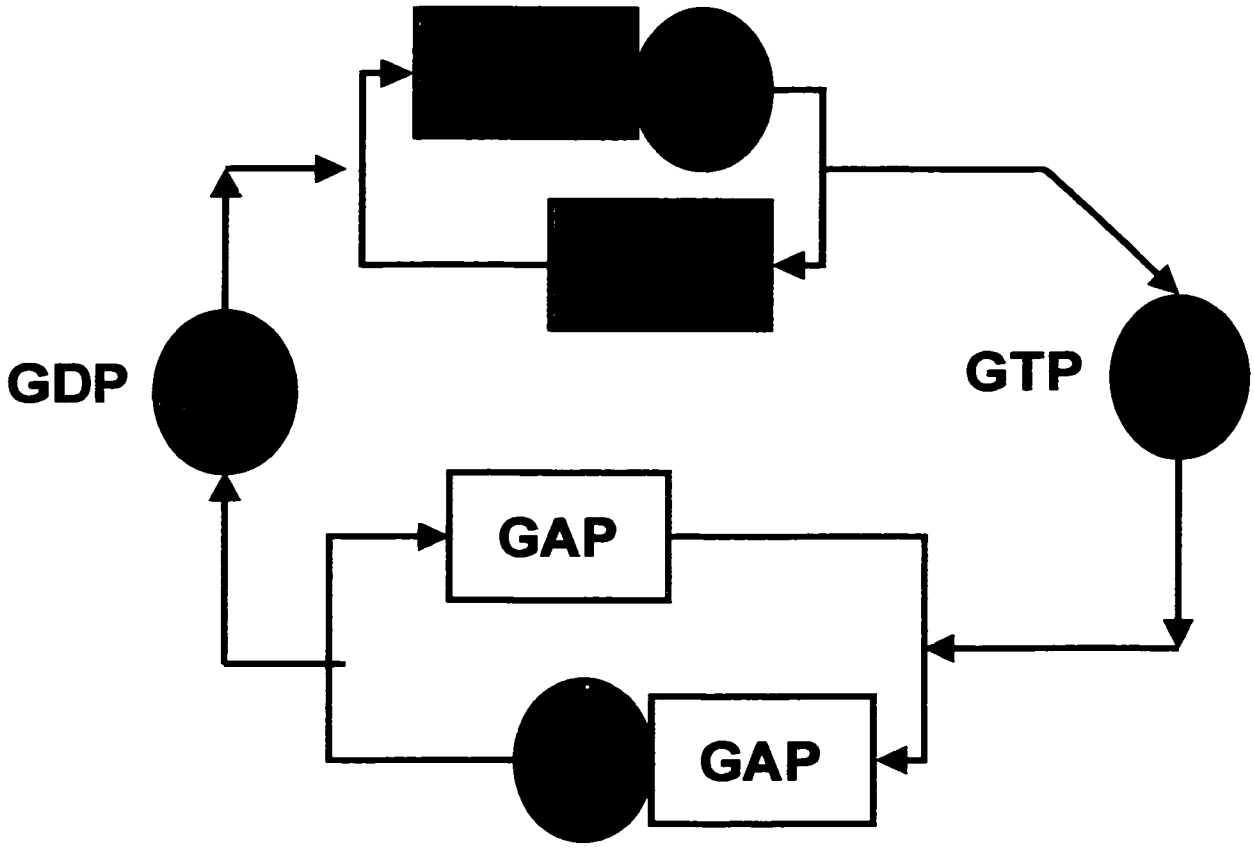

Appendix C: pIND promoter function

Schematic diagr am of promoter function in the pIND vector system. Promoter activity of the pIND vector is driven when dimerization between RXR and chimeric YgEcR nuclear receptors occrs in the presence of Muristone A. These hetero-dimers recognize E/GRE repeats located upstream of the multiple cloning site. Both RXR and YgEcR nuclear receptors are encoded on a second plasmid and are under the control of constitutive promoters.

Appendix C

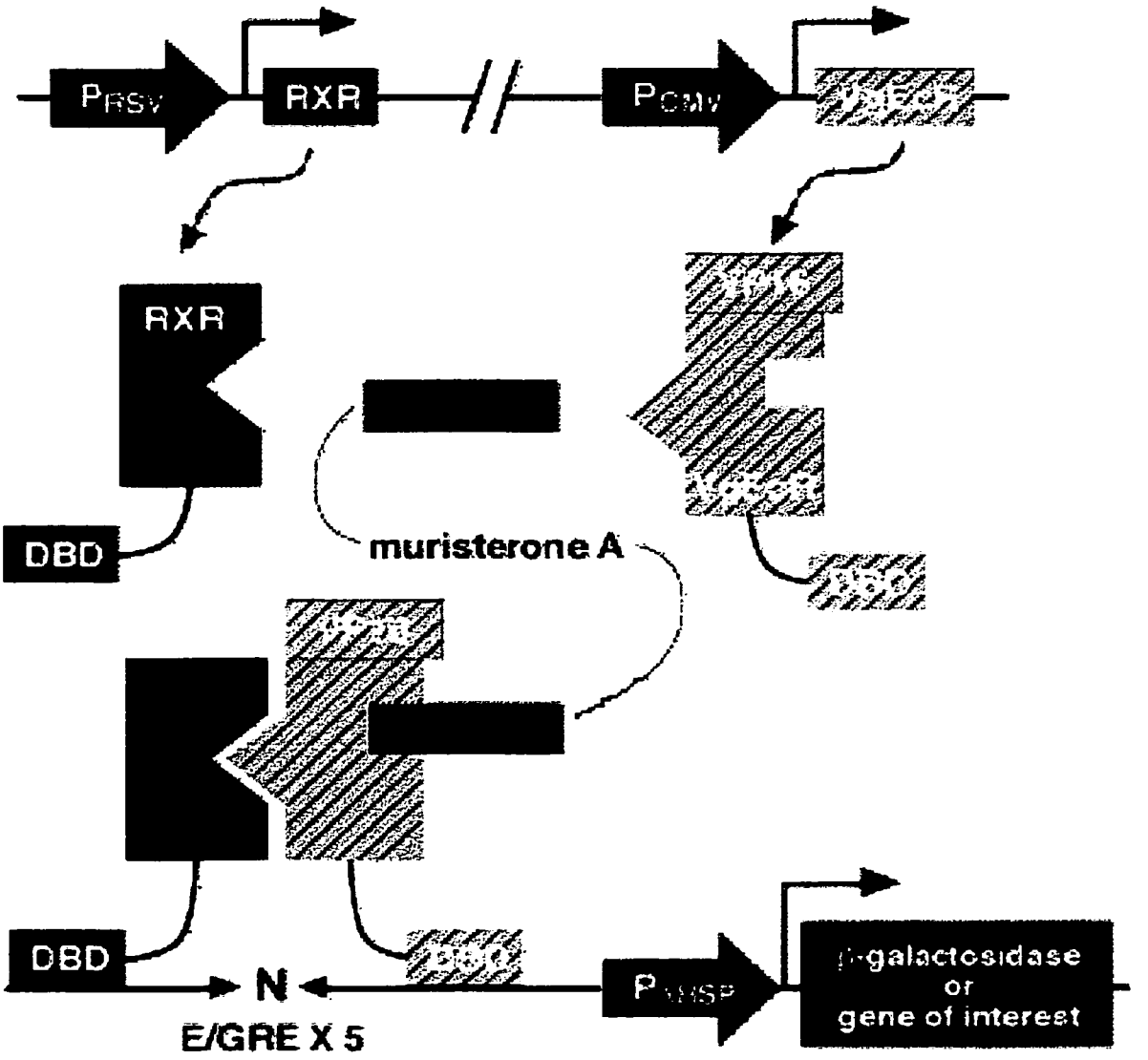

Appendix D: Caveolin-1 structural predictions

α–helical prediction was made at the Expasy website, data from the Chow-Fasman algorithm is illustrated. α_1 and α_2 denote regions of high a-helical probability as denoted in figure 4C. β-sheet prediction was made using the Levitt algorithm and the regions of high probability of forming β-sheet domains are indicated as β_1 and β_2. Hydropathy data was generated using the Kyte and Doolittle algorithm. A large hydrophobic domain is denoted by η.

Appendix D

α Helical prediction

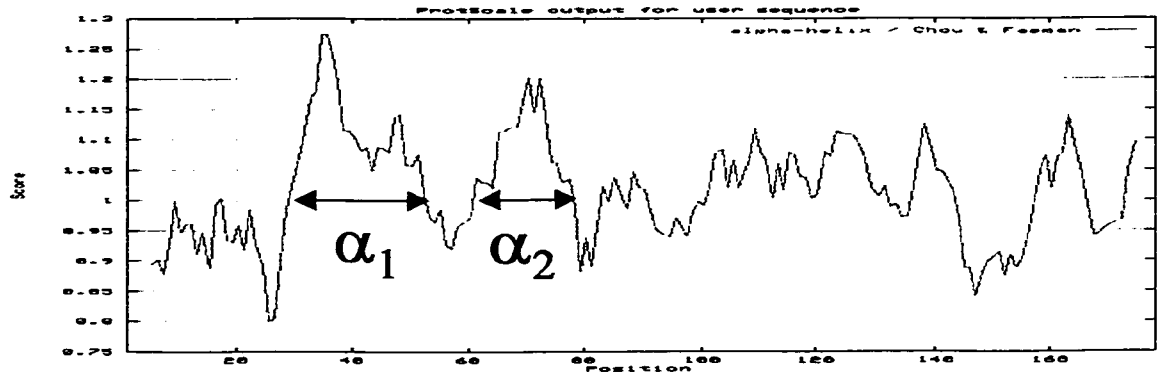

β Sheet prediction

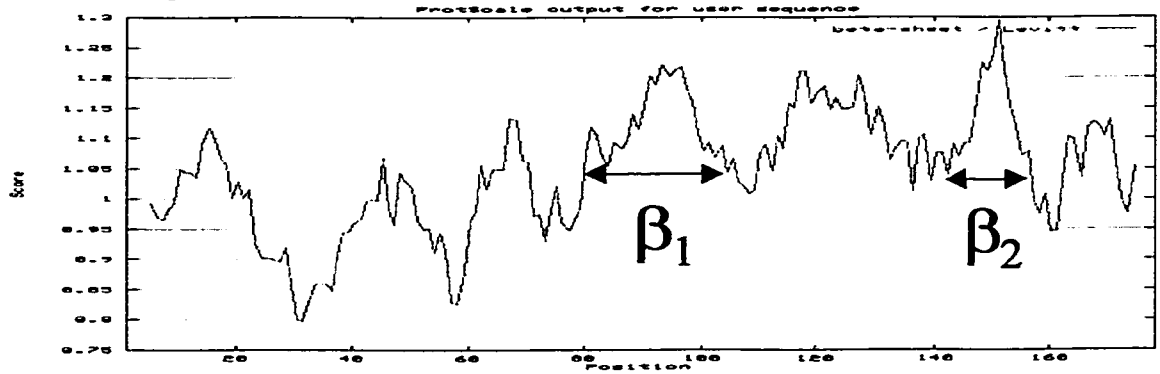

Hydropathy

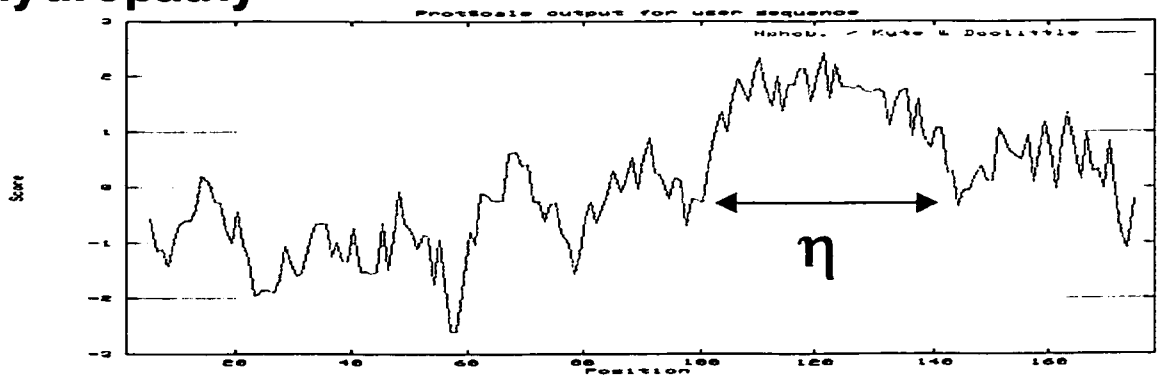

Caveolin-1 Sequence Homology

```
hCav-1 MSGGKYVDSE GHLYTVPIRE QGNIYKPNNK  AMADELSEKQ VYDAHTKEID LVNRDPKHLN
cCav-1 MSGTKYVDSE GFLYAAPVRE QGNIYKPNNK MMADELSEKA VHDVDTKEID LVNRDPKHLN
dCav-1 MSGGKYVDSE GHLYTVPIRE QGNIYKPNNK AMAEEMSEKQ VYDAHTKEID LVNRDPKHLN
mCav-1 MSGGKYVDSE GHLYTVPIRE QGNIYKPNNK AMADEVTEKQ VYDAHTKEID LVNRDPKHLN
rCav-1 MSGGKYVDSE GHLYTVPIRE QGNIYKPNNK AMADEVNEKQ VYDAHTKEID LVNRDPKHLN
       1         10        20        30        40        50        60

hCav-1 DDVVKIDFED VIAEPEGTHS FHGIWKASFT TFTVTKYWFY RLLSALFGIP MALIWGIYFA
cCav-1 DDVVKIDFED VIAEPEGTHS FDGIWKASFT TFTVTKYWFY RLLSAIFGIP MALIWGIYFA
dCav-1 DDVVKIDFED VIAEPEGTHS FDGIWKASFT TFTVTKYWFY RLLSALFGIP MALIWGIYFA
mCav-1 DDVVKIDFED VIAEPEGTHS FDGIWKASFT TFTVTKYWFY RLLSTIFGIP MALIWGIYFA
rCav-1 DDVVKIDFED VIAEPEGTHS FDGIWKASFT TFTVTKYWFY RLLSTIFGIP MALIWGIYFG
       61        70        80        90        100       110       120
```

Appendix E

Caveolin-1 Sequence Homology

hCav-1 ILSFLHIWAV VPCIKSFLIE IQCTSRVYSI YVHTVCDPLF EAVGKIFSNV RINLQKEI

cCav-1 ILSFLHIWAV VPCIRSYLIE IQCISRVYSI CIHTFCDPLF EAMGKVFSSI RATVRKEI

dCav-1 ILSFLHIWAV VPCIKSFLIE IQCISRVYSI YVHTFCDPFF EAVGKIFSNI RINMQKET

mCav-1 ILSFLHIWAV VPCIKSFLIE IQCISRVYSI YVHTFCDPLF EAIGKIFSNI RISTQKEI

rCav-1 ILSFLHIWAV VPCIKSFLIE IQCISRVYSI YVHNFCDPLF EGIGKIFSNI PISTQEEI

121 130 140 150 160 170 180

Appendix E

Caveolin-2 & 3 Sequence Homology

```
hCav-1 MDDDSYSHHS GLEYADPEKF ADSDQDRDPH RLNSHLKLG- FEDVIAEPVTT HSFDKVWICS
mCav-3 MMTEEHTDLE ARIIKDIHCK EIDLVNRDPK  NINEDIVKVD FEDVIAEPEG TYSFDGVWKV
rCav-3 MMTEEHTDLE ARIIKDIHCK EIDLVNRDPK  NINEDIVKVD FEDVIAEPEG TYSFDGVWRV
       1         10        20        30        40        50        60

hCav-1 HALFEISKYV MYKFLTVFLA IPLAFIAGIL FATLSCLHIW ILMPFVKTCL MVLPSVQTIW
mCav-3 SYTTFTVSKY WCYRLLSTLL GVPLALLWGF LFACISFCHI WAVVPCIKSY LIEIQCISHI
rCav-3 MSGGKYVDSE GHLYTVPIRE QGNIYKPNNK AMAEEMSEKQ VYDAHTKEID LVNRDPKHLN
       61        70        80        90        100       110       120

hCav-2 KSVTDVIIAP LCTSVGRCFS SVSLQLSQD
mCav-3 YSLCIRTFCN PLFAALGQVC SNIKVVLRRE G
rCav-3 YSLCIRTFCN PLFAALGQVC SNIKVVLRRE G
       121       130       140       150
```

Appendix E

Bibliography

1. Castelli, W. P. (1984) *Am.J.Med.* **76,** 4-12

2. Eisenberg, S. (1984) *J.Lipid Res.* **25,** 1017-1058

3. Yokoyama, S. Apolipoprotein-mediated cellular cholesterol efflux. Biochim.Biophys.Acta 1392, 1-15. 1998.
Ref Type: Generic

4. Tall, A. R. (1998) *Eur.Heart J.* **19 Suppl A,** A31-A35

5. Rye, K. A. and Barter, P. J. (1992) Lipid Transfer Activities and Apolipoproteins. In Rosseneu, M., editor. *Structure and Functions of Apolipoproteins*, CRC Press, Inc.,

6. Oliveira, H. C. F., Ma, L. M., Milne, R., Marcovina, S. M., Inazu, A., Mabuchi, H., and Tall, A. R. (1997) *Arterioscler.Thromb.Vasc.Biol.* **17,** 1045-1052

7. Ross, R. (1998) *Nature* **362,** 801-809

8. Ryan, R. O. (1996) *Biochem.Cell Biol.* **74,** 155-164

9. Segrest, J. P., Garber, D. W., Brouillette, C. G., Harvey, S. C., and Anantharamaiah, G. M. (1994) *Adv.Protein Chem.* **45,** 303-369

10. Havel, R. J. and Kane, J. P. (1995) Introduction: Structure and Metabolism of Plasma Lipoproteins. In Scriver, C. R., Beaudet, A. L., Sly, W. S., and Valle, D., editors. *The metabolic and molecular basis of inherited disease*, Mc Graw-Hill, Inc, New York

11. Chen, S. H., Habib, G., Yang, C. Y., Gu, Z. W., Lee, B. R., Weng, S. A., Silberman, S. R., Cai, S. J., Deslypere, J. P., and Rosseneu, M. (1987) *Science* **238,** 363-366

12. Hussain, M. M., Kancha, R. K., Zhou, Z. Y., Luchoomun, J., Zu, H. Y., and Bakillah, A. (1996) *Biochim.Biophys.Acta Lipids Lipid Metab.* **1300,** 151-170

13. Elovson, J., Chatterton, J. E., Bell, G. T., Schumaker, V. N., Reuben, M. A., Puppione, D. L., Reeve, J. R., Jr., and Young, N. L. (1988) *J.Lipid Res.* **29,** 1461-1473

14. Packard, C. J. and Shepherd, J. (1997) *Arterioscler.Thromb.Vasc.Biol.* **17,** 3542-3556

15. Mahley, R. W. (1988) *Science* **240,** 622-630

16. Dolphin, P. J. (1992) Lipolytic Enzymes and the Role of Apolipoproteins in the

Regulation of their Activity. In Rosseneu, M., editor. *Structure and Function of Apolipoproteins*, CRC Press, Inc., Boca Raton

17. Goldberg, I. J. (1996) *J.Lipid Res.* **37,** 693-707

18. Kobayashi, J., Applebaum-Bowden, D., Dugi, K. A., Brown, D. R., Kashyap, V. S., Parrott, C., Duarte, C., Maeda, N., and Santamarina-Fojo, S. (1996) *J.Biol.Chem.* **271,** 26296-26301

19. Tall, A. (1995) *Annu.Rev.Biochem.* **64,** 235-257

20. Brown, M. S. and Goldstein, J. L. (1986) *Science* **232,** 34-47

21. Anderson, R. G., Goldstein, J. L., and Brown, M. S. (1976) *Proc.Natl.Acad.Sci.U.S.A* **73,** 2434-2438

22. Francone, O. L. and Fielding, C. J. (1990) *Eur.Heart J.* **11 Suppl E:218-24,** 218-224

23. Luo, C. C., Li, W. H., and Chan, L. (1989) *J.Lipid Res.* **30,** 1735-1746

24. Li, W.-H., Tanimura, M., Luo, C.-C., Datta, S., and Chan, L. (1988) *J.Lipid Res.* 245-271

25. Barter, P. J. and Rye, K. A. (1996) *Atherosclerosis* **121,** 1-12

26. Dixon, J. L. and Ginsberg, H. N. (1992) *Semin.Liver Dis.* **12,** 364-372

27. Musliner, T. A., Long, M. D., Forte, T. M., Nichols, A. V., Gong, E. L., Blanche, P. J., and Krauss, R. M. (1991) *J.Lipid Res.* **32,** 917-933

28. Forte, T. M., Goth-Goldstein, R., Nordhausen, R. W., and McCall, M. R. (1993) *J.Lipid Res.* **34,** 317-324

29. Glomset, J. A., Assmann, G., Gjone, E., and Norum, K. R. (1995) Lecithin:Cholesterol Acyltransferase Deficiency and Fish Eye Disease. In Scriver, C. R., Beaudet, A. L., Sly, W. S., and Valle, D., editors. *The Metabolic and Molecular Bases of Inherited Disease*, McGraw-Hill, Inc., New York

30. Varban, M. L., Rinninger, F., Wang, N., Fairchild-Huntress, V., Dunmore, J. H., Fang, Q., Gosselin, M. L., Dixon, K. L., Deeds, J. D., Acton, S. L., Tall, A. R., and Huszar, D. (1998) *Proc.Natl.Acad.Sci.U.S.A* **95,** 4619-4624

31. Matveev, S., Van der Westhuyzen, D. R., and Smart, E. J. (1999) *J.Lipid Res.* **40,** 1647-1654

32. Graf, G. A., Connell, P. M., Van der Westhuyzen, D. R., and Smart, E. J. (1999) *J.Biol.Chem* **274,** 12043-12048

33. Glomset, J. A. (1968) *J.Lipid Res.* **9,** 155-167

34. Fielding, C. J. (1988) *Adv.Exp.Med.Biol.* **243,** 219-224

35. Albers, J. J., Tollefson, J. H., Faust, R. A., and Nishide, T. (1988) *Adv.Exp.Med.Biol.* **243,** 213-217

36. Fielding, C. J. and Fielding, P. E. (1995) *J.Lipid Res.* **36,** 211-228

37. Johnson, W. J., Mahlberg, F. H., Rothblat, G. H., and Phillips, M. C. (1991) *Biochim.Biophys.Acta* **1085,** 273-298

38. Kuivenhoven, J. A., Pritchard, H., Hill, J., Frohlich, J., Assmann, G., and Kastelein, J. (1997) *J.Lipid Res.* **38,** 191-205

39. Jonas, A., Sweeny, S. A., and Herbert, P. N. (1984) *J.Biol.Chem.* **259,** 6369-6375

40. Tall, A. R. (1990) *J.Clin.Invest.* **86,** 379-384

41. Babiker, A., Andersson, O., Lund, E., Xiu, R. J., Deeb, S., Reshef, A., Leitersdorf, E., Diczfalusy, U., and Björkhem, I. (1997) *J.Biol.Chem.* **272,** 26253-26261

42. Assmann, G., Von Eckardstein, A., and Funke, H. (1993) *Circulation* **87 Suppl.,** III28-III34

43. Oram, J. F. and Yokoyama, S. (1996) *J.Lipid Res.* **37,** 2473-2491

44. Rothblat, G. H., Mahlberg, F. H., Johnson, W. J., and Phillips, M. C. (1992) *J.Lipid Res.* **33,** 1091-1097

45. Brinton, E. A., Oram, J. F., Chen, C. H., Albers, J. J., and Bierman, E. L. (1986) *J.Biol.Chem.* **261,** 495-503

46. Ji, Y., Jian, B., Wang, N., Sun, Y., Moya, M. D., Phillips, M. C., Rothblat, G. H., Swaney, J. B., and Tall, A. R. (1997) *J.Biol.Chem.* **272,** 20982-20985

47. Jian, B., Delalleramoya, M., Ji, Y., Wang, N., Phillips, M. C., Swaney, J. B., Tall, A. R., and Rothblat, G. H. (1998) *J.Biol.Chem.* **273,** 5599-5606

48. Calvo, D., Gomez-Coronado, D., Lasuncion, M. A., and Vega, M. A. (1997) *Arterioscler.Thromb.Vasc.Biol.* **17,** 2341-2349

49. Babitt, J., Trigatti, B., Rigotti, A., Smart, E. J., Anderson, R. G., Xu, S., and Krieger, M. (1997) *J.Biol.Chem.* **272,** 13242-13249

50. McKnight, G. L., Reasoner, J., Gilbert, T., Sundquist, K. O., Hokland, B., McKernan, PA, Champagne, J., Johnson, C. J., Bailey, M. C., and Holly, R. (1992) *J.Biol.Chem.* **267,** 12131-12141

51. Brown, M. S., Herz, J., and Goldstein, J. L. (1997) *Nature* **388,** 629-630

52. Sargiacomo M, Scherer PE, Tang ZL, Casanova JE, and Lisanti MP (1994) *Oncogene* **9,** 2589-2595

53. Song, K. S., Li, S. W., Okamoto, T., Quilliam, L. A., Sargiacomo, M., and Lisanti, M. P. (1996) *J.Biol.Chem.* **271,** 9690-9697

54. Engelman, J. A., Zhang, X. L., Galbiati, F., and Lisanti, M. P. (1998) *FEBS Lett.* **429,** 330-336

55. Minetti, C., Sotgia, F., Bruno, C., Scartezzini, P., Broda, P., Bado, M., Masetti, E., Mazzocco, M., Egeo, A., Donati, M. A., Volonte, D., Galbiati, F., Cordone, G., Bricarelli, F. D., Lisanti, M. P., and Zara, F. (1998) *Nat.Genet* **18,** 365-368

56. Scherer, P. E., Tang, Z., Chun, M., Sargiacomo, M., Lodish, H. F., and Lisanti, M. P. (1995) *J Biol.Chem* **270,** 16395-16401

57. Kurzchalia, T. V. and Parton, R. G. (1996) *FEBS Lett.* **389,** 52-54

58. Lisanti, M. P., Scherer, P. E., Vidugiriene, J., Tang, Z., Hermanowski-Vosatka, A., Tu, Y. H., Cook, R. F., and Sargiacomo, M. (1994) *J Cell Biol.* **126,** 111-126

59. Scherer, P. E. and Lisanti, M. P. (1997) *J Biol.Chem* **272,** 20698-20705

60. Scherer, P. E., Lewis, R. Y., Volonte, D., Engelman, J. A., Galbiati, F., Couet, J., Kohtz, D. S., van Donselaar, E., Peters, P., and Lisanti, M. P. (1997) *J Biol.Chem* **272,** 29337-29346

61. Kurzchalia TV, Dupree P, and Monier S (1994) *FEBS Lett.* **346,** 88-91

62. Anderson, R. G. (1998) *Annu.Rev.Biochem.* **67,** 199-225

63. Chang, W. J., Ying, Y. S., Rothberg, K. G., Hooper, N. M., Turner, A. J., Gambliel, H. A., De Gunzburg, J., Mumby, S. M., Gilman, A. G., and Anderson, R. G. (1994) *J.Cell Biol.* **126,** 127-138

64. Michel, J. B., Feron, O., Sacks, D., and Michel, T. (1997) *J Biol.Chem* **272,** 15583-15586

65. Monier S, Parton RG, Vogel F, Behlke J, Henske A, and Kurzchalia TV (1995) *Mol.Biol.Cell* **6,** 911-927

66. Weisz, O. A., Swift, A. M., and Machamer, C. E. (1993) *J.Cell Biol.* **122,** 1185-1196

67. Voorberg, J., Fontijn, R., Calafat, J., Janssen, H., van Mourik, J. A., and Pannekoek, H. (1993) *EMBO J.* **12,** 749-758

68. Scherer, P. E., Lewis, R. Y., Volonte, D., Engelman, J. A., Galbiati, F., Couet, J., Kohtz, D. S., van Donselaar, E., Peters, P., and Lisanti, M. P. (1997) *J.Biol.Chem.* **272,** 29337-29346

69. Koleske, A. J., Baltimore, D., and Lisanti, M. P. (1995) *Proc.Natl.Acad.Sci.U.S.A* **92,** 1381-1385

70. Li, S., Song, K. S., Koh, S. S., Kikuchi, A., and Lisanti, M. P. (1996) *J Biol.Chem* **271,** 28647-28654

71. Song, K. S., Tang, Z., Li, S., and Lisanti, M. P. (1997) *J Biol.Chem* **272,** 4398-4403

72. Sargiacomo, M., Scherer, P. E., Tang, Z., Kubler, E., Song, K. S., Sanders, M. C., and Lisanti, M. P. (1995) *Proc.Natl.Acad.Sci.U.S.A* **92,** 9407-9411

73. Li, S., Okamoto, T., Chun, M., Sargiacomo, M., Casanova, J. E., Hansen, S. H., Nishimoto, I., and Lisanti, M. P. (1995) *J Biol.Chem* **270,** 15693-15701

74. Li, S., Seitz, R., and Lisanti, M. P. (1996) *J Biol.Chem* **271,** 3863-3868

75. Mastick CC, Brady MJ, and Saltiel AR (1995) *J.Cell Biol.* **129,** 1523-1531

76. Sargiacomo, M., Sudol, M., Tang, Z., and Lisanti, M. P. (1993) *J Cell Biol.* **122,** 789-807

77. Li, S., Couet, J., and Lisanti, M. P. (1996) *J Biol.Chem* **271,** 29182-29190

78. Couet, J., Li, S., Okamoto, T., Ikezu, T., and Lisanti, M. P. (1997) *J Biol.Chem* **272,** 6525-6533

79. Fra AM, Williamson E, Simons K, and Parton RG (1994) *J.Biol.Chem.* **269,** 30745-30748

80. Simons, K. and Ikonen, E. (1997) *Nature* **387,** 569-572

81. Conrad PA, Smart EJ, Ying YS, Anderson RG, and Bloom GS (1995) *J.Cell Biol.* **131,** 1421-1433

82. Harder, T. and Simons, K. (1997) *Curr.Opin.Cell Biol.* **9,** 534-542

83. Danielsen EM and van Deurs B (1995) *J.Cell Biol.* **131,** 939-950

84. Feron, O., Saldana, F., Michel, J. B., and Michel, T. (1998) *J.Biol.Chem.* **273,** 3125-3128

85. García-Cardeña, G., Oh, P., Liu, J. W., Schnitzer, J. E., and Sessa, W. C. (1996) *Proc.Natl.Acad.Sci.USA* **93,** 6448-6453

86. Shaul, P. W., Smart, E. J., Robinson, L. J., German, Z., Yuhanna, I. S., Ying, Y. S., Anderson, R. G. W., and Michel, T. (1996) *J.Biol.Chem.* **271,** 6518-6522

87. Sase, K. and Michel, T. (1997) *TCM* **7,** 28-37

88. Michel, J. B., Feron, O., Sase, K., Prabhakar, P., and Michel, T. (1997) *J.Biol.Chem.* **272,** 25907-25912

89. Schnitzer JE, Oh P, Jacobson BS, and Dvorak AM (1995) *Proc.Natl.Acad.Sci.USA* **92,** 1759-1763

90. Anderson RG, Kamen BA, Rothberg KG, and Lacey SW (1992) *Science* **255,** 410-411

91. Fielding, C. J. and Fielding, P. E. (1995) *Biochemistry* **34,** 14237-14244

92. Fielding, C. J. and Fielding, P. E. (1997) *J.Lipid Res.* **38,** 1503-1521

93. Moldovan NI, Heltianu C, Simionescu N, and Simionescu M (1995) *Exp.Cell Res.* **219,** 309-313

94. Antohe F, Dobrila L, Heltianu C, Simionescu N, and Simionescu M (1993) *Eur.J.Cell Biol.* **60,** 268-275

95. Ullrich, A., Shine, J., Chirgwin, J., Pictet, R., Tischer, E., Rutter, W. J., and Goodman, H. M. (1977) *Science* **196,** 1313-1319

96. Blackhart, B. D., Yao, Z., and McCarthy, B. J. (1990) *J.Biol.Chem.* **265,** 8358-8360

97. McLeod, R. S., Zhao, Y., Selby, S. L., Westerlund, J., and Yao, Z. (1994) *J.Biol.Chem.* **269,** 2852-2862

98. Mukherjee, S., Zha, X., Tabas, I., and Maxfield, F. R. (1998) *Biophys.J.* **75,** 1915-1925

99. Zhao, Y. W., Sparks, D. L., and Marcel, Y. L. (1996) *Biochemistry* **35,** 16510-16518

100. Zhao, Y. W., Sparks, D. L., and Marcel, Y. L. (1996) *J.Biol.Chem.* **271,** 25145-25151

101. Bilheimer, D. W., Eisenberg, S., and Levy, R. I. (1972) *Biochim.Biophys.Acta* **260,** 212-221

102. Lowry, O. H., Rosebrough, N. J., Farr, A. L., and Randall, R. J. (1951) *J.Biol.Chem.* **193,** 265-275

103. Francis, G. A., Oram, J. F., Heinecke, J. W., and Bierman, E. L. (1996)

Biochemistry **35,** 15188-15197

104. Birnboim, H. C. and Doly, J. (1979) *Nucleic Acids Res.* **7,** 1513-1523

105. Glenney, J. R. J. (1992) *FEBS Lett.* **314,** 45-48

106. Yao, Z., Blackhart, B. D., Linton, M. F., Taylor, S. M., Young, S. G., and McCarthy, B. J. (1991) *J.Biol.Chem.* **266,** 3300-3308

107. Li, S., Song, K. S., and Lisanti, M. P. (1996) *J.Biol.Chem.* **271,** 568-573

108. Teifel, M., Heine, L. T., Milbredt, S., and Friedl, P. (1997) *Endothelium* **5,** 21-35

109. Song, S. K., Li, S., Okamoto, T., Quilliam, L. A., Sargiacomo, M., and Lisanti, M. P. (1996) *J Biol.Chem* **271,** 9690-9697

110. Creighton, T. E. (1993) Protein Structure and Molecular Properties. W.H.Freeman and Co. N.Y.,

111. Zuker, M. and Jacobson, A. B. (1998) *RNA.* **4,** 669-679

112. Eaton, S. and Simons, K. (1995) *Cell* **82,** 5-8

113. Vasile, E., Simionescu, M., and Simionescu, N. (1983) *J.Cell Biol.* **96,** 1677-1689

114. Kim, M.-J., Dawes, J., and Jessup, W. (1994) *Atherosclerosis* **108,** 5-17

115. Dehouck, B., Fenart, L., Dehouck, M. P., Pierce, A., Torpier, G., and Cecchelli, R. (1997) *J.Cell Biol.* **138,** 877-889

116. Takahashi, K., Sawasaki, Y., Hata, J., Mukai, K., and Goto, T. (1990) *In Vitro Cell Dev.Biol.* **26,** 265-274

117. Oh, P., McIntosh, D. P., and Schnitzer, J. E. (1998) *J.Cell Biol.* **141,** 101-114

118. de Boer, H. C., Preissner, K. T., Bouma, B. N., and de Groot, P. G. (1995) *J.Biol.Chem* **270,** 30733-30740

119. Mackic, J. B., Stins, M., McComb, J. G., Calero, M., Ghiso, J., Kim, K. S., Yan, S. D., Stern, D., Schmidt, A. M., Frangione, B., and Zlokovic, B. V. (1998) *J.Clin.Invest* **102,** 734-743

120. Schnitzer JE and Oh P (1992) *Am.J.Physiol.* **263,** H1872-H1879

121. Schnitzer JE, Oh P, Pinney E, and Allard J (1994) *J.Cell Biol.* **127,** 1217-1232

122. Acton, S., Rigotti, A., Landschulz, K. T., Xu, S., Hobbs, H. H., and Krieger, M. (1996) *Science* **271,** 518-520

123. Fielding, C. J. and Fielding, P. E. (1997) *J.Lipid Res.* **38,** 1503-1521

124. Fielding, P. E. and Fielding, C. J. (1995) *Biochemistry* **34,** 14288-14292

125. Orso, E., Broccardo, C., Kaminski, W. E., Bottcher, A., Liebisch, G., Drobnik, W., Gotz, A., Chambenoit, O., Diederich, W., Langmann, T., Spruss, T., Luciani, M. F., Rothe, G., Lackner, K. J., Chimini, G., and Schmitz, G. (2000) *Nat.Genet.* **24,** 192-196

126. Fielding, C. J., Bist, A., and Fielding, P. E. (1999) *Biochemistry* **38,** 2506-2513

127. Fielding, C. J., Bist, A., and Fielding, P. E. (1997) *Proc.Natl.Acad.Sci.USA* **94,** 3753-3758

128. Liscum, L. and Underwood, K. W. (1995) *J.Biol.Chem* **270,** 15443-15446

129. Scherer, P. E., Okamoto, T., Chun, M., Nishimoto, I., Lodish, H. F., and Lisanti, M. P. (1996) *Proc.Natl.Acad.Sci.U.S.A* **93,** 131-135

130. Henley, J. R., Krueger, E. W., Oswald, B. J., and McNiven, M. A. (1998) *J.Cell Biol.* **141,** 85-99

131. Luetterforst, R., Stang, E., Zorzi, N., Carozzi, A., Way, M., and Parton, R. G. (1999) *J.Cell Biol.* **145,** 1443-1459

132. Christian, A. E., Haynes, M. P., Phillips, M. C., and Rothblat, G. H. (1997) *J.Lipid Res.* **38,** 2264-2272

133. Chang, C. C. Y., Chen, J., Thomas, M. A., Cheng, D., Del Priore, V. A., Newton, R. S., Pape, M. E., and Chang, T. Y. (1995) *J.Biol.Chem.* **270,** 29532-29540

134. Fra AM, Williamson E, Simons K, and Parton RG (1995) *Proc.Natl.Acad.Sci.USA* **92,** 8655-8659

135. Lange, Y. (1991) *J.Lipid Res.* **32,** 329-339

136. Smart, E. J., Ying, Y., Donzell, W. C., and Anderson, R. G. (1996) *J.Biol.Chem* **271,** 29427-29435

137. Smart EJ, Ying YS, Conrad PA, and Anderson RG (1994) *J.Cell Biol.* **127,** 1185-1197

138. Bist, A., Fielding, P. E., and Fielding, C. J. (1997) *Proc.Natl.Acad.Sci.USA* **94,** 10693-10698